# CEREBELLAR CONTRIBUTIONS TO COGNITION IN YOUNG ADULTS: A tDCS AND BRAIN IMAGING STUDY

A Dissertation

by

TED MALDONADO

Submitted to the Graduate and Professional School of
Texas A&M University
in partial fulfillment of the requirements for the degree of

DOCTOR OF PHILOSOPHY

| | |
|---|---|
| Chair of Committee, | Jessica A. Bernard |
| Committee Members, | Joseph M. Orr |
| | Darrell A. Worthy |
| | Ranjana K. Mehta |
| Head of Department, | Heather C. Lench |

August 2021

Major Subject: Psychology

ABSTRACT

The literature implicating the cerebellum and non-motor cognitive processing is quickly growing. Though there is an understanding that the cerebellum is active during non-motor task performance, little work has looked to understand why the cerebellum is active. Work in aging a disease suggest that disruptions in the cerebellum negatively impact cortical connectivity, function and processing. Critically, the cerebellum might be important for offloading cortical processing, providing support during task performance and cortical processing. The current work used transcranial direct current stimulation (tDCS) to modulate cerebellar function to better understand how changes in cerebellar output might affect cortical activation, connectivity, and behavioral performance. This work used a between-subjects design, in which participants received either anodal, cathodal, or sham stimulation over the right cerebellum before a functional and resting state magnetic resonance imaging scan where participants completed both a motor (sequence learning) and non-motor (Sternberg) task. We predicted that cathodal stimulation would improve, and anodal stimulation would hinder, task performance, connectivity, and cortical activation. Behaviorally, anodal stimulation negatively impacted behavior during late phase sequence learning. Functionally, we found that anodal stimulation resulted in increased bilateral cortical activation, particularly in parietal and frontal regions known to be involved in memory. Qualitative interpretations of the resting state data suggest anodal stimulation increases contralateral activity and decreases ipsilateral activity. This was particularly noticeable in cognitive lobules, such as Crus I and II. Additionally, we found behavioral correlates in connectivity to frontal and temporal regions in the cortex following stimulation. Assuming the change in function here parallels what occurs in aging or disease, this may provide a mechanism whereby offloading of function to the cerebellum is

negatively impacted, resulting in subsequent differences in prefrontal cortical activation patterns and performance deficits. This work has a potential to update existing compensatory models to include the cerebellum as a structure use to support cognitive processes, which has implications in remediation techniques in a number of clinical populations.

# DEDICATION

Hilary, I love you.

Mom and Dad, we did it!

# ACKNOWLEDGEMENTS

I would like to thank my advisor, Dr. Jessica Bernard, for her dedication to this dissertation. I will forever be appreciative of her support of this project and her commitment to fostering growth and curiosity. Her consistent effort to strive for excellence is something I will continue to admire.

I would like to thank my committee members, Drs. Orr, Worthy, and Mehta, for their guidance and support throughout the course of this research.

I would also like to thank LCMN and CONGA Lab members past and present for their support throughout the last five years. Jimmy, thanks for accepting my non-sense. I still do not like Crocs or Wes Anderson. Sydney, thanks for the quiz breaks and keeping me relevant in pop-culture. Bryan, thank you for your patience, it was incredibly meaningful. Hannah, thank you for your poise, your strength is amazing. Mike, thanks for letting me talk soccer so I could distract myself from imposing deadlines. Mia San Mia. Jesus, thanks for letting me sing Creed and knowing every song. Ever.

I also want to thank my wife, Hilary, for her continual and unwavering support throughout this whole journey. You earned this degree just as much as I did. I love you, and I appreciate the sacrifices you made to get US here.

Last, but certainly not least, I would like to honor my parents for their endless love and commitment to helping me succeed. Without them, I wouldn't be the person I am today, and to them I am exceedingly grateful.

# CONTRIBUTORS AND FUNDING SOURCES

## Contributors

This work was supervised by a dissertation committee consisting of Dr. Jessica Bernard (advisor) and Drs. Orr and Worthy of the Department of Psychological and Brain Sciences and Dr. Mehta of the Department of Industrial and Systems Engineering.

Abby Miller, Bryan Jackson, Hannah Ballard and Sydney Cox assisted, in part, indata collection. Bryan Jackson provided guidance and support on imaging analyses and data presentation programming. Mike Imburgio provided guidance and support on some behavioral analyses.

All work other conducted for the dissertation was completed by Ted Maldonado independently.

## Funding Sources

Graduate study was supported, in part, by a Summer Research Award from Texas A&M University.

This work was also made possible in part by National Institute on Aging under Grant Number R01AG065010. Its contents are solely the responsibility of the authors and do not necessarily represent the official views of the NIH.

# NOMENCLATURE

| | |
|---|---|
| BOLD | Blood Oxygen Level Dependent |
| DNC | Deep Cerebellar Nuclei |
| fMRI | Functional Magnetic Resonance Imaging |
| ROI | Region of Interest |
| Rs-fcMRI | Resting State Functional Connectivity Magnetic Resonance Imaging |
| RT | Reaction Time |
| tDCS | Transcranial Direct Current Stimulation |
| TMS | Transcranial Magnetic Stimulation |

TABLE OF CONTENTS

Page

LIST OF FIGURES

Page

LIST OF TABLES

Page

# CHAPTER I

# GENERAL INTRODUCTION

Dr. Jeremy Schmahmann, a professor of neurology at Harvard and Massachusetts General Hospital, once quipped that the cerebellum is the "Rodney Dangerfield of the brain", a sentiment meant to indicate the cerebellum "don't get no respect" from scientists. Most research seems content with understanding the role the cerebellum plays in balance and motor movement. However, a growing body of work has also suggested the cerebellum is involved in non-motor cognitive processing, such a language, planning, emotion processing, and working memory (King et al., 2019; Leiner et al., 1989, 1991; Schmahmann et al., 2019; Stoodley et al., 2012). Understanding the role that the cerebellum plays in motor and non-motor processing can provide significant insights into how information is processed. It can further inform remediation techniques that might help overcome deficits resulting from neural infarcts as well as the normative differences and changes that occur with aging.

## General Cerebellar Overview

This cerebellum is a unique structure located in the posterior portion of the brain, under the occipital and temporal lobes. Though the cerebellum is only 10% of the total volume of the brain, it contains half of the neurons (Ghez, 1991) and is almost 80% of the surface area of the cortex (Sereno et al., 2020). The cerebellum consists of a right and left hemisphere and a midline structure called the vermis. Across these three regions, there are 32 lobules, in which anterior lobules (lobules I-V) are thought to be motor oriented and posterior lobules (lobules VI-X) are non-motor oriented (Diedrichsen, King, Hernandez-Castillo, Sereno, & Ivry, 2019; King, Hernandez-Castillo,

Poldrack, Ivry, & Diedrichsen, 2019; Stoodley & Schmahmann, 2010), though secondary motor representations do emerge in lobules VIIIa and VIIIb (Stoodley & Schmahmann, 2009).

The cytoarchitecture of the cerebellum is remarkably uniform (Ghez, 1991). The cerebellum is composed of three cellular layers consisting primarily of molecular, Purkinjie, and granular cells. Communication between the cerebellum and cortex occurs via the deep cerebellar nuclei (DCN) and thalamus. Broadly, signal from mossy fibers innervate granule cells which project to parallel fibers that innervate inhibitory Purkinjie cells, the primary cell group in the cerebellum. Purkinjie cells then project to the DCN which project to the thalamus, and profusely to the cortex (Ghez, 1991).

The uniform cytoarchitecture suggests that the cerebellum likely engages in the same information processing (Ghez, 1991; Ito, 2008; Ramnani, 2006) across each lobule, with projections that are sent to various regions of the cortex (Buckner et al., 2011; Ito, 2008; Ramnani, 2006), though some have speculated this might not be entirely accurate (Diedrichsen et al., 2019). Briefly, it is believed that the cerebellum encodes internal models of processes completed by the cortex (Ito, 2008), such that a copy of the information used by the cortex is sent and stored in the cerebellum (Ramnani, 2006), as part of a forward model. These models can be seen when we begin to understand why we are not able to tickle ourselves (Blakemore et al., 1998; Blakemore et al., 2000). Here, the cerebellum perceives decreased activation in the somatosensory cortex during a self-tickle, compared to increased activation during an externally generated tickle (Blakemore et al., 1998). This information is stored in the cerebellum and is used to predict the consequences of our movements (i.e. the tickle), by providing a signal that is used to cancel the response to the stimulation (i.e. eliminate sensation of a self-tickle). Internal models are broadly used to account for the role the cerebellum plays in non-motor cognitive processing as well. Indeed, primate work

has found distinct connections between the prefrontal cortex and motor cortex to the cerebellum (Kelly & Strick, 2003; Middleton & Strick, 2001). Critically, projections from the prefrontal cortex terminated in crus I and II, whereas motor cortex projects terminated in anterior regions of the cerebellum.

Converging evidence in human neuroimaging also supports these distinct closed-loop circuits. These projections are broadly replicated in humans using diffusion tensor imaging (Salmi et al., 2010) and further replicated in a developmental sample (Bernard et al., 2015). Further, parcellation work has shown distinct cerebellar activation with analogous cortical regions (Buckner et al., 2011; Diedrichsen et al., 2019). Notably, cerebellar connections with the cortex are cross-lateralized. At rest, work has found distinct cerebello-cortical circuits with the motor cortex, the dorsal lateral prefrontal cortex, the medial prefrontal cortex, and the anterior prefrontal cortex (Krienen & Buckner, 2009). Further, the default mode, salience, and executive networks have received distinct inputs from the cerebellum (Habas et al., 2009). O'Reilly and colleagues (2010) have furthered this understanding by demonstrating functional zones in the cerebellum such that anterior regions of the cerebellum have specific networks with motor, somatosensory, visual, and auditory cortices; however, posterior lobes are part of networks with the prefrontal and posterior parietal cortices (Bernard et al., 2012; Diedrichsen et al., 2019; King et al., 2019; O'Reilly et al., 2010). This was further supported by work using anatomical and self-organizing map approaches which found lobular boundaries of the human cerebellum might not directly align with functional boundaries, though anatomical boundaries can be useful when understanding circuits linking the cerebellum and the cortex (Bernard et al., 2012). Additional work provides more support suggesting that regions of the cerebellum are functionally coupled with specific

cerebral networks, such that there are three distinct maps of the cerebral cortex in the cerebellum (Buckner et al., 2011).

## Cerebellum and Motor Learning

The cerebellum is commonly and historically implicated in motor function and motor learning (Bernard & Seidler, 2014; Holmes, 1939). However, over the past several decades, there has been a wealth of work implicating the cerebellum in non-motor cognitive processing (Buckner, 2013; Chen & Desmond, 2005; Schmahmann, 2018; Schmahmann & Sherman, 1998; Stoodley et al., 2012). Specifically, there are cognitive components that play a role in learning new motor skills (Doyon, Gabitov, Vahdat, Lungu, & Boutin, 2018), with some work suggesting that working memory is one of the primary cognitive functions involved in the learning process (Bo & Seidler, 2009). Briefly, in a motor sequence learning task there are two learning phases (Doyon et al., 2018; Doyon et al., 1997; Karni et al., 1998). During initial learning, the brain structures involved include the striatum, the cerebellum, the hippocampus, the spinal cord, motor cortical regions such as the premotor cortex, SMA, pre SMA, and the anterior cingulate, as well as prefrontal and parietal areas. Critically, during initial learning, intricate interactions between brain structures are thought to establish the motor routines necessary to learn new motor behaviors and to create optimal representations of a sequence, or other complex motor behavior. During this initial learning phase, it is thought that cognitive processes are needed for optimization. Specifically, working memory is thought to be involved as an individual must repeatedly maintain and then update pieces of information in order to learn a sequence (Anguera et al., 2010, 2012; Bo & Seidler, 2009; Seidler et al., 2012). As the sequence is better maintained and performance is optimized, the resulting representation of the motor sequence is processed by a cortico-striatal circuit consisting primarily of the striatum, motor cortical regions, and parietal cortices. In this later learning phase, it is

thought that the newly learned motor sequence is completed in a more automatized fashion. Should new information need to be added, or further enhanced, then the motor sequence is pulled from this cortico-striatal network so the new information can be added in a consolidation-like process (Doyon et al., 2018). Critically, work has suggested that the cerebellum is particularly active in the early learning phase when procedural memories are created (Bernard & Seidler, 2013; Doyon et al., 2018), in part due to the cognitive processes necessary during initial practice that is used to optimize the execution of the learn sequence. However, cerebellar activation then decreases as execution becomes more automatic (Imamizu et al., 2000). A cortico-striato cerebellar network model has been developed to more succinctly explain the specific role the cerebellum plays in motor learning (Penhune & Steele, 2012). In this model, the cerebellum chooses the optimal internal model, the basal ganglia learn the appropriate response associations and motor chunks, and the motor cortex, likely with input from the prefrontal and parietal lobes, stores the newly learned information.

## Cerebellum and Non-Motor Cognition

Patient work has indicated that lesions in the posterior cerebellum result in marked deficits in cognition (Ilg et al., 2013; Richter et al., 2007; Schmahmann & Sherman, 1998; Timmann et al., 2008, 2009). The deficits were seen primarily in executive functions such as planning, set shifting, verbal fluency, abstract reasoning and working memory (Schmahmann & Sherman, 1998). However, difficulties were also experienced in spatial cognition. Individuals also experienced personality changes such as blunting of affect and inappropriate behavior along with language deficits. This has subsequently been supported by imaging work showing infarcts in the posterior cerebellum result in deficits in working memory and verbal fluency tasks (Ilg et al., 2013; Richter et al., 2007). Even more, brief disruption of cerebellar function using transcranial magnetic

stimulation (TMS) negatively impacted working memory performance (Desmond et al., 2005; Rami et al., 2003).

Subsequent imaging work has shown distinct cerebellar activations during the completion of language, working memory, spatial processing, and emotion processing tasks (Chen & Desmond, 2005; Diedrichsen et al., 2019; King et al., 2019; Stoodley et al., 2012; Stoodley & Schmahmann, 2009). Initial work suggested that working memory activations were found in lobules VI, VII, VIIIa. Bilaterally, EF activations were found in lobules VI, VII, VIIIb, Crus I, and Crus II, while language activations were localized to lobules VI, crus I, crus II. Spatial activations were left lateralized in lobule VI (Stoodley et al., 2012b, 2012a). Tract tracing in non-human primates has demonstrated closed loop circuits between the cerebellum, thalamus and the cortex in non-human primates (Dum & Strick, 2003; Kelly & Strick, 2000) and parallel circuits have also been mapped in the human brain (Bernard et al., 2012, 2013, 2016; Krienen & Buckner, 2009; Loewenstein et al., 2012; Palesi et al., 2015; Salmi et al., 2010). Even more, functional parcellations of the cerebellum map to specific regions within the cerebellum (Buckner et al., 2011).

## Transcranial Direct Current Stimulation

Clearly there are ethical limitations to inducing cerebellar lesions, but recent work has developed the use of noninvasive neural modulation techniques to investigate function after temporarily altering processing in a particular brain region. Through the use of magnets or electricity, we are able to temporarily mimic the effects one might experience with a lesion to better understand the cerebellum's role in cognitive processing. Transcranial direct current stimulation (tDCS) is not necessarily a novel technique, as the ancient Greeks would apply electric eels to the scalp as a remedy to multiple issues (Priori, 2003; Sarmiento et al., 2016). However,

modern use of tDCS allows researchers to increase or decrease the underlying neural activity in a region of the brain to better understand processing in both health and disease across a number of domains (Grimaldi et al., 2014).

Typical cortical tDCS protocols apply either a positive (anodal) or a negative (cathodal) current to the scalp for 5 to 25 minutes at 0.5 to 2 mA (Ferrucci et al., 2015; Nitsche et al., 2005). Anodal stimulation is thought to increase underlying neural activation which typically results in a positive increase in performance. Alternatively, cathodal stimulation reduces underlying neural activation which typically results in a negative decrease in performance. These same protocols had been applied to the cerebellum; however, recent work using optogenetics in rodents suggested that the polarity might be reversed in the cerebellum (Galea et al., 2009; Grimaldi et al., 2016). When no stimulation was applied to the cerebellum, Purkinje cells sent an inhibitory signal to the DCN. The DCN then sent an excitatory projection to the thalamus, which then projected to the cerebellar cortex. When anodal stimulation was applied, this exciteed the inhibitory Purkinje circuit, resulting in an increase in inhibitory function on the DCN which resulted in a decrease in cerebellar output to the cortex. Alternatively, cathodal stimulation applied to the cerebellum inhibited the inhibitory Purkinje circuit, which resulted in a decreased inhibitory projection on the DCN, which ultimately resulted in an increase in cerebellar output to the cortex (Doyon et al., 2018; Galea et al., 2009).

**Motor tDCS.** Cerebellar tDCS has a strong history of modulating motor performance particularly during motor learning and motor adaptation paradigms (Buch et al., 2017). Anodal stimulation to the cerebellum has enhanced online task performance by reducing errors (Cantarero et al., 2015), increased response latencies on a serial reaction time task (Jongkees et al., 2019), has enhanced motor adaptation in both younger and older individuals (Doppelmayr et al., 2016; Hardwick & Celnik, 2014), and improved implicit sequence learning (Ehsani et al., 2016; Ferrucci

et al., 2013; Samaei et al., 2017; Shimizu et al., 2017). However, this literature is mixed (Ballard et al., 2019; Maldonado & Bernard, 2021; Nguemeni et al., 2021), though this might be due to methodological variability (Horvath et al., 2014). For instance, some studies which found improved task performance following anodal stimulation (Ferrucci et al., 2013; Jongkees et al., 2019) placed their electrode such that stimulation would affect both the right and left cerebellum, whereas other placed the stimulating electrode over the right cerebellum and found anodal stimulation hindered task performance (Ballard et al., 2019). These, and other methodological considerations (Horvath et al., 2014), might explain the mixed nature of these results.

Imaging work has looked to understand changes in cerebellar and cortical activations following stimulation in relation to behavioral performance. Work by Liebrand and colleagues (2020) found that anodal stimulation over the right cerebellum enhanced sequence learning, accompanied by increased right M1, left cerebellum lobule VI, left inferior frontal gyrus and right inferior parietal lobule activations. Additionally, connectivity analyses demonstrated decreased connectivity from the putamen to the cerebellum, resulting in decreased inhibition of the cerebellum. Stimulation to the left M1 did not show these behavioral and cortical changes (Liebrand et al., 2020). Alternatively, recent work has applied cathodal stimulation to the cerebellum that led to a disinhibition of the dentate nucleus (Küper et al., 2019), though there was no change in cortical activation during a simple motor learning task.

Similar to the behavioral literature, methodological considerations might explain the contrasting results (Horvath et al., 2014). Specifically, there is a growing literature that suggests the effect of stimulation can be eliminated when a behavioral task is completed concurrently with stimulation (Quartarone et al., 2004), which occurred during the study conducted by Liebrand and colleagues. Further, study design might also explain divergent outcomes. Liebrand and colleagues

used a within subject design, in which participants completed stimulation and behavioral tasks on three different occasions. Küper and colleagues used a between-subjects design. Critically, tDCS results may magnify individual differences, which are lost when averaged across groups (Horvath et al., 2014), making it difficult to quantify unique tDCS responses and could simplify more complex patterns in behavior after stimulation.

Together, behavioral and imaging work strongly support a role for the cerebellum in motor learning and motor adaptation. Further, cerebellar tDCS seems to be a viable mechanism for understanding cerebellar contributions in the motor domain. Critically, behavioral data is mixed, and there is limited imaging work to accurately makes sense of the existing behavioral data. Thus, it is important that future work continue to combine behavioral and imaging methodologies, to provide more accurate understanding of how cortical change relates to behavior, and how cerebellar tDCS moderates this change.

**Non-Motor Cerebellar tDCS**. Cerebellar tDCS has also modulated non-motor performance particularly in language, executive function (e.g., working memory and inhibition), and attentional control tasks (Grimaldi et al., 2014; Oldrati & Schutter, 2018). A recent meta-analysis has suggested cerebellar tDCS might affect motor performance more than cognitive performance (Oldrati & Schutter, 2018), although how cerebellar tDCS is administered might be the reason for these key differences (Horvath et al., 2014; Rice et al., 2021). This includes electrode placement (Rice et al., 2021), the use of sham stimulation, and electric current influencers, such as electrode attachment method (Horvath et al., 2014). Further it was suggested that task complexity and the measure used as the dependent variable could partially explain the difference in the impact of cerebellar tDCS on non-motor cognitive performance (Oldrati & Schutter, 2018). This is clearly evident in the literature discussed below.

The work investigating language processing in the cerebellum broadly focuses on language and speech disorders and mechanisms for remediating impairment (Leggio et al., 2020). A detailed discussion of clinical populations is outside the scope of the current work; however, there is some work in healthy adults that demonstrates the role the cerebellum might play in language processing. Most of the cerebellar tDCS literature examining language combines tDCS and fMRI to ask and answer more targeted questions about the role the cerebellum plays in language, such as language processing (D'Mello et al., 2017; Miall et al., 2016), production (Turkeltaub et al., 2016), and storage (Macher et al., 2014). Broadly, anodal tDCS has been found to increase activity during language function (D'Mello et al., 2017). Specifically, anodal tDCS has increased Crus I and Crus II activation and connectivity in language networks. Anodal tDCS has also increased functional connectivity between the cerebellum and areas involved in the motor control of speech (Turkeltaub et al., 2016). Alternatively, work has found that anodal tDCS resulted in less activation in the right cerebellar lobule VIIb (Macher et al., 2014), specifically during the late encoding phase during a phonological storage task. A recent study found that anodal tDCS to the posterolateral cerebellum improved accuracy on a sentence completion task, and increased activation in left frontal and temporal cortices (Rice et al., 2021).

In regard to working memory, cathodal tDCS has impaired performance on a forward and backwards digit span task (Boehringer et al., 2013) and a verb generation task (Spielmann et al., 2017), but increased performance on a paced auditory serial addition and subtraction task (Pope & Miall, 2012), particularly as cognitive demands increased. Other work has shown both anodal and cathodal stimulation impaired the practice dependent improvement in reaction time during a Sternberg task (Ferrucci et al., 2008). More recently, work has applied both anodal and cathodal stimulation to both the right cerebellum and left dorsal lateral prefrontal cortex while participants

completed a Sternberg task (Maldonado & Bernard, 2021). Results found that when collapsing across regions, anodal stimulation negatively impacted RT, particularly when cognitive processing was high. Alternatively, anodal stimulation improved accuracy under medium load levels, and cathodal stimulation hindered accuracy under high load.

There is also a growing literature suggesting cerebellar tDCS does not affect working memory performance when applied to the cerebellum. A within subjects study applying anodal, cathodal and sham stimulation before the completion of an n-back task found no effects of load or stimulation (van Wessel et al., 2016). Similarly, a within subjects study applying cathodal and sham stimulation to the right cerebellum found no effect of stimulation on working memory task performance (Maldonado, Goen, Eakin, & Bernard, 2019). A between subjects tDCS study in which anodal or sham stimulation was applied to the cerebellum found no effects of stimulation on task performance for an implicit categorization task (Verhage et al., 2017). Under similar circumstances, researchers failed to find effects of stimulation on an implicit categorization learning task (Steiner et al., 2016), a probabilistic classification learning task (Majidi et al., 2017), and a serial reaction time task (Ambrus et al., 2016).

The work looking at the cerebellum in inhibitory control is limited and mixed. Initial work using a within subjects design did not find an effect of stimulation on a Stroop task (Maldonado, Goen, Imburgio, Eakin, & Bernard, 2019), and this null result was replicated in a subsequent between subjects design (Maldonado & Bernard, 2021). However, this might be due to task complexity. Other work has found cathodal stimulation reduced the number of commission errors in a go/no-go task (Wynn et al., 2019). Alternatively, commission errors were increased following cathodal stimulation in a subsequent study (Mannarelli et al., 2020).

Much of the work focused on attention applied tDCS to cortical regions, generally finding that anodal stimulation improves attentional control (Bolognini, Fregni, et al., 2010; Bolognini, Olgiati, et al., 2010; Coffman et al., 2012; Roy et al., 2015), though cathodal stimulation might also be beneficial in improving aspects of attention (Moos et al., 2012). However, recent work has also applied tDCS to the cerebellum and found anodal stimulation reduced reaction time on both congruent and incongruent trials of an attention network test (Mannarelli et al., 2019). Alternatively, cathodal stimulation only reduced reaction times for congruent trials. This work suggests that the cerebellum degraded the ability to process complex stimuli in which errors were present, ultimately providing evidence that the cerebellum is involved in error processing and the perception of conflicting signals (Mannarelli et al., 2019).

Together, both behavioral and imaging results clearly demonstrate that the cerebellum is involved in non-motor cognitive processing and cerebellar tDCS is a viable method of examining this relationship, though like with motor learning, the results have been mixed. With that said, the variability and heterogeneity in methodology across studies is likely contributing, at least in part, to these mixed results. Similar to motor processing however, the literature is not always consistent, and the imaging work needed to further clarify behavioral outcomes is, to date, limited. Therefore, work is needed to continue to assess the role the cerebellum plays in non-motor cognitive processing to further determine how the cerebellum is involved, particularly in relation to cerebellar cortical interactions that help support behavioral processing. To this end, the addition of an imaging parameter can elucidate how the changes in cortical and cerebellar connectivity and activation resulting from cerebellar stimulation affects behavior.

## Conclusion

Taken together, the literature suggests that the cerebellum is involved in both motor and non-motor processing. However, limited work has directly examined how the cerebellum might support motor and non-motor processing. Critically, there is a growing literature to suggest tDCS is a useful technique for assessing how the cerebellum is involved in motor and non-motor processing. Therefore, this dissertation looks to examine the role of the cerebellum in motor and non-motor processing by using cerebellar tDCS over the right cerebellum, before the completion of a sequence learning (motor) and a verbal working memory (non-motor) task that were completed in the magnetic resonance imaging environment. The first chapter will examine behavioral performance on both a sequence learning and working memory task, and also the functional activation related to this behavioral performance, following cerebellar tDCS. The second chapter of this dissertation will look at resting state cortico-cerebellar connectivity in young adults. Specifically, we are interested it understanding how cerebellar tDCS might modulate connectivity to provide greater insight into how the cerebellum might communicate with the cortex. Together these studies will provide novel insights into the role the cerebellum plays in motor and non-motor cognitive processing.

The first study (Chapter 2) looked to understand cerebellar and cortical activation in relation to behavioral performance after stimulation. Previous work has strongly relied on behavioral data (Boehringer et al., 2013; Ferrucci et al., 2008; Majidi et al., 2017; Maldonado et al., 2019; Pope & Miall, 2012; Spielmann et al., 2017; van Wessel et al., 2016; Verhage et al., 2017) with tDCS, but the results have typically been mixed. In regard to sequence learning, we found a significant effect of stimulation on reaction time, such that the magnitude in change in RT was significantly greater following cathodal stimulation between middle learning and random phase, compared to anodal and sham. Additionally, we saw anodal stimulation have a negative

impact on accuracy, particularly in late learning phases. This is in line with previous behavioral work from our group which found a similar effect following anodal stimulation (Ballard et al., 2019). When examining the functional data, we found that anodal stimulation resulted in greater bilateral cortical activation in frontal and parietal regions during sequence learning compared to random button presses. Further, within this effect, the anodal stimulation group saw greater parietal activation compared to the cathodal stimulation group. In regard to working memory task performance, we only found an effect of stimulation on reaction time, such that anodal and cathodal stimulation both improved reaction time compared to sham. Functional data demonstrated increased bilateral frontal activation following anodal stimulation during high load, compared to low load. However, a similar pattern of results was found following cathodal stimulation when comparing high load to medium load. Broadly, we concluded that anodal stimulation might degrade cerebellar processing and output to the cortex which ultimately resulted in greater cortical activation to compensate for the loss of cerebellar resources. Similar effects are found in aging (Bernard et al., 2013) and disease (Allen et al., 2007; Bai et al., 2009). This manuscript is currently in preparation.

In the second study (Chapter 3), we used resting state functional connectivity MRI (rs-fMRI) to investigate networks of the human cerebellum. The current work diverges slightly from previous work (Buckner et al., 2011; Habas et al., 2009; Krienen & Buckner, 2009; O'Reilly et al., 2010), such that we used a lobular approach, using anatomically defined regions as opposed to a functional parcellation. Though cerebellar tDCS did not significantly alter cortico-cerebellar connectivity, there were striking patterns of change which are worth noting. Specifically, we found that after anodal stimulation there were robust contralateral correlations with frontal, parietal, and temporal lobes, that were not present in the sham stimulation group. This was particularly

noticeable when crus I and II were used as the seed regions. Though the group contrasts were not significant, this visual interpretation of the results provided initial data to suggest anodal stimulation altars resting state connectivity between the cerebellum and the cortex. This was further supported by correlations between cerebello-cortical connectivity and task performance in frontal and temporal regions of the cortex after cathodal and anodal stimulation. Future work is needed to support this finding and determine the underlying mechanism and provide further understanding of why this modification might occur. This manuscript is currently in preparation.

Together, this work looked to provide initial evidence for the cerebellum as a component for existing scaffolding models, further supporting cerebellar inclusion into models describing cortical activation in health and disease.

# CHAPTER II

# ANODAL TRANSCRANIDAL DIRECT CURRENT STIMULATION TO THE CEREBELLUM INCREASES CORTICAL ACTIVATION IN MOTOR AND NON-MOTOR PROCESSING: A tDCS AND fMRI STUDY

## Introduction

Interest in the role the cerebellum plays in non-motor cognitive processing has increased over the last 30 years (Buckner, 2013). This was initially driven by patient work which demonstrated that lesions in the posterior cerebellum resulted in degraded cognitive performance (Ilg et al., 2013; Richter et al., 2007; Schmahmann & Sherman, 1998; Timmann et al., 2008, 2009). Subsequent imaging work demonstrated posterior cerebellar activation (King et al., 2019; Stoodley et al., 2012; Stoodley & Schmahmann, 2010) during a number of non-motor tasks, such as working memory (Bellebaum & Daum, 2007; Desmond et al., 1997; Hautzel et al., 2009; Hayter et al., 2007; Stoodley et al., 2012), updating (Jahanshahi et al., 2000), inhibition (Neau et al., 2000), set shifting (Ravizza & Ivry, 2001; Schall et al., 2003), and planning tasks (Lie et al., 2006). Further, these activations are functionally connected to regions in the cortex (Bernard et al., 2016; Diedrichsen, King, Hernandez-Castillo, Sereno, & Ivry, 2019; Dum & Strick, 2003; Kelly & Strick, 2000; King et al., 2019; Palesi et al., 2015; Ramnani, 2006; Sen et al., 2010; Stoodley et al., 2012b; Stoodley & Schmahmann, 2009), with structural data demonstrating white matter tracts linking the cerebellum and cortex in the human brain (Salmi et al., 2010). Recent work has further demonstrated that coactivations between the prefrontal cortex and the cerebellum can predict performance on learning and executive function tasks (Reineberg et al., 2015).

Models for sequence learning suggest learning happens over time in distinct phases (Doyon, Gabitov, Vahdat, Lungu, & Boutin, 2018; Doyon et al., 1997; Karni et al., 1998). It is thought there is need for cognitive processing during the early learning phase, in which some work suggests working memory is needed to make motor chucks (Bo & Seidler, 2009). Critically, the cerebellum is also particularly active in the early learning phase when procedural memories are created (Bernard & Seidler, 2013; Doyon et al., 2018), though the cerebellum might also be active due to its role in cognitive processing (Ballard, Goen, Maldonado, & Bernard, 2019; Schmahmann, 2018; Schmahmann, Guell, Stoodley, & Halko, 2019; Stoodley, Valera, & Schmahmann, 2012b). Indeed, imaging work has demonstrated areas in the prefrontal cortex, typically involved in cognitive processing, are also active during early learning stages of motor adaptation tasks (Anguera et al., 2010, 2012), and during explicit sequence tasks (Aizenstein et al., 2004; Eliassen et al., 2001; Honda et al., 1998; Sakai et al., 1998; Schendan et al., 2003). Indeed, closed loop cerebello-thalamic-cortical circuits between cortical regions involved in cognition and the cerebellum have been found (Bernard, Orr, & Mittal, 2016; Dum & Strick, 2003; Kelly & Strick, 2000; Palesi et al., 2015; Ramnani, 2006; Sen, Kawaguchi, Truong, Lewis, & Huang, 2010; Stoodley, Valera, & Schmahmann, 2012b; Stoodley & Schmahmann, 2009), providing evidence for cerebello-cortical interactions during task performance. Taken together, this literature provides evidence for cerebellar involvement in cognitive aspects of initial motor sequence learning.

This cerebello-cortical interaction has likely evolved for the processing of internal models created in the cerebellum (Ramnani, 2006, 2014). Briefly, it is believed that the cerebellum encodes internal models (i.e. forward or inverse) of processes completed by the cortex (Ito, 2008), such that a copy of the information used by the cortex is sent and stored in the cerebellum (Ramnani, 2006), in order to complete a process precisely. A forward model will use these copies

to predict the expected result of a motor command, but uses error learning to update the command if the predicted outcome does not match the desired outcome. An inverse model will choose the copies necessary to achieve a desired outcome. Critically, these internal models are continually updated based on an input-output relationship between motor commands and their consequences (Ito, 2008). Any degradation of these models can contribute to behavioral decline and performance decrements (Bernard & Seidler, 2014; Ilg et al., 2013; Schmahmann & Sherman, 1998). This theory of internal models is broadly used to account for the role the cerebellum plays in non-motor cognitive processing.

Despite a growing literature demonstrating cerebellar activation during nonmotor cognitive processing, little work has investigated how the cerebellum is involved in cortical processing. Past work in aging suggests the cerebellum might provide the cortex with processing resources, such that when output from the cerebellum is degraded, performance suffers (Bernard & Seidler, 2014). That is, when tasks become more automatic, individuals can rely more on internal models and cerebellar processing, freeing up cortical resources, particularly if tasks become increasingly complicated. Recent advancements in non-invasive stimulation, such as transcranial direct current stimulation (tDCS) allow us to explore the role the cerebellum plays in cognition. tDCS increases (anodal) or decreases (cathodal) neural activity using a small amount of electrical current in order to understand the behavioral contributions of specific brain regions in pseudo isolation. Behaviorally, this results in an increase or decrease in motor (Reis & Fritsch, 2011) or non-motor functioning (Coffman et al., 2014), when applied to the cortex. However, the cellular structure of the cerebellum seems to reverse this effect. Specifically, anodal stimulation excites inhibitory cells in the cerebellum which in turn results in decreased signal to the cortex. Alternatively, cathodal

stimulation inhibits the inhibitory cells, resulting in increased signal to the cortex (Galea et al., 2009; Grimaldi et al., 2016).

Behavioral effects broadly fall in line with the polarity specific effects of cerebellar tDCS (Ballard et al., 2019; Block & Celnik, 2013; Buch et al., 2017; Cantarero et al., 2015; Ferrucci et al., 2013; Galea, Vazquez, Pasricha, Orban De Xivry, & Celnik, 2011; Hardwick & Celnik, 2014; Jongkees et al., 2019; Liebrand et al., 2020; Pope & Miall, 2012; Shah, Nguyen, & Madhavan, 2013). Briefly, cathodal stimulation results in task improvement, while anodal stimulation hampers performance (Shah et al., 2013), particularly during late learning (Ballard et al., 2019). Similar work examining non-motor cognitive processing again demonstrated cathodal stimulation over the right cerebellum improved performance, and anodal stimulation impaired performance. Briefly, cathodal stimulation has improved performance in both working memory (Pope & Miall, 2012) and inhibition tasks (Mannarelli et al., 2019; Wynn et al., 2019) whereas anodal stimulation has typically hindered task performance in verbal memory tasks (Ferrucci et al., 2008).

Imaging work in conjunction with tDCS is also typically mixed (D'Mello et al., 2017; Küper et al., 2019; Macher et al., 2014; Rice et al., 2021; Turkeltaub et al., 2016). However, past work has demonstrated anodal stimulation decreased activation in the right cerebellar lobule VIIb during the late encoding phase of a phonological storage task (Macher et al., 2014). Additionally, cathodal stimulation has not modulated cortical activation patterns, though led to disinhibition of the dentate nucleus (Küper et al., 2019), in line with past optogenetic work (Galea et al., 2009; Grimaldi et al., 2016).

Taken together, there is a growing literature implicating the cerebellum in broader cortical processing. Further, we see that cerebellar tDCS is able to modulate cerebellar output, ultimately affecting behavioral performance. However, the results are often mixed but the imaging work

needed to accurately interpret the behavioral results is limited. Therefore, we are interested in understanding how the cerebellum might interact with the cortex to support cortical processing, as such we combined cerebellar tDCS and fMRI to understand this cerebello-cortical interaction. In the current study, participants were placed in one of three stimulation conditions (anodal, cathodal, or sham) and completed both motor (sequence learning) and non-motor (Sternberg) tasks to better understand how the cerebellum is recruited during performance and how this impacts cortical processing. Stimulation was applied to the right cerebellum. We predict increased cortical activation following cathodal stimulation to the right cerebellum and decreased activation following anodal stimulation following both the Sequence learning and Sternberg task.

## Methods

### Participants

Seventy-five healthy, young adults participated in this study and were provided monetary compensation for their time. Exclusion criteria included left handedness, history of neurological or mood disorders, skin conditions, and history of concussion. Data was not collected for one participant because the participant did not wish to complete the experiment after providing consent. For the Sternberg data, an additional two participants were not analyzed because task accuracy was below 20% (n=1) and a computer error interrupted data recording (n=1). Three participants were excluded from the sequence learning analysis due to computer errors (n=2) and excessive movement (n=1). Thus, seventy-four right-handed participants (38 female) ages 18 to 30 (*M*= 22.03 years, *SD*= 3.44) were included in the analyses. Participants were randomly assigned to either the anodal (sequence n=25; Sternberg n=23), cathodal (sequence n=24; Sternberg n=25), or sham (sequence n=22; Sternberg n=24) stimulation condition. All procedures completed by

participants were approved by the Texas A&M University Institutional Review Board and conducted according to the principles expressed in the Declaration of Helsinki.

**Procedure**

The entire experiment took approximately two hours to complete. Stimulation was completed and behavioral data were collected within 80 minutes. Following the completion of the consent form, participants completed a basic demographic survey, followed by tDCS (see below for details). Participants were blind to the stimulation types. Following stimulation, participants completed a computerized Sternberg (Sternberg, 1966) and sequence learning (Kwak et al., 2012) task in the MRI environment while brain imaging data were collected. Tasks were administered in a pre-determined random order (for more details, see below).

**tDCS Stimulation Parameters**

Participants were randomly assigned to receive either cathodal, anodal, or sham stimulation using a Soterix 1x1 tES system. Each electrode was placed in a saline soaked sponge (6 mL per side), with the stimulation electrode placed two cm below and four cm lateral of the inion over the right cerebellum, and the return electrode placed on the right deltoid (Ferrucci, Cortese, & Priori, 2015).

To ensure proper connection with the scalp, an initial 1.0 mA current was set for 30 seconds. If contact quality was below 40%, adjustments, such as moving hair to increase the electrode's contact with the scalp, were made and contact quality was rechecked. Following a successful re-check, participants completed a 20-minute stimulation session at 2 mA (Ferrucci et al., 2015; Grimaldi et al., 2014, 2016). During the stimulation conditions, maximum stimulation intensity was reached in 30 seconds and maintained for 20 minutes, and then would return to 0 mA. During sham conditions, maximum stimulation intensity would be reached, but would then

immediately return to 0 mA. There was no additional stimulation during the 20-minute session. Stimulation was followed by the completion of the behavioral tasks in the scanner.

**Behavioral Tasks**

In total, task administration started about 20 minutes after stimulation and the tasks took approximately 35 minutes to complete. This is within the 90 minute window in which stimulation is thought to be effective (Nitsche & Paulus, 2001). However, task order was counterbalanced across participants to mitigate the impact of time after stimulation on task performance.

*Sequence Learning*. The sequence task (Kwak et al., 2012) was administered via computer using PsychoPy (Peirce et al., 2019; Peirce, 2007). Participants were shown four empty rectangles and instructed to indicate the location of the rectangle that was filled as quickly as possible via button press. Though the stimuli were presented for 200ms, the participant had 800ms to respond before the next stimulus appeared. Random blocks (R) had 18 trials and sequence (S) blocks had 36 trials. During sequence trials, participants had to learn a six-element sequence (1-3-2-3-4-2), which was repeated six times within a block. The order of the task was as follows: R-S-S-S-R-R-S-S-S-R-R-S-S-S-R. For the purposes of analysis here, the first three sequence blocks were considered early learning, the central sequence blocks were middle learning, and the last sequence blocks were considered late learning. Dependent variables used to estimate learning were mean reaction time for correct trials and average total accuracy.

*Sternberg*. The Sternberg Task (Sternberg, 1966) was administered via computer using PsychoPy v3.1.2 (Peirce et al., 2019; Peirce, 2007). At the beginning of a trial, participants were given six seconds to remember a string of either one, five or seven capitalized letters, which represent low, medium, and high load, respectively. Following the presentation of the study letters, participants were shown individual lower-case letters and told to indicate whether the letter was

one of the study letters shown at the beginning of the trial, via button press. Each letter was displayed for 1200ms, separated by a fixation cross that lasted 800ms. Each participant completed three runs of this task. Within each run, a participant completed three blocks of 25 trials each, for a total of 225 trials. Dependent variables were average reaction time for correct trials and accuracy.

**Behavioral Data Analysis**

Statistical analyses were conducted in R (Team, 2018), using the *lme4* (Bates et al., 2015) package, and p-value estimates were determined using the *lmerTest* package (Kuznetsova et al., 2017). A $p<.05$ threshold was used as the cut-off for significance. When necessary, the *emmeans* package (Lenth et al., 2018) was used to follow-up on significant effects. These comparisons of estimated marginal means used Bonferroni-corrected *p*-values.

Task data was analyzed using liner mixed effects models using restricted maximum likelihood, as it produces unbiased estimates of variance and covariance parameters, and is ideal for mixed effect models with small samples. Learning phase (early, middle, late) was included as a fixed factor for the sequence task, with all random trials included for comparison. Load (low, medium, and high) was included as a fixed factor for the Sternberg task. Stimulation type (cathodal, anodal, or sham stimulation) was included as a fixed effect and subject was included as a random effect for both tasks. A model was completed for both reaction time for correct trials and accuracy across both tasks.

**fMRI Procedures**

*Data Acquisition.* fMRI data was collected at the Texas A&M Translational Imaging Center with a 3-T Siemens Magnetom Verio scanner using a 32-channel head coil. Three scans with alternate phase encoding directions were used to collect blood oxygen level dependent (BOLD) whole brain scans with a multiband factor of 4 (number of volumes = 134, repetition time

[TR] = 2000 ms, echo time [TE] = 27 ms; flip angle [FA] = 52°, 3.0 × 3.0 × 3.0 mm3 voxels; 56 slices, interleaved, slice thickness=3.00mm, field of view (FOV) = 300 × 300 mm; time = 4:40 min). An additional high resolution T1 weighted whole brain anatomical scan was taken (sagittal; GRAPPA with acceleration factor of 2; TR = 2400 ms; TE = 2.07 ms; 0.8 x 0.8 x 0.8 mm3 voxels; 208 slices, interleaved, slice thickness= 0.8; FOV = 256 × 256 mm; FA = 8°; time = 7:02 min) for data normalization.

*fMRI data pre-processing and analysis.* Images were converted from DICOM format to NIFTI files and organized into a Brain Imaging Data Structure (BIDS) using bidskit (v 2019.8.16; Mike Tyszak, 2016). Functional images were encoded using opposite phase encoding directions. For distortion correction, single 4D images were taken for each participant from each phase encoding direction and were merged. Then fieldmap images were created using FSL's topup to unwrap images (Andersson et al., 2003).

FMRI data were processed using FEAT (FMRI Expert Analysis Tool) Version 6.00, part of FSL (FMRIB's Software Library, www.fmrib.ox.ac.uk/fsl). Registration to high resolution structural and/or standard space images was carried out using FLIRT (Jenkinson et al., 2002; Jenkinson & Smith, 2001). Registration from high resolution structural to standard space was then further refined using FNIRT nonlinear registration (Andersson, Jenkinson, & Smith, 2007; Andersson, Jenkinson, & Smith, 2007). The following pre-statistics processing was applied: motion correction using MCFLIRT (Jenkinson et al., 2002); slice-timing correction using Fourier-space time-series phase-shifting; non-brain removal using BET (Smith, 2002); spatial smoothing using a Gaussian kernel of FWHM 5mm; grand-mean intensity normalization of the entire 4D dataset by a single multiplicative factor. ICA was carried out using MELODIC (Beckmann & Smith, 2004), to investigate the possible presence of unexpected artifacts or activation. Time-series

statistical analysis was carried out using FILM with local autocorrelation correction (Woolrich et al., 2001). Subject level variables were modeled using fix effects and group level comparisons were modeled using FLAME 1 & 2 mixed effects. The subject level contrast collapsed across stimulation condition and contrasted activation conditions between sequence learning phases types (early, middle and late) and working memory loads (low, medium, high). Group level analyses (cathodal, anodal, sham) were thresholded non-parametrically using clusters determined by $z>3.1$ and a (corrected) cluster significance threshold of $p=0.05$ (Worsley, 2001).

*ROI Analysis.* Region of interest (ROI) analyses were also conducted to determine if stimulation affected signal in specific ROIs. Here, we used masks (Figure 2.1) that covered bilateral parietal cortices, bilateral frontal cortices, and bilateral crus I using masks from an existing repository of functional ROIs (Shirer et al., 2012). These masks were fed into FSL's Featquery, which calculated percent signal change for each subject for both the sequence learning and Sternberg task. ANOVAs were conducted to determine if there were significant differences in mean percent signal change in an ROI within each stimulation condition (cathodal, anodal, sham). Mean percent signal change was assessed for each individual (i.e. left crus I) and combined (i.e. left and right frontal lobe) ROI, in order to look at signal change within hemispheres (i.e. left crus I) and possible interactions between hemispheres (i.e. left and right frontal lobe). Pearson correlations were also run for each ROI within each stimulation condition to see if performance was related to signal change. These comparisons were corrected using Bonferroni-corrected *p*-values.

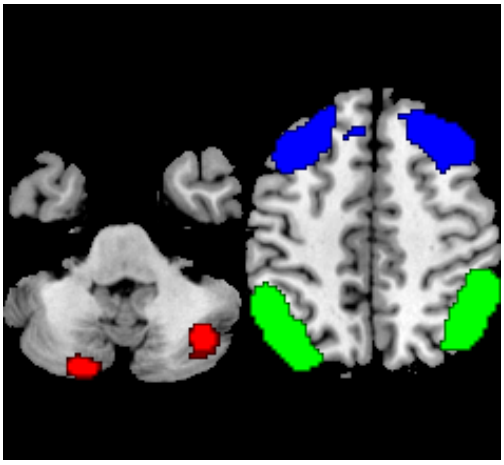

**Figure 2.1 Regions of interest used to examine percent signal change (Shirer et al., 2012). Red= Crus I; Blue=Frontal Gyrus; Green=Parietal Gyrus.**

## Results

### Sternberg Task

**Table 2.1 Mean RT and accuracy for the Sternberg task by Load, Region, and Stimulation Condition.**

| | | Reaction Time (ms) | | Accuracy | |
|---|---|---|---|---|---|
| Load | Stimulation | Mean | SD | Mean | SD |
| Low | Anodal | 500.97 | 131.49 | 0.97 | 0.18 |
| Low | Cathodal | 506.79 | 121.54 | 0.98 | 0.15 |
| Low | Sham | 541.77 | 127.06 | 0.99 | 0.11 |
| Medium | Anodal | 652.43 | 197.95 | 0.93 | 0.26 |
| Medium | Cathodal | 649.92 | 198.77 | 0.92 | 0.27 |
| Medium | Sham | 676.84 | 195.10 | 0.91 | 0.28 |
| High | Anodal | 667.76 | 247.57 | 0.85 | 0.36 |
| High | Cathodal | 666.20 | 246.53 | 0.85 | 0.36 |
| High | Sham | 686.15 | 262.03 | 0.84 | 0.36 |

Participants were randomly assigned to either the anodal (n=23), cathodal (n=25), or sham (n=24) condition. Mean reaction times and accuracy on the Sternberg task can be found in Table 2.1 and are depicted visually in Figure 2.2. When examining the fixed effects of reaction time, there was a significant effect of load [($F(2, 9800) = 665.74$, $p < .001$)], such that reaction times for each load condition were significantly different from each other ($ps < .001$). This demonstrates the

increase in difficulty associated with increased load. We also found a significant effect of stimulation [($F(2, 68.9) = 4.20$, $p = .011$)], such that reaction times following anodal ($p = .038$) and cathodal ($p = 0.035$) stimulation were both significantly quicker relative to sham. We did not find a stimulation by load interaction [($F(4, 9800) = 1.05$, $p = .380$)]. Taken together, both anodal and cathodal stimulation improved reaction time.

With respect to accuracy, we only found an effect of load [($F(2, 10{,}290) = 194.93$, $p < .001$)], such that accuracy was best on low ($p < 0.001$) load, then medium load ($p < .001$), and then high load ($p < .001$). We did not find an effect of stimulation [($F(2, 69) = 0.026$, $p = .974$)], or a load by stimulation interaction [($F(4, 10{,}290) = 1.29$, $p = .271$)].

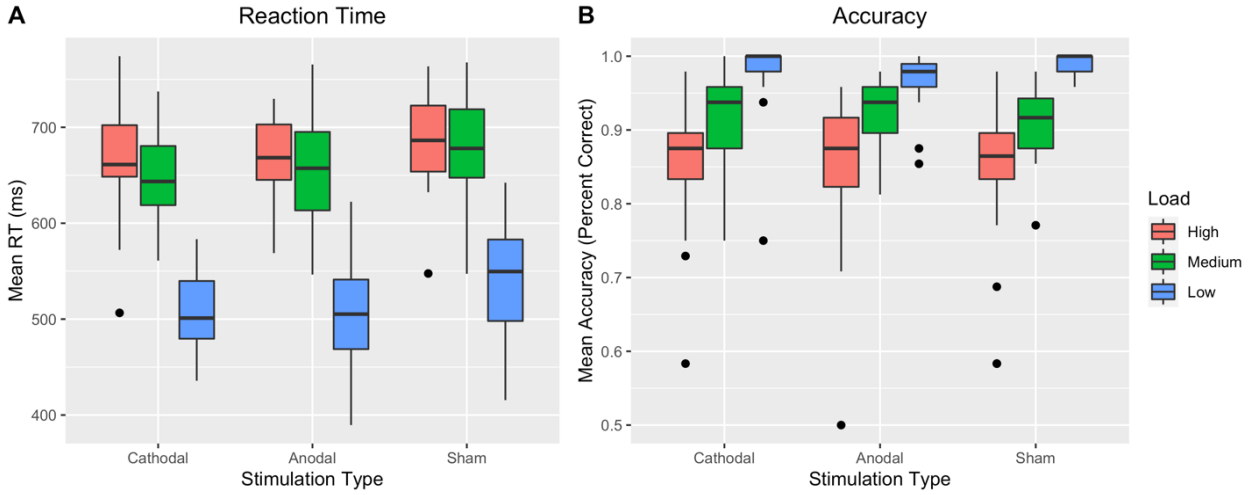


**Figure 2.2 Mean RT and accuracy for the Sternberg task by Load and Stimulation Condition. Dots indicate outliers. Whiskers represent the interquartile range. Both anodal and cathodal stimulation improved reaction time.**

One issue that might affect behavior outcomes is task order and stimulation decay. Even though task order was counterbalanced to mitigate any effect of stimulation decay, it is still possible to that the effect of stimulation was no longer present during the task completed second. Below we included task order in our behavioral analysis to investigate whether performance differenced depending on task order.

In addition to the effects on reaction time we already describe, we do not find any additional effects of order for reaction time (Figure 2.3; *ps*>.090).

In addition to the effects on accuracy we already describe, we found a three-way interaction between stimulation, load and order for accuracy (Figure 2.3; p> .001). Specifically, accuracy was better following cathodal stimulation during high load trials, when Sternberg was completed second (*p*=.023). Also, accuracy was better following sham stimulation during high load, if Sternberg was completed first (*p*=.0167). No other effects were significant (*ps*> .214). We did not find an effect of order (*p*=.781), or stimulation by order (*p*=.241), or load by order (*p*=.474) interactions.

Together, we do not see a decline in performance when a task is completed second, broadly indicating that there was no decay in stimulation during task completion. Indeed, stimulation duration does modulate the time needed for cortical activation to return to baseline (Nitsche & Paulus, 2001). Specifically, 9 minutes of stimulation resulted in 30 minutes of effect and 13 minutes resulted in over 90 minutes of effect. Therefore, 20 minutes of stimulation should ensure the effect of stimulation was present for the duration of the scanning session, which was completed well within 90 minutes of stimulation. It should be worth noting that we might be experiencing an effect of comfort. That is, as participants get more familiar with responding to stimuli in a scanner, their performance improves.

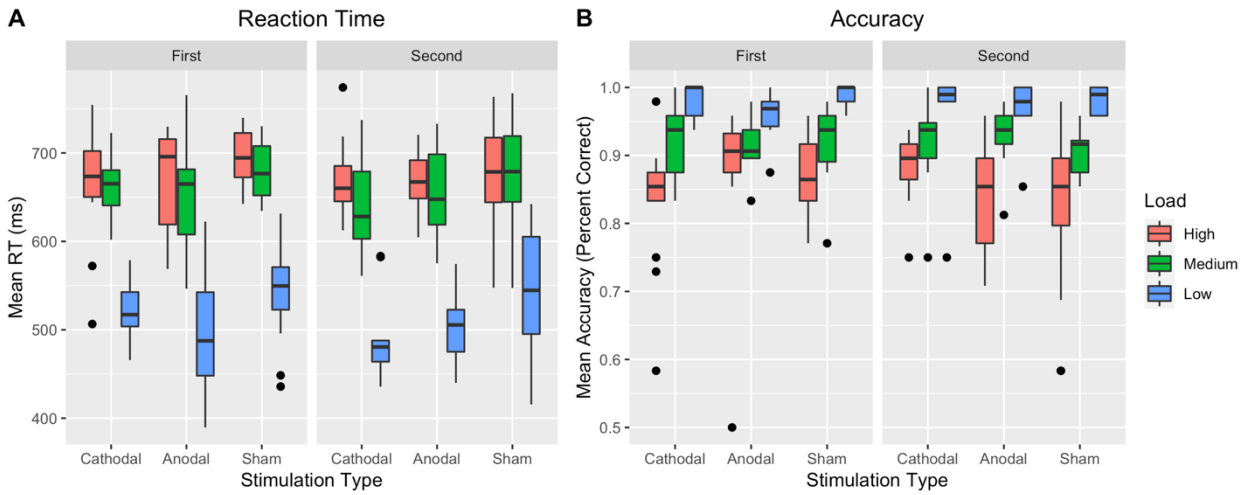


**Figure 2.3 Mean RT and accuracy for the Sternberg task by Load, Stimulation Condition and Task Order. Dots indicate outliers. Whiskers represent the interquartile range.**

We first looked at the significant activation patterns in the sham stimulation group. Activation foci are reported in Table 2.2 and depicted visually in Figure 2.4.

Under low load, we saw significant activation in the right middle occipital gyrus. Under medium load, we saw significant activations in the left inferior parietal lobe and right inferior occipital lobe. Under high load, we saw activation in the left inferior frontal gyrus, left inferior parietal lobe, left supplemental motor area, right inferior occipital lobe, right insula, and the vermis in the cerebellum.

When examining load contrasts during sham stimulation, we found frontal and parietal regions showed larger activations during high load than low load. These included the left and right inferior frontal lobe, left middle frontal gyrus, left and right inferior parietal lobe, and the left supplemental motor area. Additionally, subcortical regions such as the thalamus and right crus I in the cerebellum also showed greater activity when contrasting the high load relative to low load conditions. Finally, there was greater activation in the right inferior frontal and left inferior parietal lobes under high load, compared to medium load. There were no significant activations when comparing medium against low load. Together, we found the expected load effects (Sternberg,

1966) and activation in the frontal and parietal regions one would expect when completing a verbal working memory task (Emch et al., 2019).

**Table 2.2 Significant clusters following sham stimulation during a Sternberg task.**

| Load | Region | Voxels | MNI Coordinates | | | Z |
|---|---|---|---|---|---|---|
| | | | x | y | z | |
| Low | Right Middle occipital gyrus | 445 | 34 | -88 | 4 | 5.27 |
| Medium | Right Inferior occipital gyrus | 497 | 38 | -86 | -4 | 6.28 |
| | Left Inferior parietal, but supramarginal and angular gyri | 109 | -40 | -46 | 44 | 5.67 |
| High | Left Inferior frontal gyrus, opercular part | 448 | -44 | 10 | 22 | 5.26 |
| | Left Inferior parietal, but supramarginal and angular gyri | 305 | -40 | -44 | 42 | 5.83 |
| | Left Supplementary motor area | 247 | -4 | 6 | 56 | 5.67 |
| | Right Insula | 170 | 42 | 16 | -8 | 5.6 |
| | Right Inferior occipital gyrus | 123 | 36 | -86 | 0 | 5.29 |
| | Vermis VIII, cerebellum | 107 | -2 | -64 | -36 | 5.35 |
| High > Low | Left Inferior frontal gyrus, triangular part | 849 | -46 | 22 | 30 | 7.18 |
| | Right Inferior frontal gyrus, triangular part | 678 | 46 | 30 | 32 | 8.26 |
| | Left Supplementary motor area | 504 | -2 | 20 | 52 | 6.07 |
| | Left Inferior parietal, but supramarginal and angular gyri | 332 | -34 | -60 | 46 | 6.58 |
| | Right Insula | 267 | 32 | 24 | -2 | 6.14 |
| | Left Middle frontal gyrus | 194 | -30 | 54 | 12 | 6.5 |
| | Right Inferior parietal, but supramarginal and angular gyri | 159 | 44 | -44 | 42 | 6.2 |
| | Left Thalamus | 144 | -4 | -24 | 8 | 5.08 |
| | Right Thalamus | 121 | 8 | -10 | 10 | 5.33 |
| | Right Crus I, cerebellum | 106 | 10 | -72 | -26 | 6.07 |
| High > Medium | Right Inferior frontal gyrus, opercular part | 211 | 38 | 14 | 10 | 5.58 |
| | Left Inferior parietal, but supramarginal and angular gyri | 118 | -36 | -42 | 34 | 5.58 |

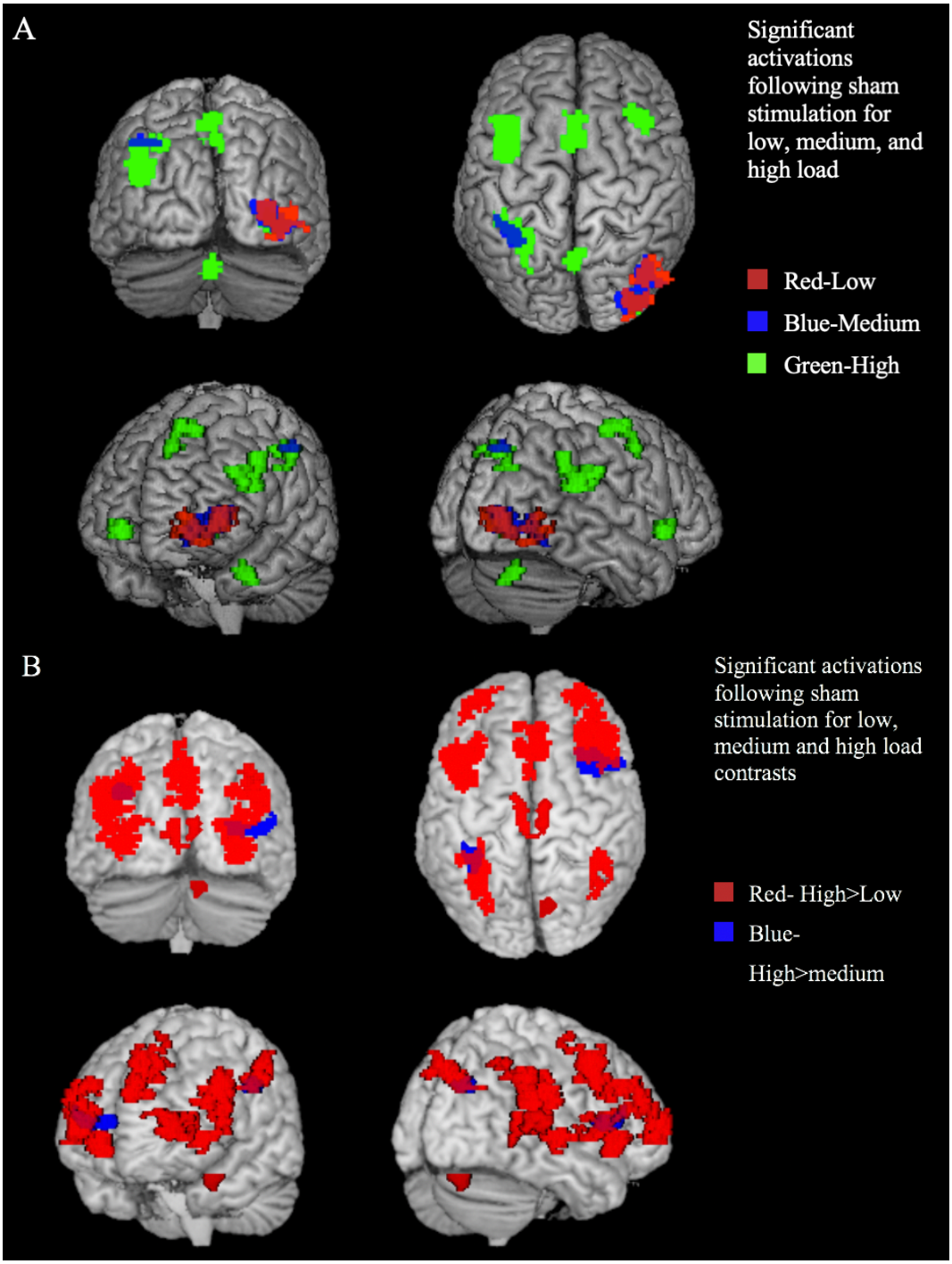


**Figure 2.4 Significant activations in the sham stimulation group during a Sternberg task. (A) Significant activations following sham stimulation for low, medium and high load; Red=Low Load; Blue=Medium Load; Green=High Load; (B) Significant activations following sham stimulation for low, medium and high load contrasts; Red=greater activation following high load compared to low load; Blue= greater activation during high load compared to medium load.**

We next looked at the effect of active stimulation on load in the cathodal and anodal stimulation groups. Activation foci are reported in Table 2.3 and depicted visually in Figure 2.5.

*Low*. In the cathodal stimulation group, there was significant activation in the right middle temporal gyrus and left supplemental motor area during the low load condition. Further, activation was significantly greater in the right putamen, right inferior parietal lobe, and the left paracentral lobule when the cathodal group was compared to the anodal stimulation group. There were no significant activations following anodal stimulation during the low load condition.

*Medium*. There were no significant activations following anodal or cathodal stimulation.

*High*. Cathodal stimulation resulted in a number of activations in cortical and subcortical regions such as the right medial superior frontal gyrus, the right middle frontal gyrus, right middle cingulum and lobule VIIb in the cerebellum. Additional activations were found in the right angular gyrus, right inferior parietal regions, right insula, right inferior temporal, and left superior temporal poles. Anodal stimulation resulted only in activation in the left inferior frontal lobe. Further activations following cathodal stimulation were greater in the right inferior, middle and superior temporal lobes, right inferior parietal lobe, and lobule VIII in the cerebellum compared to anodal stimulation.

Taken together, stimulation, particularly cathodal stimulation, increased activations in key memory and language centers in the brain. This further provides evidence that cathodal cerebellar stimulation results in increased cerebellar output to non-motor regions during verbal working memory tasks (Grimaldi et al., 2016).

**Table 2.3 Significant clusters following stimulation during a Sternberg task.**

| Load | Stimulation | Region | Voxels | MNI Coordinates | | | Z |
|---|---|---|---|---|---|---|---|
| | | | | x | y | z | |
| Low | Cathodal | Right Middle temporal gyrus | 215 | 42 | -72 | 0 | 5.16 |
| | | Left Supplementary motor area | 108 | -4 | -16 | 58 | 4.76 |
| | Cathodal > Anodal | Right Lenticular nucleus, putamen | 287 | 30 | -14 | 4 | 4.74 |
| | | Right Inferior parietal, but supramarginal and angular gyri | 266 | 40 | -36 | 54 | 4.82 |
| | | Left Paracentral lobule | 174 | 0 | -24 | 54 | 4.92 |
| High | Cathodal | Right Superior frontal gyrus, medial | 472 | 6 | 34 | 42 | 5.32 |
| | | Right Angular gyrus | 280 | 36 | -54 | 38 | 5.15 |
| | | Right Insula | 258 | 36 | 22 | -6 | 6.07 |
| | | Right Middle frontal gyrus | 232 | 38 | 42 | 8 | 5.05 |
| | | Right Lobule VIIb, cerebellum | 221 | 6 | -76 | -44 | 5.04 |
| | | Right Inferior parietal, but supramarginal and angular gyri | 164 | 48 | -46 | 56 | 5.45 |
| | | Right Inferior temporal gyrus | 147 | 48 | -62 | -12 | 5.72 |
| | | Left Temporal pole: superior temporal gyrus | 120 | -48 | 16 | -10 | 5.03 |
| | | Right Median cingulate and paracingulate gyri | 115 | -2 | -6 | 30 | 4.97 |
| | Anodal | Left Inferior frontal gyrus, triangular part | 128 | -46 | 30 | 28 | 4.73 |
| | Cathodal > Anodal | Left Lobule VIII, cerebellum | 260 | -12 | -66 | -36 | 4.64 |
| | | Right Superior temporal gyrus | 159 | 52 | -16 | 2 | 4.73 |
| | | Right Inferior parietal, but supramarginal and angular gyri | 147 | 52 | -52 | 40 | 4.54 |
| | | Right Middle temporal gyrus | 139 | 54 | -42 | 8 | 4.73 |
| | | Right Inferior temporal gyrus | 116 | 50 | -56 | -10 | 5.53 |

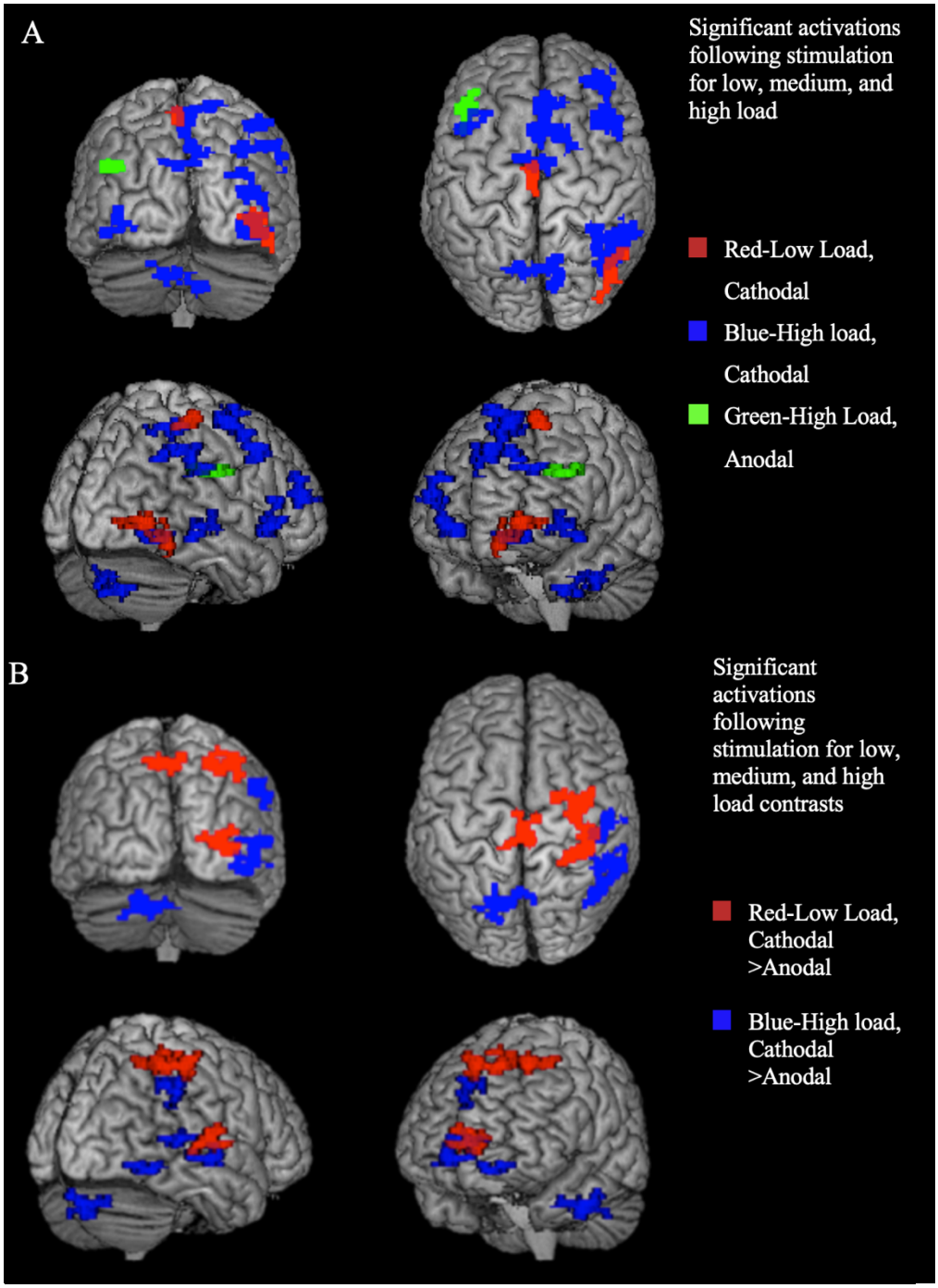


**Figure 2.5 Significant activations following stimulation during a Sternberg task. (A) Significant activations following stimulation for low, medium and high load; Red=Low Load following cathodal stimulation; Blue=High load following cathodal stimulation; Green=High Load following anodal stimulation. (B) Significant contrasts following stimulation for low, medium, and high load contrasts; Red=activations greater following cathodal stimulation compared to anodal stimulation during low load trials; Blue=**

**activations greater following cathodal stimulation compared to anodal stimulation during high load trials.**

We next looked at the effect of stimulation on load contrasts. Activations are reported in Table 2.4 and depicted visually in Figure 2.6.

*High > Low*. Cathodal stimulation resulted in increased activation during high load in left inferior and right superior frontal regions, left precentral gyrus, left thalamus, and right insula. Anodal stimulation resulted in greater activations to the right angular gyrus. Additionally, there were greater activations in the left superior, left and right inferior, and right middle frontal lobes during high load relative to low in the anodal stimulation group.

*High > Medium*. Cathodal stimulation resulted in greater activation in frontal, occipital, and parietal regions such as the left superior frontal lobe, left middle occipital lobe, supramarginal gyrus, left angular, and left precentral lobe during high load compared to medium load. Additionally, greater activation was also seen in the right crus I in the cerebellum. Following anodal stimulation, there was greater activation in frontal regions such as the right inferior frontal lobe, and the left superior frontal lobe during the high load condition as compared to medium.

*Medium > Low*. Here, anodal stimulation resulted in greater activation in the left insula under medium load compared to low load. There were no significant activation differences following cathodal stimulation.

Together, these results show that frontal and parietal activations were greater when processing was high, and in the anodal stimulation group, we saw bilateral activation of the frontal lobes, consistent with our scaffolding hypothesis wherein additional resources may be needed to make up for the down regulation of the cerebellum with anodal tDCS (Bernard et al., 2013; Filip et al., 2019).

**Table 2.4 Significant contrast clusters following stimulation during a Sternberg task.**

| Load | Stimulation | Region | Voxels | MNI Coordinates | | | Z |
|---|---|---|---|---|---|---|---|
| | | | | x | y | z | |
| High > Low | Cathodal | Left Thalamus | 420 | -4 | -20 | 12 | 6.98 |
| | | Right Superior frontal gyrus, medial | 339 | 6 | 34 | 46 | 5.9 |
| | | Right Insula | 289 | 38 | 22 | -2 | 6.71 |
| | | Left Precental gyrus | 258 | -38 | 6 | 50 | 6.19 |
| | | Left Inferior frontal gyrus, orbital part | 170 | -38 | 24 | -2 | 6.88 |
| | Anodal | Left Superior frontal gyrus, dorsolateral | 2300 | -18 | 62 | 14 | 7.37 |
| | | Left Superior frontal gyrus, medial | 313 | -2 | 28 | 46 | 6.05 |
| | | Right Middle frontal gyrus | 266 | 38 | 18 | 40 | 5.19 |
| | | Right Angular gyrus | 204 | 34 | -70 | 50 | 7.87 |
| | | Right Inferior frontal gyrus, triangular part | 198 | 48 | 22 | 4 | 5.73 |
| | | Right Inferior frontal gyrus, orbital part | 111 | 38 | 44 | -4 | 5.65 |
| High > Medium | Cathodal | Left Superior frontal gyrus, medial | 380 | 2 | 42 | 44 | 6.5 |
| | | Right Crus I, cerebellum | 337 | 32 | -66 | -36 | 5.49 |
| | | Left Middle occipital gyrus | 144 | -42 | -76 | 40 | 4.75 |
| | | Right Supramarginal gyrus | 135 | 60 | -40 | 34 | 5.34 |
| | | Left Angular gyrus | 111 | -44 | -56 | 30 | 4.89 |
| | | Left Precental gyrus | 106 | -40 | 6 | 42 | 5.68 |
| | Anodal | Right Inferior frontal gyrus, opercular part | 148 | 44 | 8 | 22 | 5.92 |
| | | Left Superior frontal gyrus, medial | 134 | -10 | 26 | 42 | 4.95 |
| | | Left Superior frontal gyrus, medial | 133 | -4 | 56 | 28 | 5.85 |
| | | Right Insula | 108 | 32 | 18 | 0 | 4.28 |
| Medium > Low | Anodal | Left Insula | 102 | -36 | 20 | -2 | 5.05 |

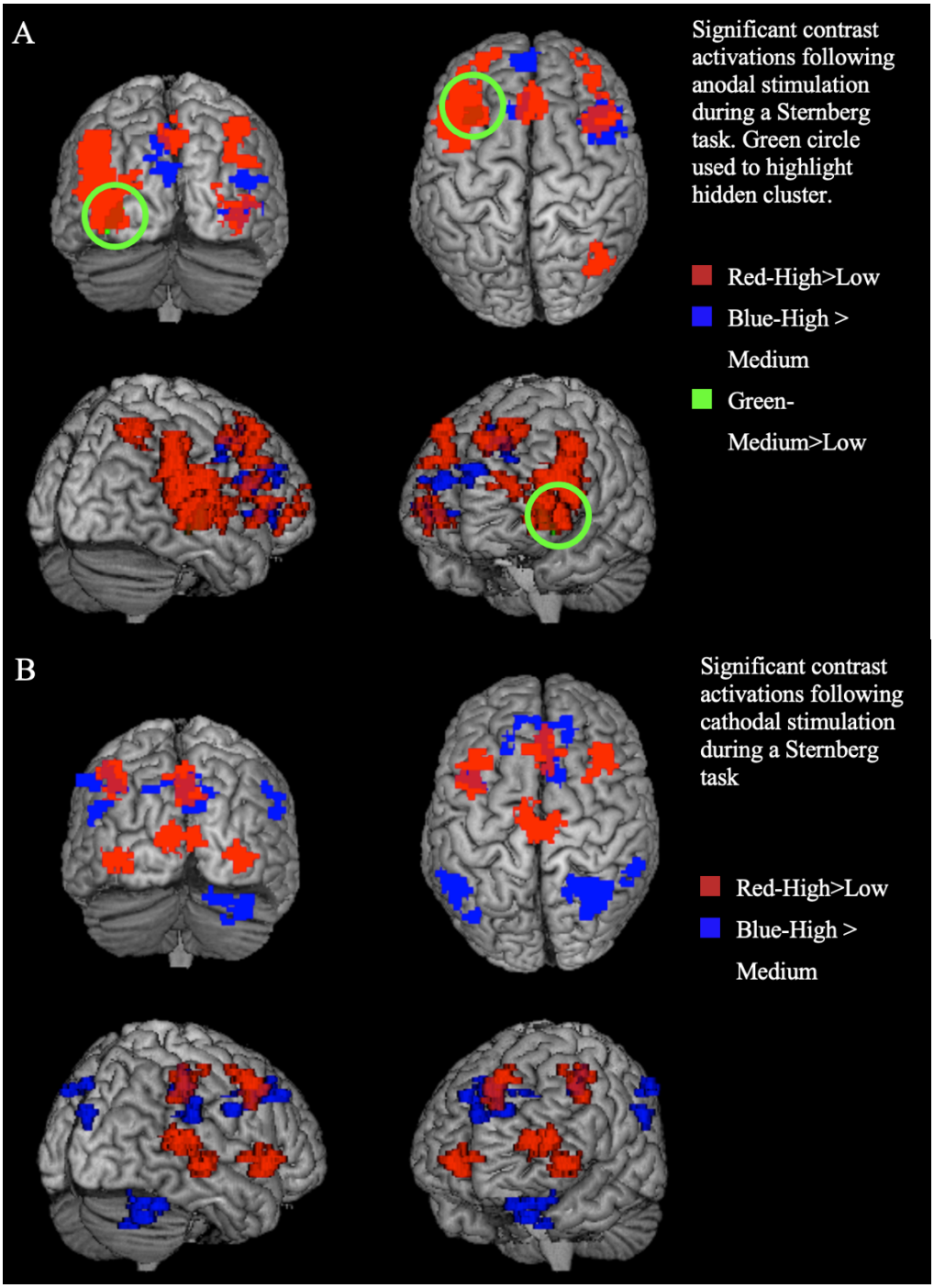


**Figure 2.6 Significant contrast activations following stimulation during a Sternberg task. (A) Significant contrast activations following anodal stimulation during a Sternberg task; Red = high > low load following anodal stimulation; Blue= high > medium load following anodal stimulation; Green = medium > low load following anodal stimulation. (B) Significant contrast activations following cathodal stimulation during a Sternberg task; Red=high > low load following cathodal stimulation; Blue= high > medium load following cathodal stimulation.**

**Sequence Learning**

**Table 2.5 Mean RT and accuracy for the sequence learning task by Phase, Region, and Stimulation Condition.**

| | | Accuracy | | Reaction Time (ms) | |
|---|---|---|---|---|---|
| **Phase** | **Stimulation** | **Mean** | **SD** | **Mean** | **SD** |
| Early | Anodal | 0.96 | 0.20 | 350.74 | 132.50 |
| Early | Cathodal | 0.97 | 0.18 | 336.04 | 117.12 |
| Early | Sham | 0.96 | 0.18 | 359.10 | 126.63 |
| Late | Anodal | 0.95 | 0.23 | 293.23 | 135.62 |
| Late | Cathodal | 0.98 | 0.15 | 285.94 | 120.03 |
| Late | Sham | 0.97 | 0.17 | 311.98 | 131.05 |
| Middle | Anodal | 0.97 | 0.17 | 315.96 | 131.02 |
| Middle | Cathodal | 0.97 | 0.18 | 298.33 | 114.57 |
| Middle | Sham | 0.98 | 0.15 | 330.50 | 133.81 |
| Random | Anodal | 0.94 | 0.23 | 407.36 | 104.51 |
| Random | Cathodal | 0.95 | 0.22 | 409.86 | 103.70 |
| Random | Sham | 0.96 | 0.21 | 422.30 | 111.79 |

Participants were randomly assigned to either the anodal (n=25), cathodal (n=24), or sham (n=22) condition. Mean reaction times (RT) and accuracy for the sequence learning task can be found in Table 2.5 and depicted visually in Figure 2.7. First, we found a significant phase by stimulation interaction [($F$(6, 28,332) = 4.96, $p$ < .001)], such that the magnitude in change in RT is significantly greater following cathodal stimulation between middle learning and random button presses, compared to anodal and sham. Additionally we found a significant effect of learning phase [($F$(3, 28,332) = 1,796.79, $p$ < .001)], such that reaction times for early, middle, late, and random learning trials were all significantly different from one another ($p$s < .001). There was no effect of stimulation [($F$(2, 68) = 0.693, $p$ = .504)].

When looking at accuracy, we found a phase by stimulation interaction [($F$(6, 30,592) = 3.74, $p$ = .001)], such that accuracy was lower during late learning following anodal stimulation, compared to sham ($p$ =.020) and cathodal ($p$ < .002) stimulation. There was no main

effect of stimulation on accuracy [($F(3, 68) = 1.54$, $p = .223$)], though we did find an effect of phase [($F(3, 30{,}592) = 16.15$, $p < .001$)], such that accuracy was worse for early learning, followed by late learning, and lastly middle learning. Taken together, RT was improved following cathodal stimulation during middle learning and accuracy was negatively impacted following anodal stimulation during later learning phases.

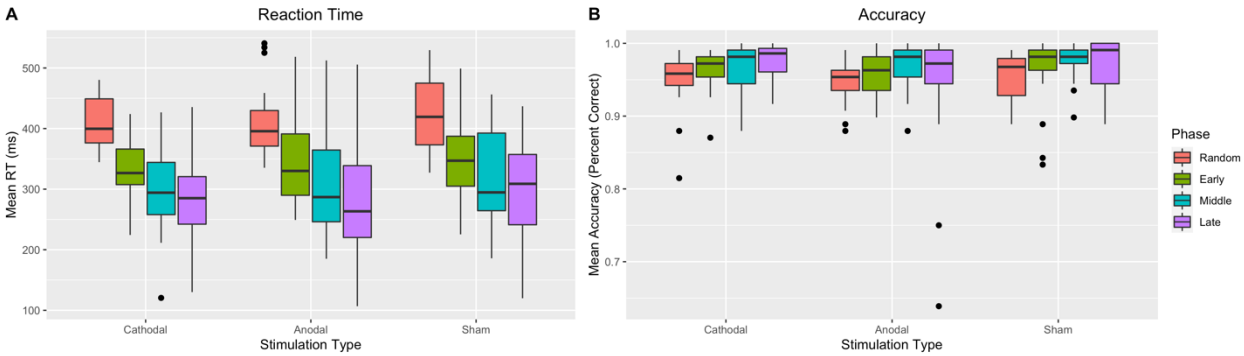


**Figure 2.7 Mean RT and accuracy for the sequence learning task by Phase and Stimulation Condition. Dots indicate outliers. Whiskers represent the interquartile range. Accuracy was negatively impacted following anodal stimulation during later learning phases.**

In addition to the effects on reaction time we already describe, we found a marginal effect of order (Figure 2.8; $p = .052$), such that RT was faster when sequence was second. We also found a three-way interaction between stimulation, phase and order for RT ($p > .001$). Specifically, RT was better following anodal stimulation during early learning trials, when sequence was completed second ($p = .040$). No other effects were significant ($p > .09$). We did not find stimulation by order ($p = .842$) or phase by order ($p = .107$) interactions.

In addition to the effects on accuracy we already describe, we found phase by order interaction (Figure 2.8; $p < .001$), such that accuracy was better for random trials when the sequence task was completed first. We also found a three-way interaction between stimulation, phase and order for accuracy ($p = .042$). Specifically, accuracy was better following sham stimulation during early learning trials, when sequence was completed second ($p = .033$). No other

effects were significant (*ps* > .09). We did not find an effect of order (*p*=.393), or a stimulation by order (*p*=.747) interaction.

Similar to Sternberg, order effects indicate that completing a task second was of benefit. Again, perhaps indicating that participants were more familiar with how to respond to stimuli in the scanner.

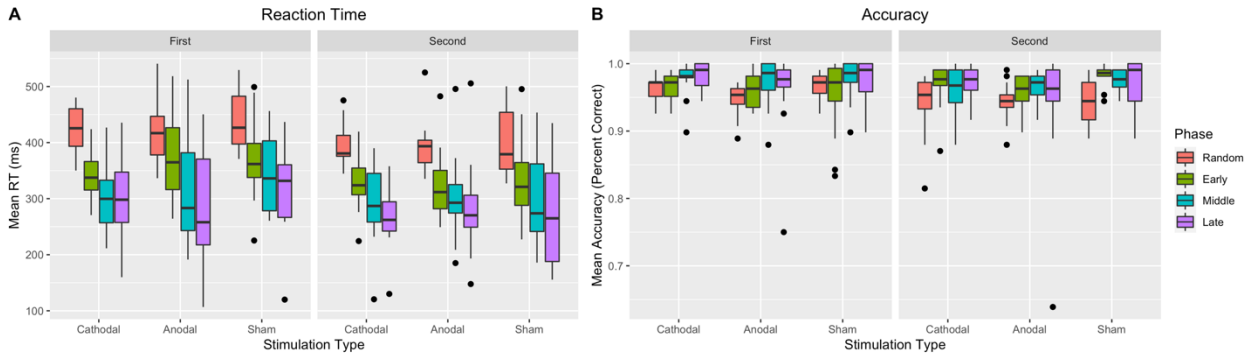


**Figure 2.8 Mean RT and accuracy for the sequence learning task by Phase, Stimulation Condition, and Task Order. Dots indicate outliers. Whiskers represent the interquartile range.**

We first looked at the activation patterns in the sham stimulation group. Activation foci are reported in Table 2.6 and depicted visually in Figure 2.9.

During random trials, activations were present in the left putamen, left supplemental motor area, left and right inferior frontal gyrus, left middle cingulum, left superior and right middle temporal gyrus, left calcarine, right Heschl gyrus and right thalamus. During sequence learning common motor network regions, such as the left postcentral gyrus, left supplemental motor area, right paracentral lobule, and right precentral gyrus were active during task performance. Additionally, left caudate, right putamen, left posterior cingulum, left Heschl gyrus, right insula, and right cuneus were also active during sequence learning. Additionally, activations were greater activation in the left supplementary motor area, left precentral gyrus, left lingual gyrus, and the left inferior occipital gyrus during sequence trials, compared to random button press trials.

When examining sequence learning during the early learning phase, activation was found in the left lingual gyrus and right calcarine fissure. During middle sequence learning the sham group showed activations in the left calcarine fissure, left supplemental motor area, right middle cingulum gyrus, right superior occipital lobe, left superior and right middle frontal cortex, the left and right fusiform gyrus, left middle and right superior occipital lobe, and the left and right precentral gyrus. During late learning activation was seen only in the left cuneus.

Together, these activation patters are consistent with canonical findings of cortical motor activation (Dhamala et al., 2003; Newton et al., 2008; Seidler et al., 2005; Wei et al., 2017), and patterns typically seen during explicit motor sequence learning (Aizenstein et al., 2004; Bischoff-Grethe et al., 2004).

**Table 2.6 Significant clusters associated with explicit motor sequence learning following sham stimulation.**

| Phase | Region | Voxels | MNI Coordinates | | | Z |
|---|---|---|---|---|---|---|
| | | | x | y | z | |
| Random | Left Calcarine fissure and surrounding cortex | 18101 | -10 | -66 | 16 | 8.41 |
| | Left Lenticular nucleus, putamen | 1388 | -16 | 18 | -2 | 6.72 |
| | Right Inferior frontal gyrus, triangular part | 732 | 50 | 26 | 24 | 5.93 |
| | Left Median cingulate and paracingulate gyri | 606 | -8 | 16 | 42 | 6.02 |
| | Left Inferior frontal gyrus, opercular part | 468 | -40 | 4 | 28 | 6.42 |
| | Left Superior temporal gyrus | 338 | -46 | -22 | 8 | 5.22 |
| | Right Heschl gyrus | 298 | 48 | -12 | 10 | 5.93 |
| | Right Middle temporal gyrus | 254 | 68 | -40 | 4 | 4.98 |
| | Left Supplementary motor area | 194 | -4 | -2 | 64 | 4.92 |
| | Right Middle temporal gyrus | 150 | 48 | -14 | -12 | 4.96 |
| | Right Thalamus | 147 | 10 | -16 | 12 | 4.52 |
| | Right Middle frontal gyrus | 141 | 38 | 8 | 50 | 5.01 |
| Sequence | Right Cuneus | 8722 | 14 | -68 | 22 | 7.22 |

| | | | | | | |
|---|---|---|---|---|---|---|
| | Left Supplementary motor area | 718 | -6 | 2 | 56 | 6.18 |
| | Left Postcentral gyrus | 582 | -42 | -16 | 48 | 6.01 |
| | Left Heschl gyrus | 291 | -54 | -10 | 10 | 4.9 |
| | Left Posterior cingulate gyrus | 276 | -4 | -30 | 30 | 4.78 |
| | Right Precental gyrus | 258 | 36 | -18 | 44 | 4.93 |
| | Right Lenticular nucleus, putamen | 249 | 26 | 12 | -6 | 4.97 |
| | Left Caudate nucleus | 191 | -14 | 22 | -2 | 5.19 |
| | Right Paracentral lobule | 158 | 12 | -40 | 56 | 4.69 |
| | Right Insula | 147 | 34 | 20 | 6 | 5.01 |
| Sequence> Random | Left Supplementary motor area | 196 | -6 | 2 | 56 | 6.25 |
| | Left Precental gyrus | 186 | -38 | -6 | 50 | 5.29 |
| | Left Lingual gyrus | 176 | -16 | -84 | -6 | 6.73 |
| | Left Inferior occipital gyrus | 123 | -38 | -86 | -6 | 6.01 |
| Early | Right Calcarine fissure and surrounding cortex | 781 | 8 | -72 | 20 | 6.13 |
| | Left Lingual gyrus | 251 | -14 | -76 | -6 | 5.23 |
| Middle | Left Middle occipital gyrus | 553 | -28 | -72 | 36 | 5.75 |
| | Left Precental gyrus | 512 | -42 | -2 | 54 | 5.29 |
| | Right Precental gyrus | 275 | 48 | -12 | 54 | 4.9 |
| | Right Fusiform gyrus | 235 | 30 | -58 | -4 | 5.24 |
| | Left Fusiform gyrus | 228 | -34 | -70 | -12 | 5.22 |
| | Right Superior occipital gyrus | 225 | 18 | -82 | 36 | 4.6 |
| | Right Median cingulate and paracingulate gyri | 146 | 8 | 4 | 40 | 4.99 |
| | Right Middle frontal gyrus | 139 | 34 | 6 | 52 | 4.99 |
| | Left Supplementary motor area | 129 | 0 | 10 | 54 | 4.87 |
| | Left Superior frontal gyrus, dorsolateral | 121 | -20 | 0 | 66 | 4.72 |
| | Left Calcarine fissure and surrounding cortex | 101 | -20 | -66 | 8 | 4.65 |
| Late | Left Cuneus | 3570 | -2 | -80 | 32 | 6.31 |

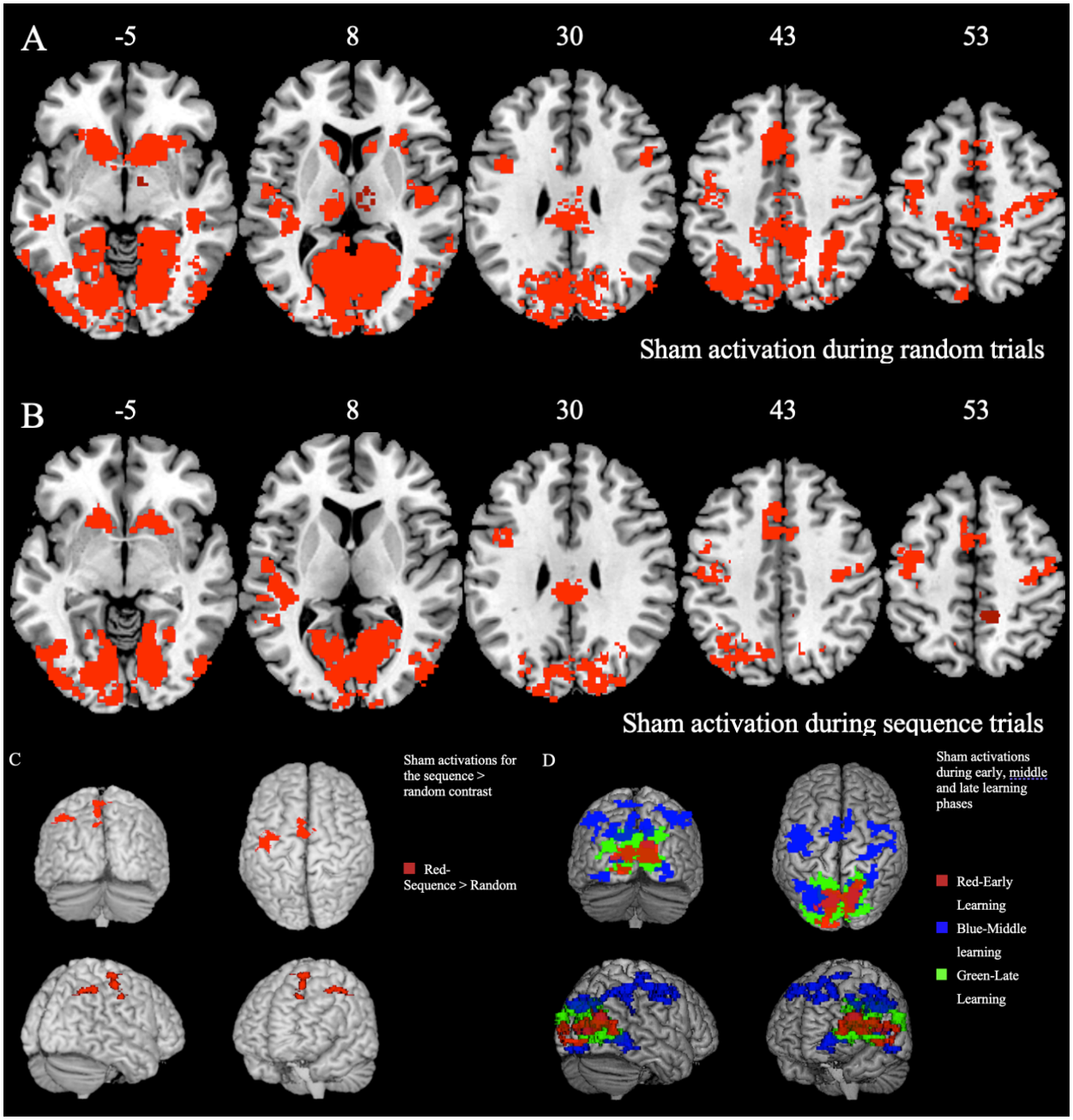


**Figure 2.9 Significant activations in the sham stimulation group during a Sequence learning task. (A) Sham activation during random trials. (B) Sham activation during sequence trials. (C) Sham activations for the sequence > random contrast; (D) Sham activations during early, middle, and late learning phases, Red=Early learning; Blue=Middle learning; Green= Late learning.**

We next looked at the significant patterns of activation following stimulation in the anodal and cathodal groups. Activation foci are reported in Table 2.7 and depicted visually in Figure 2.10.

*Random*. The anodal stimulation group had activation in right cuneus, right precuneus, right insula, left postcentral and precentral gyri, and left middle cingulum (Figure 2.10A). Cathodal stimulation resulted in activations in the right calcarine fissure, the right precuneus, the right inferior frontal lobe, the left postcentral gyrus, the right superior temporal pole, the right insula, and the right superior and left middle temporal lobe.

*Sequence*. Anodal stimulation saw activation in the left supplemental motor area, the left middle temporal lobe, and the left middle frontal lobe, the left middle cingulum, the left insula, the right precentral gyrus, right cuneus, the right and left thalamus, and the left and right putamen (Figure 2.10B). The cathodal stimulation group again showed similar activation patterns to sham, though there were activations in left middle occipital lobe and left and right middle temporal lobes. Together, we see the expected motor regions, with the inclusion of some cognitive regions (i.e. left middle frontal and temporal lobes), that would facilitate sequence learning.

*Sequence>random*. When examining activations that were greater during sequence trials compared to random trials (Figure 2.10C), we found greater bilateral cortical activation following anodal stimulation, with activations in the left middle frontal gyrus, left supplemental motor area, left inferior occipital lobe, right angular, right fusiform gyrus, left and right inferior parietal, and left and right insula. There was also activation in subcortical regions, particularly the thalamus. Following cathodal stimulation, we found only activations in the left thalamus and left supplemental motor region.

Further, we investigated the statistical differences between the stimulation groups (Figure 2.10D). The anodal stimulation group had increased activation in the right angular gyrus, left

inferior parietal lobe, left precentral gyrus, and lobules IV-VI in the cerebellum compared to cathodal stimulation. Further, anodal stimulation resulted in larger activation in the right middle frontal lobe and right lobule VI in the cerebellum when compared to the sham group. This is consistent with our scaffolding hypothesis, wherein there was additional cortical activation after stimulation to the cerebellum that is thought to downregulate its function and output (Bernard et al., 2013).

**Table 2.7 Significant contrast clusters following stimulation during a Sequence learning task.**

| Phase | Stimulation | Region | Voxels | MNI Coordinates | | | Z |
|---|---|---|---|---|---|---|---|
| | | | | x | y | z | |
| Random | Cathodal | Right Calcarine fissure and surrounding cortex | 11099 | 12 | -62 | 16 | 7.62 |
| | | Right Precuneus | 3550 | 4 | -42 | 54 | 6.13 |
| | | Right Inferior frontal gyrus, opercular part | 358 | 44 | 6 | 24 | 5.02 |
| | | Left Postcentral gyrus | 271 | -58 | -4 | 20 | 4.95 |
| | | Right Temporal pole: superior temporal gyrus | 183 | 50 | 10 | -14 | 5.15 |
| | | Right Insula | 167 | 30 | 18 | 6 | 5.02 |
| | | Right Superior temporal gyrus | 160 | 46 | -26 | -2 | 5.31 |
| | | Left Middle temporal gyrus | 128 | -48 | -36 | 2 | 4.97 |
| | Anodal | Right Cuneus | 15095 | 6 | -76 | 32 | 9.97 |
| | | Right Precuneus | 1849 | 6 | -42 | 48 | 6.33 |
| | | Left Anterior cingulate and paracingulate gyri | 687 | -6 | 18 | 28 | 6.03 |
| | | Left Postcentral gyrus | 410 | -56 | -8 | 30 | 5.28 |
| | | Left Precental gyrus | 135 | -48 | 12 | 36 | 5.22 |
| | | Right Insula | 115 | 38 | 20 | -8 | 5.7 |
| Sequence | Cathodal | Left Calcarine fissure and surrounding cortex | 5009 | -4 | -70 | 12 | 6.6 |
| | | Right Supplementary motor area | 3008 | 2 | -2 | 58 | 5.32 |
| | | Right Inferior temporal gyrus | 254 | 50 | -58 | -12 | 5.22 |
| | | Left Middle occipital gyrus | 244 | -20 | -100 | -2 | 5.12 |

| | | | | | | | |
|---|---|---|---|---|---|---|---|
| | | Left Lenticular nucleus, pallidum | 200 | -8 | 4 | 2 | 4.92 |
| | | Left Middle frontal gyrus | 189 | -36 | 44 | 18 | 5.67 |
| | | Left Middle temporal gyrus | 140 | -48 | -38 | 6 | 5.14 |
| | | Right Middle temporal gyrus | 122 | 52 | -36 | 2 | 4.66 |
| | | Right Olfactory cortex | 107 | 18 | 12 | -12 | 4.91 |
| | | Left Middle occipital gyrus | 106 | -28 | -74 | 32 | 4.78 |
| | Anodal | Right Cuneus | 12038 | 10 | -78 | 36 | 7.7 |
| | | Left Supplementary motor area | 1438 | -4 | 14 | 46 | 6.07 |
| | | Left Median cingulate and paracingulate gyri | 520 | -6 | -24 | 30 | 5.32 |
| | | Right Precental gyrus | 277 | 44 | -16 | 52 | 5.33 |
| | | Left Median cingulate and paracingulate gyri | 223 | -14 | -36 | 46 | 4.93 |
| | | Right Thalamus | 218 | 8 | -18 | 4 | 5.7 |
| | | Left Insula | 170 | -38 | 14 | 4 | 6.04 |
| | | Left Lenticular nucleus, putamen | 166 | -14 | 14 | -4 | 4.85 |
| | | Left Thalamus | 164 | -8 | -18 | 8 | 5.43 |
| | | Right Insula | 143 | 34 | 26 | 6 | 5.23 |
| | | Right Lenticular nucleus, putamen | 130 | 18 | 14 | -6 | 4.94 |
| | | Left Middle temporal gyrus | 124 | -62 | -52 | 18 | 5.82 |
| | | Left Middle frontal gyrus | 111 | -30 | 46 | 24 | 5.76 |
| | Cathodal | Left Thalamus | 259 | -6 | -26 | 10 | 4.93 |
| | | Left Supplementary motor area | 153 | 0 | -6 | 56 | 5.26 |
| Sequence > Random | Anodal | Left Inferior parietal, but supramarginal and angular gyri | 1987 | -40 | -40 | 42 | 7.13 |
| | | Left Supplementary motor area | 932 | -6 | 16 | 44 | 6.11 |
| | | Right Inferior parietal, but supramarginal and angular gyri | 819 | 36 | -46 | 42 | 6.93 |
| | | Left Inferior occipital gyrus | 464 | -46 | -72 | -4 | 6.26 |
| | | Right Fusiform gyrus | 329 | 38 | -70 | -16 | 5.63 |

| | | | | | | |
|---|---|---|---|---|---|---|
| | Left Insula | 268 | -34 | 18 | 6 | 5.7 |
| | Left Thalamus | 219 | -8 | -16 | 10 | 5.51 |
| | Right Angular gyrus | 189 | 36 | -56 | 54 | 5.8 |
| | Right Insula | 147 | 40 | 18 | 4 | 5.09 |
| | Right Thalamus | 110 | 10 | -18 | 4 | 5.12 |
| | Left Middle frontal gyrus | 100 | -32 | 46 | 24 | 4.84 |
| Cathodal > Sham | | | | | | |
| | Right Caudate nucleus | 145 | 8 | 0 | 12 | 5.93 |
| Anodal > Sham | Right Middle frontal gyrus | 116 | 28 | 50 | 2 | 4.83 |
| | Right Lobule VI, cerebellum | 104 | 38 | -44 | -28 | 4.97 |
| Anodal > Cathodal | Left Inferior parietal, but supramarginal and angular gyri | 446 | -40 | -40 | 42 | 5.67 |
| | Right Angular gyrus | 326 | 42 | -48 | 38 | 5.23 |
| | Right Angular gyrus | 193 | 28 | -58 | 52 | 4.76 |
| | Left Lobule IV & V, cerebellum | 154 | -20 | -40 | -30 | 4.47 |
| | Left Precental gyrus | 122 | -60 | 6 | 32 | 5.08 |
| | Right Lobule VI, cerebellum | 108 | 32 | -46 | -26 | 5.01 |

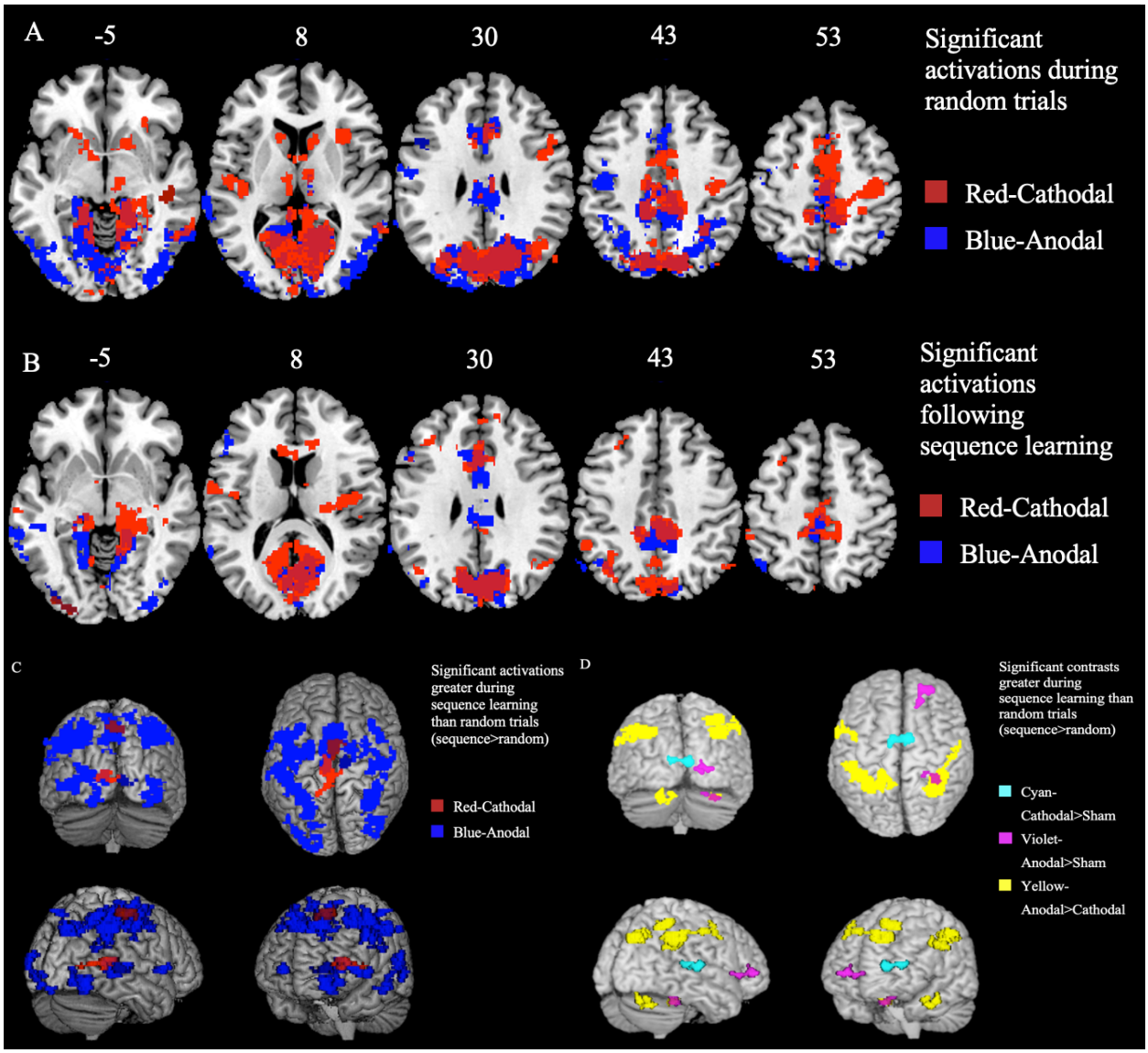


**Figure 2.10 Significant activations following stimulation during a sequence learning task. (A) Significant activations during random trials; Red=Cathodal Stimulation; Blue=Anodal Stimulation; (B) Significant activations following sequence learning; Red=Cathodal Stimulation; Blue=Anodal Stimulation; (C) Significant activations greater during sequence learning than random trials (sequence>random); Red=Cathodal Stimulation; Blue=Anodal Stimulation; (D) Significant contrasts greater during sequence learning than random trials (sequence>random); Cyan= activations greater following cathodal stimulation compared to sham stimulation; Violet= activations greater following anodal stimulation compared to sham stimulation; Yellow= activations greater following anodal stimulation compared to cathodal stimulation.**

We next examined activations within each learning phase to demonstrate how stimulation might alter activations during each learning phase. Activations are reported in Table 2.8 and depicted visually in Figure 2.11.

*Early*. In the anodal stimulation group, we saw activation in the right calcarine fissure and left middle occipital lobe. Cathodal stimulation resulted in right paracentral lobule, left caudate, left supplemental motor area and left precuneus activation. Additionally, there was greater right caudate activation following cathodal stimulation compared to sham.

*Middle*. Anodal stimulation resulted in activations in the left insula, left precentral gyrus, right superior frontal lobe, right inferior temporal lobe, right superior parietal lobe, left anterior and middle cingulum, left middle occipital lobe, right middle occipital lobe, and right lingual gyrus. Additionally, anodal stimulation resulted in greater activation in the right precuneus compared to cathodal stimulation. There were no significant activations following cathodal stimulation during the middle learning blocks.

*Late*. In the cathodal stimulation group during the late learning blocks, we saw extensive activation. This included the right middle temporal lobe, the left superior frontal lobe, the left precuneus, the right postcentral gyrus, the right insula, the right lingual gyrus, the right inferior frontal lobe, the right precentral gyrus, the right supplemental motor area, the right calcarine fissure, and the left and right middle frontal lobes. Activation was also found in the left thalamus. Anodal stimulation resulted in activations in the right inferior parietal lobe, right lingual gyrus, left precentral gyrus, right middle occipital lobe, right fusiform area, and the left cuneus.

Taken together, we began to see differences in how simulation might affect sequence learning. During middle learning anodal stimulation seemed to increase bilateral parietal and occipital lobe activations. However, during late learning cathodal stimulation resulted in more

frontal and parietal activations. This polarity specific change in cortical activation following cerebellar stimulation provided insight as to how the cerebellum helped during sequence learning.

**Table 2.8 Significant clusters of activation associated with different stages of learning (early, middle, and late) during an explicit sequence learning task. Each stimulation group, as well as group contrasts are reported below.**

| Phase | Stimulation | Region | Voxels | MNI Coordinates | | | Z |
|---|---|---|---|---|---|---|---|
| | | | | x | y | z | |
| Early | Cathodal | Left Precuneus | 1404 | -4 | -80 | 48 | 5.74 |
| | | Left Supplementary motor area | 151 | 0 | -12 | 56 | 4.52 |
| | | Right Paracentral lobule | 142 | 12 | -30 | 56 | 4.95 |
| | | Left Caudate nucleus | 115 | -8 | 12 | -2 | 4.71 |
| | Anodal | Left Middle occipital gyrus | 854 | -36 | -90 | -2 | 8.53 |
| | | Right Calcarine fissure and surrounding cortex | 165 | 14 | -64 | 20 | 4.68 |
| | Cathodal > Sham | Right Caudate nucleus | 119 | 20 | 16 | 10 | 5.24 |
| Middle | Anodal | Right Lingual gyrus | 1062 | 16 | -88 | -10 | 6.83 |
| | | Left Middle occipital gyrus | 985 | -28 | -64 | 32 | 6.09 |
| | | Right Superior occipital gyrus | 470 | 26 | -68 | 36 | 6.83 |
| | | Left Median cingulate and paracingulate gyri | 445 | 0 | 8 | 40 | 5.4 |
| | | Left Thalamus | 330 | -6 | -20 | 4 | 5.4 |
| | | Left Anterior cingulate and paracingulate gyri | 282 | -6 | 20 | 28 | 5.63 |
| | | Right Superior parietal gyrus | 281 | 38 | -56 | 56 | 5.68 |
| | | Right Inferior temporal gyrus | 253 | 54 | -54 | -10 | 5.41 |
| | | Right Superior frontal gyrus, dorsolateral | 234 | 26 | 6 | 64 | 4.85 |
| | | Left Precental gyrus | 147 | -46 | 6 | 38 | 5.09 |
| | | Left Insula | 119 | -40 | 14 | 2 | 4.96 |
| | | Left Median cingulate and paracingulate gyri | 115 | -2 | -18 | 34 | 4.65 |
| | Anodal > Cathodal | Right Precuneus | 233 | 10 | -78 | 56 | 5.24 |
| Late | Cathodal | Right Calcarine fissure and surrounding cortex | 1903 | 10 | -62 | 12 | 6.37 |

| | | | | | | |
|---|---|---|---|---|---|---|
| | Left Thalamus | 767 | -8 | -18 | 6 | 5.57 |
| | Right Supplementary motor area | 646 | 2 | -6 | 56 | 5.74 |
| | Right Middle frontal gyrus | 562 | 34 | 54 | 18 | 5.51 |
| | Left Middle frontal gyrus | 427 | -26 | 38 | 22 | 5.61 |
| | Right Precental gyrus | 307 | 46 | -16 | 46 | 5.2 |
| | Right Inferior frontal gyrus, orbital part | 243 | 22 | 42 | -4 | 4.94 |
| | Right Lingual gyrus | 225 | 22 | -46 | -2 | 5.84 |
| | Left Precuneus | 212 | -4 | -44 | 40 | 5.77 |
| | Right Insula | 166 | 36 | 14 | 6 | 4.93 |
| | Right Postcentral gyrus | 153 | 34 | -28 | 56 | 5.36 |
| | Right Inferior frontal gyrus, triangular part | 132 | 58 | 28 | 8 | 4.67 |
| | Left Superior frontal gyrus, orbital part | 123 | -24 | 46 | -4 | 5.51 |
| | Right Middle temporal gyrus | 107 | 52 | -42 | 0 | 5.03 |
| | Left Cuneus | 2506 | -14 | -86 | 16 | 6 |
| | Right Fusiform gyrus | 394 | 34 | -72 | -14 | 5.72 |
| | Right Middle occipital gyrus | 249 | 32 | -78 | 10 | 5.93 |
| Anodal | Left Precental gyrus | 184 | -48 | 2 | 32 | 4.99 |
| | Right Lingual gyrus | 162 | 20 | -62 | 0 | 4.68 |
| | Right Inferior parietal, but supramarginal and angular gyri | 126 | 30 | -54 | 50 | 4.7 |

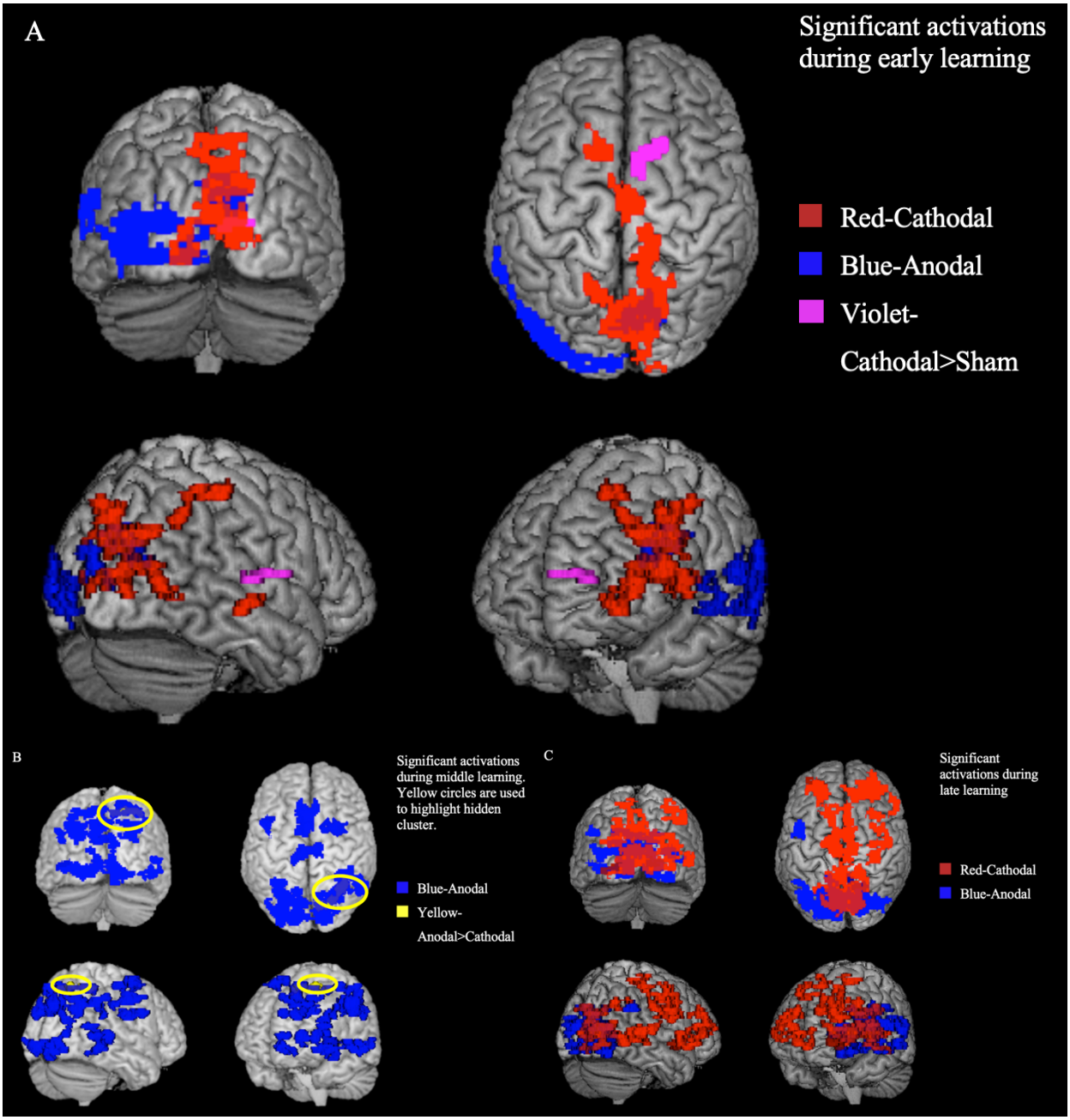


**Figure 2.11 Significant activations by learning phase following stimulation during an explicit sequence learning task. (A) Significant activations during early learning; Red=Cathodal Stimulation; Blue=Anodal Stimulation; Violet= activations greater following cathodal stimulation compared to sham stimulation; (B) Significant activations during middle learning; Blue=Anodal Stimulation; Yellow= activations greater following anodal stimulation compared to cathodal stimulation; (C) Significant activations during late learning; Red=Cathodal Stimulation; Blue=Anodal Stimulation.**

Lastly, we examined contrasts of learning phase with general sequence learning and the activations that were greater in sequence, when compared to random trials. We report all activations in Table 2.9 and highlight patterns of results visually in Figure 2.12. Notable patterns and findings are highlighted below.

Activations that were greater during middle learning, compared to early learning, following anodal stimulation (Figure 2.12A) were larger in the left inferior parietal lobe, the left precuneus, and the right superior parietal lobe. Critically, we also found greater activation in left lobule VI and right crus I in the cerebellum. Further, activation in the right crus I was greater in the anodal stimulation group compared to cathodal stimulation.

Next, we compared late learning to the middle learning blocks (Figure 2.12B). Following cathodal stimulation, there was increased activation in the right precentral gyrus compared to sham stimulation, and greater activation in the left middle cingulum compared to anodal stimulation. No other contrasts or analyses were significant.

We also looked at the effect stimulation had on contrasts between learning phases with the sequence>random contrast (Figure 2.12C). First, we examined activation in the middle>early contrast. Cathodal stimulation resulted it activations in the left fusiform gyrus, the left middle occipital lobe, the right caudate, the left precentral gyrus, the left and right calcarine, the right superior frontal lobe, and the right thalamus. Furthermore, cathodal stimulation resulted in larger activations to the right putamen, right supplemental motor area, left lingual gyrus, the left hippocampus, the right thalamus, and crus II in the cerebellum, compared to sham. Following cathodal stimulation, there were larger activations in the right superior frontal lobe, and the left and right crus I in the cerebellum, compared to anodal stimulation.

When we examined the middle > late contrast, we found greater activation in the right median cingulate following anodal stimulation compared to sham (Figure 2.12D). Additionally, following anodal stimulation there were greater activations in the left thalamus, right caudate, and in the vermis, compared to cathodal stimulation.

Together, we saw effects of stimulation, but the effects varied with learning phase. Specifically, we saw increased activation in the anodal stimulation group during the middle learning blocks compared to early learning, but an effect of cathodal stimulation when middle learning blocks were compared to late learning. Previous work suggests that as a sequence becomes more automatized, the influence of the cerebellum diminishes (Doyon et al., 2018; Imamizu et al., 2000). Perhaps anodal stimulation inhibited the learning process which manifests behaviorally as poor accuracy in late learning. Cathodal stimulation, on the other hand, opens up cortical resources in order to maintain automatization of a newly learned sequence as learning progresses.

**Table 2.9 Significant contrast clusters following stimulation during a Sequence learning task by learning phase.**

| Phase | Stimulation | Region | Voxels | MNI Coordinates | | | Z |
|---|---|---|---|---|---|---|---|
| | | | | x | y | z | |
| Sequence; Early < Middle | Anodal | Right Superior parietal gyrus | 272 | 32 | -60 | 60 | 6.1 |
| | | Right Crus I, cerebellum | 224 | 36 | -60 | -30 | 5.75 |
| | | Left Precuneus | 167 | -10 | -62 | 58 | 5.78 |
| | | Left Lobule VI, cerebellum | 157 | -28 | -60 | -30 | 5.06 |
| | | Left Inferior parietal, but supramarginal and angular gyri | 139 | -44 | -42 | 52 | 5.17 |
| | Anodal > Cathodal | Right Crus I, cerebellum | 109 | 28 | -78 | -22 | 4.78 |

| | | | | | | | |
|---|---|---|---|---|---|---|---|
| | Sham > Cathodal | Right Caudate nucleus | 332 | 20 | 16 | 10 | 5.49 |
| Sequence; Middle < Late | Cathodal > Sham | Right Precental gyrus | 102 | 34 | -24 | 56 | 4.61 |
| | Cathodal > Anodal | Left Median cingulate and paracingulate gyri | 130 | -6 | -42 | 36 | 4.72 |
| | Sham > Anodal | Right Precuneus | 116 | 10 | -50 | 36 | 5.29 |
| Sequence > Random; Early < Middle | Anodal > Cathodal | Left Crus I, cerebellum | 384 | -20 | -82 | -22 | 5.59 |
| | | Right Crus I, cerebellum | 215 | 28 | -78 | -22 | 5.42 |
| | | Right Medial frontal gyrus, orbital part | 158 | 10 | 36 | -10 | 5.02 |
| | Sham > Anodal | Right Median cingulate and paracingulate gyri | 190 | 0 | -18 | 48 | 4.34 |
| | | Left Precuneus | 133 | -14 | -36 | 70 | 4.94 |
| | | Left Lenticular nucleus, putamen | 121 | -30 | -12 | 10 | 4.83 |
| | Sham > Cathodal | Right Lenticular nucleus, putamen | 519 | 24 | 2 | 6 | 5.07 |
| | | Right Hippocampus | 339 | 16 | -34 | 2 | 5.04 |
| | | Left Superior frontal gyrus, dorsolateral | 307 | -18 | -4 | 56 | 4.97 |
| | | Left Hippocampus | 297 | -34 | -30 | 2 | 4.88 |
| | | Left Crus I, cerebellum | 241 | -22 | -82 | -24 | 5.49 |
| | | Left Lingual gyrus | 229 | -10 | -90 | -12 | 5.26 |
| | | Right Supplementary motor area | 169 | 12 | 6 | 62 | 4.83 |
| | | Left Thalamus | 103 | -6 | -2 | 10 | 4.19 |
| Sequence > Random; Middle > Late | Anodal > Sham | Right Median cingulate and paracingulate gyri | 133 | 16 | -46 | 38 | 5.13 |
| | Anodal > Cathodal | Left Thalamus | 195 | -10 | -16 | 20 | 4.78 |
| | | Right Caudate nucleus | 141 | 18 | -8 | 22 | 4.2 |
| | | Vermis VII, cerebellum | 131 | 0 | -74 | -22 | 4.71 |
| | Sham > Cathodal | Right Thalamus | 130 | 12 | -20 | 4 | 4.92 |

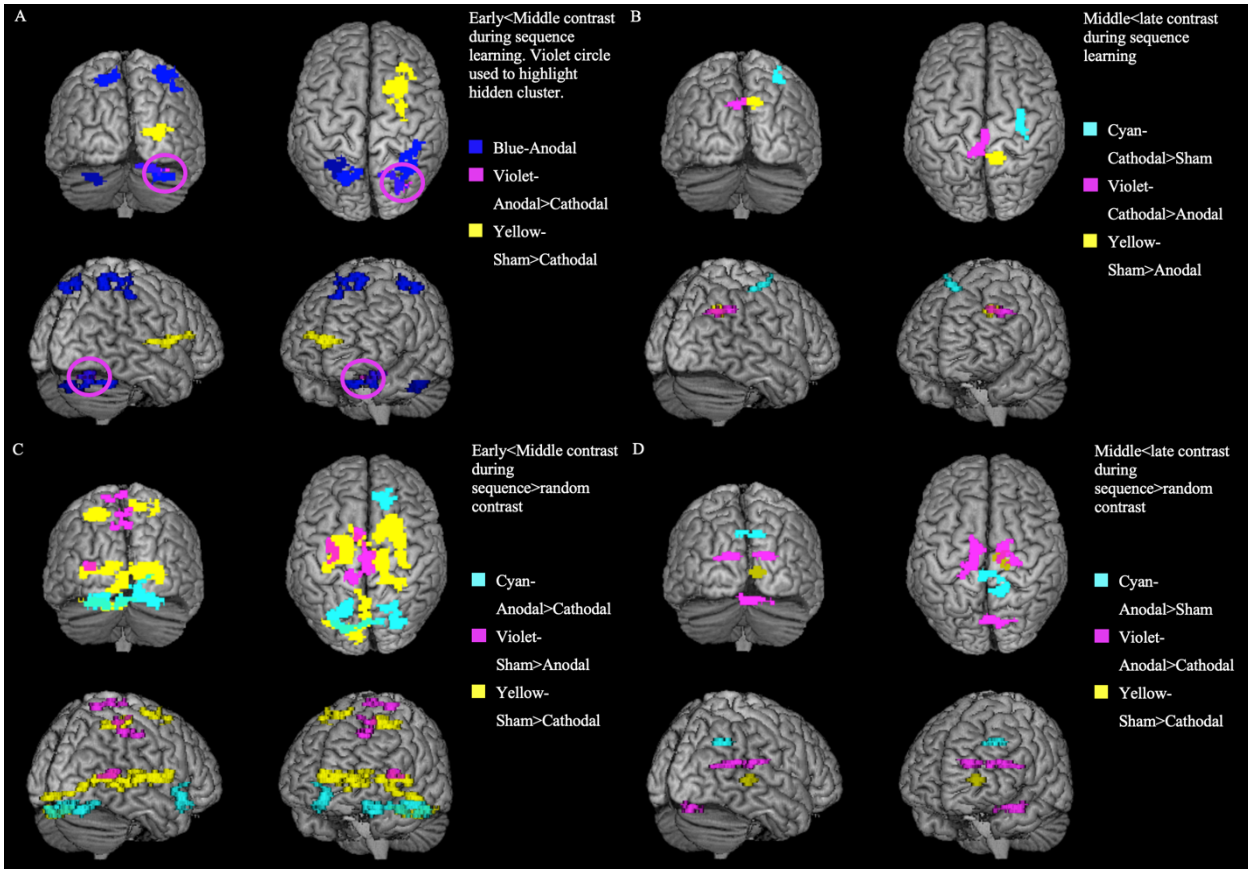


**Figure 2.12 Significant activations following stimulation during a Sequence learning task. (A) Early<Middle contrast during sequence learning; Blue=Anodal Stimulation; Violet= activations greater following anodal stimulation compared to sham stimulation; Yellow= activations greater following sham stimulation compared to cathodal stimulation; (B) Middle<late contrast during sequence learning; Cyan= activations greater following cathodal stimulation compared to sham stimulation; Violet= activations greater following cathodal stimulation compared to anodal stimulation; Yellow= activations greater following sham stimulation compared to anodal stimulation; (C) Early<Middle contrast during sequence>random contrast; Cyan= activations greater following anodal stimulation compared to cathodal stimulation; Violet= activations greater following sham stimulation compared to anodal stimulation; Yellow= activations greater following sham stimulation compared to cathodal stimulation; (D) Middle<late contrast during sequence>random contrast; Cyan= activations greater following anodal stimulation compared to sham stimulation; Violet= activations greater following anodal stimulation compared to cathodal stimulation; Yellow= activations greater following sham stimulation compared to cathodal stimulation.**

*ROI analysis.* ROI analysis looked to understand whether stimulation modulated mean signal change in crus I, frontal regions or parietal regions. For both the Sternberg (Figure 2.13, *p*s> .060) and sequence learning (Figure 2.14, *p*s> .124) tasks, stimulation did not significantly

modulate the percent signal change in crus I, frontal regions or parietal regions, either laterally or bilaterally. We do want to note one trend level effect that did emerge. We found a marginal effect of stimulation ($p$ =.060) on mean signal change in the frontal lobes bilaterally during the Sternberg task. This was driven by greater signal change following cathodal stimulation compared to anodal stimulation ($p$= .072). Though non-significant, this might provide further evidence to support an increase in cortical activation following cathodal stimulation (Grimaldi et al., 2016).

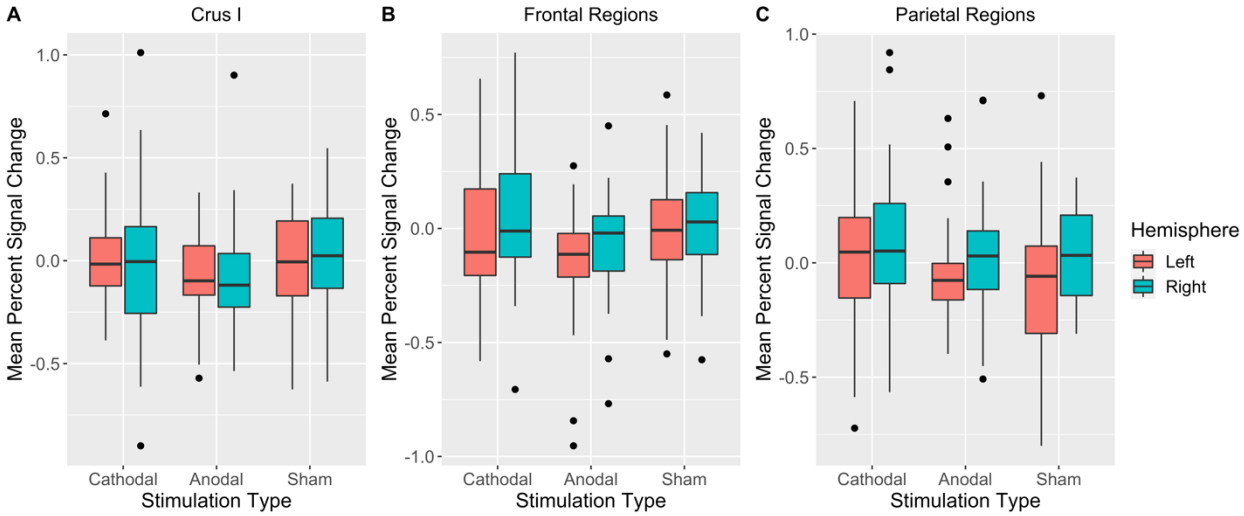


**Figure 2.13 Mean percent signal change by stimulation condition for the Sternberg task.**

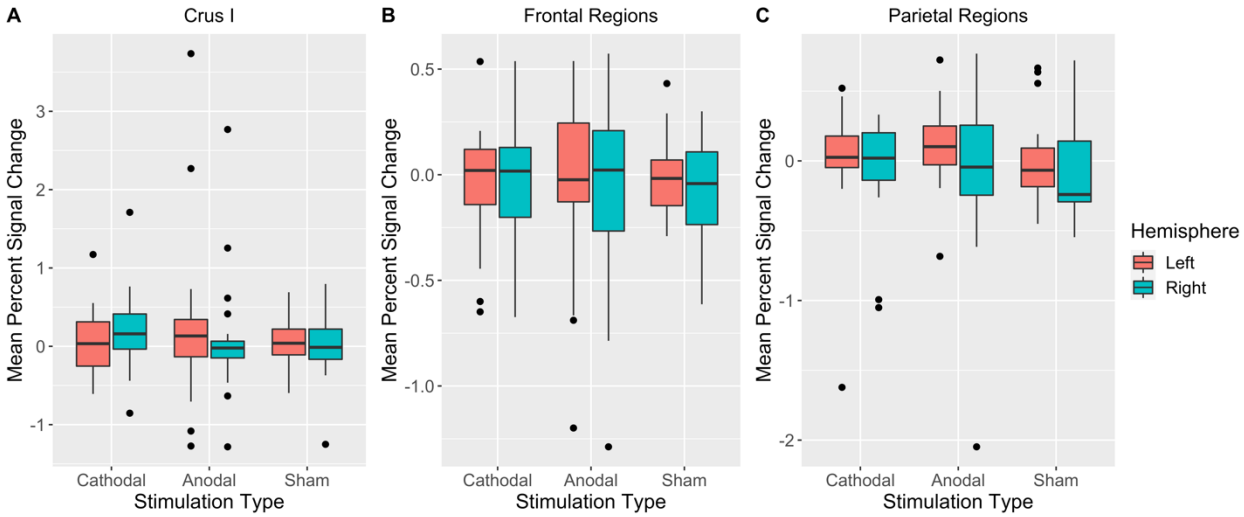


**Figure 2.14 Mean percent signal change by stimulation condition for the Sequence learning task.**

A correlation analysis was also conducted to see if signal change was associated with Sternberg (Table 2.10) or sequence learning (Table 2.11) performance. During Sternberg task performance, accuracy increased as signal increased in the left parietal lobe following cathodal stimulation ($p$ =.013, Figure 2.15A), but decreased as signal increased following anodal stimulation ($p$ =.050). Similarly, accuracy increased as signal increased in the right parietal lobe following cathodal stimulation ($p$ =.037). During sequence learning, reaction time increased as signal increased in the right parietal lobe ($p$ =.014, Figure 2.15B) following anodal stimulation. However, these effects did not survive a Bonferroni multiple comparison correction.

**Table 2.10 Correlation matrix for percent signal change in Crus I, frontal and parietal regions during a Sternberg task.**

| | | Sternberg | | | | | |
|---|---|---|---|---|---|---|---|
| | | Cathodal | | Anodal | | Sham | |
| | | r | p | r | p | r | p |
| Reaction Time | Left Crus I | -0.179 | 0.392 | 0.059 | 0.788 | 0.017 | 0.936 |
| Accuracy | Left Crus I | 0.260 | 0.209 | -0.014 | 0.949 | 0.166 | 0.437 |
| Reaction Time | Left Parietal Lobe | 0.136 | 0.516 | 0.130 | 0.553 | -0.141 | 0.511 |
| Accuracy | Left Parietal Lobe | 0.491 | 0.013 | -0.413 | 0.050 | 0.010 | 0.965 |
| Reaction Time | Left Frontal Lobe | 0.394 | 0.051 | -0.253 | 0.244 | 0.013 | 0.951 |
| Accuracy | Left Frontal Lobe | 0.386 | 0.057 | 0.052 | 0.813 | -0.059 | 0.783 |
| Reaction Time | Right Crus I | 0.208 | 0.319 | -0.056 | 0.799 | 0.194 | 0.364 |
| Accuracy | Right Crus I | 0.076 | 0.716 | -0.070 | 0.750 | 0.170 | 0.428 |
| Reaction Time | Right Parietal Lobe | -0.083 | 0.692 | -0.169 | 0.442 | -0.080 | 0.708 |
| Accuracy | Right Parietal Lobe | 0.420 | 0.037 | -0.390 | 0.066 | 0.034 | 0.876 |
| Reaction Time | Right Frontal Lobe | 0.029 | 0.891 | -0.250 | 0.251 | 0.087 | 0.687 |
| Accuracy | Right Frontal Lobe | 0.239 | 0.250 | -0.007 | 0.973 | -0.096 | 0.656 |

**Table 2.11 Correlation matrix for percent signal change in Crus I, frontal and parietal regions during a sequence learning task.**

| | | Sequence | | | | | |
|---|---|---|---|---|---|---|---|
| | | Cathodal | | Anodal | | Sham | |
| | | r | p | r | p | r | p |
| Reaction Time | Left Crus I | 0.167 | 0.435 | -0.165 | 0.429 | -0.158 | 0.482 |
| Accuracy | Left Crus I | -0.131 | 0.542 | 0.033 | 0.877 | -0.188 | 0.402 |
| Reaction Time | Left Parietal Lobe | 0.236 | 0.267 | 0.182 | 0.384 | -0.188 | 0.402 |
| Accuracy | Left Parietal Lobe | -0.226 | 0.288 | 0.082 | 0.698 | -0.256 | 0.250 |
| Reaction Time | Left Frontal Lobe | 0.248 | 0.242 | -0.017 | 0.935 | -0.062 | 0.785 |
| Accuracy | Left Frontal Lobe | 0.072 | 0.739 | 0.065 | 0.756 | -0.137 | 0.544 |
| Reaction Time | Right Crus I | 0.058 | 0.786 | -0.073 | 0.728 | -0.012 | 0.959 |
| Accuracy | Right Crus I | -0.157 | 0.463 | -0.039 | 0.853 | 0.247 | 0.267 |
| Reaction Time | Right Parietal Lobe | 0.197 | 0.356 | 0.483 | 0.014 | 0.027 | 0.907 |
| Accuracy | Right Parietal Lobe | -0.065 | 0.764 | -0.150 | 0.474 | -0.511 | 0.015 |
| Reaction Time | Right Frontal Lobe | 0.226 | 0.289 | 0.300 | 0.145 | 0.214 | 0.338 |
| Accuracy | Right Frontal Lobe | 0.229 | 0.283 | -0.034 | 0.872 | -0.050 | 0.826 |

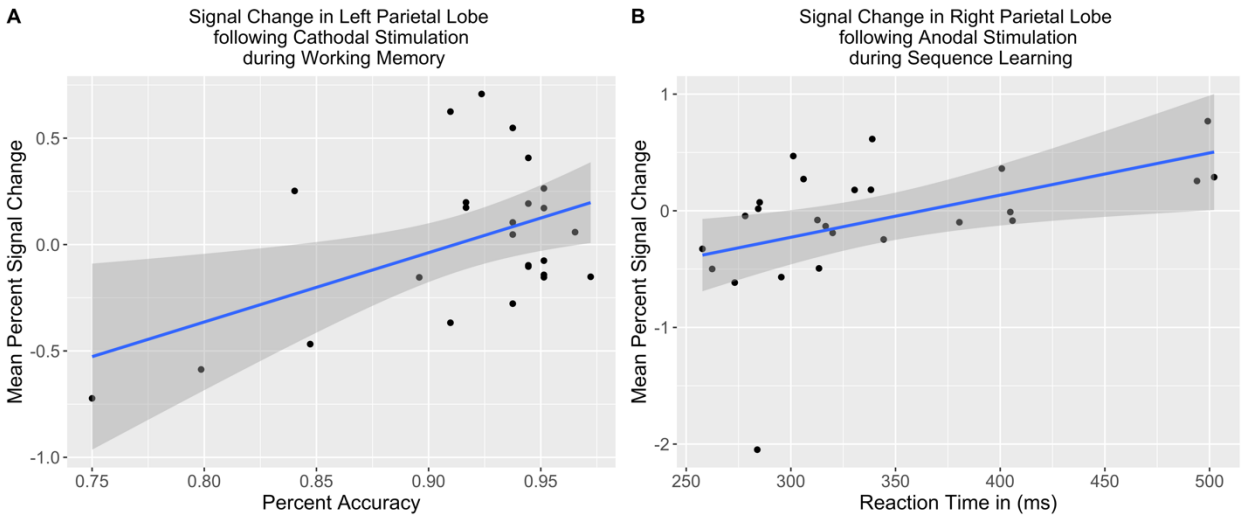


**Figure 2.15 Correlations between mean percent signal change and task performance following stimulation. (A) Mean percent signal change in the left parietal lobe following cathodal stimulation during a working memory task. (B) Mean percent signal change in the right parietal lobe following anodal stimulation during a sequence learning task.**

## Discussion

The literature implicating the cerebellum in cognitive processing is growing (Buckner, 2013; Schmahmann et al., 2019; Stoodley, 2012; Stoodley et al., 2012b), but little work has

examined how this structure interacts with the cortex during non-motor tasks. Critically, recent aging work has implicated the cerebellum in cortical scaffolding (Bernard & Seidler, 2014; Filip et al., 2019), suggesting that the cerebellum is recruited as a support system for cognitive processing through the use of internal models to support automatized processing. Further, past work using tDCS over the right cerebellum to modulate cognitive processing has been mixed (Boehringer et al., 2013; D'Mello et al., 2017; Ferrucci et al., 2008; Küper et al., 2019; Macher et al., 2014; Majidi et al., 2017; Pope & Miall, 2012; Rice et al., 2021; Spielmann et al., 2017; Turkeltaub et al., 2016; van Wessel, Claire Verhage, Holland, Frens, & van der Geest, 2016; Verhage, Avila, Frens, Donchin, & van der Geest, 2017). Therefore, we combined tDCS and fMRI to better understand how activation patterns might relate to behavioral performance and to understand what role the cerebellum might play in cognitive processing, particularly in conjunction with processing in the cerebral cortex. Together, this stands to provide novel insights into the potential cerebellar scaffolding mechanism. Thus, following anodal, cathodal, or sham stimulation, participants completed a motor learning (explicit sequence learning) or verbal working memory (Sternberg) task. Broadly, we found increased cortical activation following anodal stimulation across task domains, implicating the cerebellum as a critical scaffold for cortical processing (Bernard & Seidler, 2014; Filip et al., 2019), particularly when cerebellar output is thought to be degraded. Results and implications are discussed below.

**Working Memory**

Behaviorally, we found the expected effect of load, such that performance (both reaction time and accuracy) was best for low load, followed by medium load, and finally worst for high load. We did not find an effect of stimulation on accuracy during performance of the Sternberg task, but we did find that both anodal and cathodal stimulation improved reaction time. Though

we predicted performance decrements following anodal stimulation and performance increases following cathodal stimulation, these findings are partially supported by previous work. Specifically, cathodal tDCS improved response latencies on paced auditory serial addition and subtraction tasks, particularly as cognitive demands increased (Pope & Miall, 2012). However, our results oppose similar work which found both anodal and cathodal stimulation negatively impacted reaction time Sternberg task performance (Ferrucci et al., 2008; Maldonado & Bernard, 2021). Though we acknowledge that reaction time is not the only measure of working memory performance, the current data mimic the mixed nature of this literature. In regard to accuracy, there was no effect of stimulation, though accuracy was high, perhaps making it difficult for stimulation to modulate task performance.

Functionally, activations following sham stimulation generally align with past work examining activations following a verbal working memory task (Emch et al., 2019). Critically, a network of frontal and parietal regions as well as crus I in the cerebellum, were active. This is consistent with past work implicating these regions in verbal working memory tasks (Emch et al., 2019; Jonides et al., 1997, 1998). Critically, these activations were particularly robust when cognitive load was high (Jonides et al., 1997), further replicating effects of load on activation (Cappell et al., 2010; Reuter-Lorenz & Cappell, 2008).

Activations following real stimulation (both cathodal and anodal) are also consistent with past work (Emch et al., 2019; Jonides et al., 1997, 1998) and could explain the behavioral effect we found on reaction time. Behaviorally, we saw both anodal and cathodal stimulation improve reaction time. Functionally, when examining activation following cathodal stimulation under high load, we found activations in frontal, parietal and cerebellar regions associated with verbal working memory (Jonides et al., 1997). However, when contrasting high and low load following anodal

stimulation, we found greater frontal activations to the inferior, middle and frontal lobes, which are also regions implicated in verbal working memory task performance (Emch et al., 2019; Jonides et al., 1997, 1998). We propose that this effect of anodal stimulation is of significance, as the increased bilateral cortical activation may be compensation as a result of diminished cerebellar output, given what is known about the impact of anodal stimulation on the cerebellum (Galea et al., 2009; Grimaldi et al., 2016). In the current work, this compensatory response following anodal stimulation might have been effective and helped improve behavioral performance as measured by reaction time, while with cathodal stimulation individuals recruited the expected regions.

Work by Macher and colleagues applied anodal stimulation to the right cerebellum which resulted in poorer performance on a modified Sternberg task, though cathodal stimulation did not affect performance (Macher et al., 2014). Critically, this work also found attenuated signal in the right cerebellum, and decreased functional connectivity to the posterior parietal cortex following anodal stimulation. This attenuated signal to the cortex following anodal stimulation is of significance, and in line with our predictions. In the current work, it is possible that connectivity to the frontal lobes was also attenuated following anodal stimulation, as might be predicted by Grimaldi et al (2016), resulting in the need for more cortical processing to ensure successful task completion. That is, if the cerebellum was not processing information from the cortex adequately, more cortical resources would be needed to make up for this, resulting in increased cortical activation. The internal models stored in the cerebellum, and used to help support cortical processing, might have been negatively impacted following anodal stimulation, hindering task performance (Bernard & Seidler, 2014; Filip et al., 2019; Ito, 2008). Therefore, in this specific data set, cathodal stimulation did result in a behavioral boost manifesting as improved reaction time during a verbal working memory task. But we might also be observing an effective

compensatory reaction in frontal lobes, such that when anodal stimulation diminished cerebellar output and degraded internal models during high cognitive load tasks, the cortex was able to successfully recruit more neural resources, which ultimately improved reaction time following anodal stimulation.

**Sequence Learning**

Behaviorally, we found a significant effect of stimulation on both reaction time and accuracy. For reaction time, we found the magnitude in change in RT was significantly greater following cathodal stimulation between middle learning and random button presses, compared to anodal and sham. For accuracy, we found that the anodal stimulation group showed significantly worse accuracy during late phase learning. This is consistent with previous findings from our group (Ballard et al., 2019), though differs from two other studies that suggest anodal stimulation improves sequence learning ability (Ferrucci et al., 2013; Jongkees et al., 2019). However, some methodological discrepancies could cause this result. Specifically, both studies (Ferrucci et al., 2013; Jongkees et al., 2019) placed their electrode such that stimulation would affect both the right and left cerebellum. The current work only applied stimulation targeting the right cerebellum (Ferrucci, Cortese, & Priori, 2015). Applying anodal stimulation to both the left and right hemisphere could negatively impact any cerebellar output to the cortex, not just communication from the right cerebellum. Additionally, Ferrucci and colleagues used a within subjects design in which participants completed both anodal and sham stimulation at least one week apart, and within each session completed the same behavioral task before and after stimulation (Ferrucci et al., 2013). This could naturally result in a learning effect. Further, while Ferrucci used a 20 minute, 2mA, stimulation session, Jongkees used a 20 minutes, 1 mA session while participants were completing the task, a procedure that is thought to reduce the effect of stimulation (Horvath et al.,

2014; Quartarone et al., 2004). Though the sequence learning task completed in the current work is similar to those complete in previous work, the methodological differences could ultimately induce an alternative effect.

With respect to the lower accuracy during late learning in the anodal stimulation group, work implicating the cerebellum in motor learning suggests the cerebellum is particularly active during early motor learning when procedural memories are created (Bernard & Seidler, 2013; Doyon et al., 2018). Critically, during late learning, the cortex increasingly relies on the internal models that should be created during early learning to complete tasks more automatically. These models have been refined, hence the lower amount of activation (Imamizu et al., 2000). However, if these internal models were not adequately formed during early learning this could result in poor performance during late learning. It is possible that anodal stimulation was disrupting the formation of these models, particularly in early learning, which had an adverse impact on accuracy in late learning.

Our imaging data suggested anodal stimulation increased cortical activations, in key frontal (Emch et al., 2019; Jonides et al., 1997), parietal (Lissek et al., 2013) and cerebellar (Stoodley, 2012) regions associated with non-motor cognition. Critically, the activations in parietal regions were greater following anodal stimulation when compared to cathodal, demonstrating how disruptive anodal stimulation might be to task performance and cortical processing. This mimics the effect we saw during the Sternberg task, in which anodal stimulation seemed to increase cortical activation, presumably due to degraded cerebellar output and associated processing, in an effort to maintain task performance. Perhaps the cerebellum was supporting the working memory processes needed to complete a sequence learning task, but anodal stimulation degraded the cerebellar output necessary to support this process, requiring increased activation in parietal

regions associated with working memory (Berryhill & Olson, 2008; Lissek et al., 2013). This provides further evidence to suggest that the cerebellum plays a supporting role in mon-motor cognitive processing and degradation of cerebellar output has functional and behavioral consequences.

Contrary to the current findings, recent work found anodal stimulation improves sequence learning, particularly in middle to late learning phases (Liebrand et al., 2020). These behavioral findings were supported by increased learning-specific activity in right M1, left cerebellum lobule VI, left inferior frontal gyrus and right inferior parietal lobule during anodal tDCS compared to sham. However, several methodological considerations might help understand this discrepancy. First, task performance was completed online, that is stimulation was applied as participants completed a task. There is a growing literature that suggests the effect of tDCS stimulation can be eliminated when a behavioral task is completed concurrently with stimulation (Horvath et al., 2014). This interference effect has been demonstrated in both cognitive (Antal et al., 2007) and motor (Quartarone et al., 2004) paradigms. Critically, even the act of thinking about motor movements could eliminate the effect of tDCS (Quartarone et al., 2004) if this occurs while the stimulation is being applied. Thus, it is possible that there was no real effect of anodal stimulation, and the behavioral results were normal task performance. Further, the primary change seems to be in reaction time, but there is no effect on accuracy, which we find in the current work. As Liebrand and colleagues (2020) used a within subject design, even with counterbalancing, it is possible that the simplicity of the task naturally resulted in improved reaction time, regardless of stimulation condition or condition order. Therefore, key methodological differences might explain why behavioral outcomes differed between the two studies. We should note however, Liebrand and colleagues showed changes in activation that are consistent with increased cortical activation as a

result of degraded cerebellar output following anodal tDCS. Therefore, it is possible that anodal stimulation did modulate cortical activation similar to what is found in the current work, but the behavioral outcomes were negated, due to the online nature of stimulation.

In our work, we saw increased bilateral cortical activation in parietal regions typically active during sequence learning (Lissek et al., 2013). It is possible that even though we saw an increase in activation to compensate for this loss, the compensation was not enough, which resulted in poor performance in late learning. In terms of internal models, we speculate that those that would have been created during early learning and were not developed adequately, such that in late learning we see poor accuracy as a result of degraded output from the cerebellum, and poorly formed internal models. This would result in a greater need for cortical processing, but it might also explain why accuracy still suffered, as not enough cortical resources were brought on. Since the cerebellum is no longer able to provide resources to the cortex, cortical activations increased to complete the task efficiently (Bernard et al., 2013; Filip et al., 2019). Critically, we saw a decrease in accuracy in late learning following anodal stimulation, which might be a behavioral consequence of degraded cerebellar output, especially when the cortex was not able to fully compensate for the loss of cerebellar resources.

**The Cerebellum as a Scaffolding Structure**

The current work looked to better understand the role the cerebellum played in cognitive processing. In both a verbal working memory and sequence learning task, we have found that anodal stimulation resulted in increased bilateral cortical activation, in regions previously associated with these tasks (Emch et al., 2019; Jonides et al., 1997, 1998; Lissek et al., 2013), compared to sham or cathodal stimulation. Optogenetic work strongly suggested that anodal stimulation to the cerebellum would excite inhibitory Purkinje cells, ultimately decreasing signal

to the cortex (Galea et al., 2009; Grimaldi et al., 2016). The current work suggested that the cortex may compensate for this lost input and processing from the cerebellum, by increasing cortical activation. Therefore, it is possible that the cerebellum provides additional resources to help support cortical processing. Specifically, internal models stored in the cerebellum are used for greater automaticity on well learned tasks (Ito, 2008; Ramnani, 2006, 2014). However, when cerebellar outputs are degraded, there are negative behavioral implications (Bernard & Seidler, 2014; Filip et al., 2019). Interestingly, some of this increased cortical activation occurred when cognitive processing demands were higher. This was particularly notable during high load in the Sternberg task, perhaps indicating that the cerebellum was increasingly relied upon when cortical regions were taxed. That is, some offloading of processing via internal models may occur when tasks get more difficult. If this was inhibited due to cerebellar dysfunction, age differences, or, as was the case here, due to stimulation, more cortical resources may be needed to maintain performance.

Past work in aging (Bernard et al., 2013) and disease (Allen et al., 2007; Bai et al., 2009) has suggested that degraded cerebellar output negatively impacts cortical connectivity and activation. Cerebellar resources might be important for cortical processing, as they may provide crucial scaffolding for performance and function (Bernard et al., 2013; Filip et al., 2019). Indeed, a recent imaging meta-analysis indicated that the cerebellum in advanced age might be able to engage in compensatory scaffolding for motor tasks, but there was decreased overlap across cognitive tasks compared to young adults, perhaps contributing to performance differences (Bernard et al., 2020). In advanced age cerebellar volume declines (Bernard & Seidler, 2013a; Hoogendam et al., 2012; Koppelmans et al., 2015) and there is a decrease in connectivity with the cortex (Bernard et al., 2013; Ferreira & Busatto, 2013). These differences are behaviorally

relevant, as internal models for procedures are formed in the cerebellum and are used to guide behavior (Ito, 2008; Ramnani, 2006). If internal models are not efficiently processed due to degraded white matter and smaller lobular volume in the cerebellum in advanced age, this might result in motor and cognitive performance deficits (Bernard & Seidler, 2014). However, several compensatory scaffolding models argued that deteriorating neural structures in advanced age resulted in increased activations in cortical regions to compensate for these losses (Cabeza, 2002; Cabeza et al., 2018; Cabeza, Anderson, Locantore, & McIntosh, 2002; Park & Reuter-Lorenz, 2009; Reuter-Lorenz & Campbell, 2008; Reuter-Lorenz & Park, 2014). Critically, these models focused primarily on the prefrontal cortex and largely ignored non-cortical structures such as the cerebellum.

Based on the current work, anodal tDCS seemed to mimic this disrupted cerebellar function, ultimately decreasing cerebellar output, which disrupted cortical processing. This then resulted in the need for increased cortical activation, to maintain task performance. This was seen most clearly in sequence learning, where anodal stimulation resulted in bilateral parietal and additional frontal activation, and decreased accuracy during late learning. We propose that the initial creation of internal models was disrupted and the models were not created properly/optimally. Then, during late learning, when the internal models were needed to complete the tasks more automatically, we saw poor task performance (i.e. reduced accuracy in late learning), because the models were degraded and not useful for task performance (Bernard & Seidler, 2014). This was compounded by the effect of anodal stimulation on cortical activity. We suggest that anodal stimulation also negatively impacted output of the cerebellum via closed-loop circuits with the cortex (Coffman et al., 2011; Kelly & Strick, 2003; Middleton & Strick, 2001),

reducing the influence the cerebellum had on cortical processing and now the cortex is no longer able to rely on the cerebellum for support, and must recruit resources elsewhere.

This work ultimately suggests that if the cerebellum is not functioning optimally, there is a greater need for cortical resources. In specific populations, such as aging (Bernard et al., 2013) and disease (Allen et al., 2007; Bai et al., 2009), there are already limitations on cortical resources and these individuals are more likely to tax these resources during lower levels of cognitive processing. The current work provides initial evidence for why there might be a need for greater cortical activation, specifically as a relates to the cerebellum. Previous work simply indicated that the cerebellum is active during task performance (King et al., 2019; Schmahmann, 2018; Stoodley, 2012), but the current work suggested that the cerebellum is helping support cortical processing, through a scaffolding mechanism, which ultimately helps the cortex in task processing. Thus, the implications of this work might be able to explain, in part a compensatory mechanism of dysfunction in behavior across illnesses. Further, this work has a potential to update existing compensatory models to include the cerebellum as a structure use to support cognitive processes, which has implications in remediation techniques in a number of clinical populations (Ferrucci, Bocci, Cortese, Ruggiero, & Priori, 2016; van Dun & Manto, 2018).

**Limitations**

While our findings provide a novel understanding of the role the cerebellum plays in cognitive processing, there were a few limitations worth noting. First, was electrode size. While a large portion of the literature has used the traditional 1x1 montage to modulate cerebellar function (Ambrus et al., 2016; Ballard et al., 2019; Boehringer et al., 2013; Cantarero et al., 2015; Ferrucci et al., 2008; Hardwick & Celnik, 2014; Jongkees et al., 2019; Majidi et al., 2017; Pope & Miall, 2012; Spielmann et al., 2017; Steiner et al., 2016; van Wessel et al., 2016; Verhage et al., 2017),

it is possible that stimulation occurred outside of the right cerebellum due to spread of the signal. Thus, we likely impacted a greater region of the cerebellum beyond the lateral posterior region we targeted, potentially including ventral cortical areas, in addition to spinal signal and surrounding musculature. Future work might look to incorporate HD-tDCS that allows for more focal targeting of brain regions (Datta et al., 2009; Datta et al., 2016; Dmochowski et al., 2011; Huang et al., 2017; Villamar et al., 2013). Critically the cerebellum, particularly lobules I-IV are tucked away beneath the cortex, and it would be important to have a more precise and accurate targeting of these lobules to increase the changes of functional change in the cortex and behavior. Additionally, work using TMS and theta burst stimulation have also proved useful (Minks et al., 2010; Oberman et al., 2011; Tremblay et al., 2016; Valero-Cabré et al., 2017).

A second limitation was task difficulty, particularly during the Sternberg task. Though the current task seemed to be reasonably difficult in terms of memory load for young adults (Cowan, 2001), accuracy levels across all groups were ~ 90%. Therefore, there was not much room for modulation of task performance. Even though this might have limited our ability to find performance differences, we were still able to provide important new insights.

**Conclusions**

The current work looked to better understand what role the cerebellum might have during nonmotor cognitive processing, by applying anodal, cathodal, and sham stimulation over the right cerebellum prior to completing a motor and non-motor task. Broadly, we found cathodal stimulation resulted in a performance boost, and anodal stimulation hindered task performance. This effect of anodal stimulation also resulted in increased cortical activation, presumably a result of a compensatory mechanism due to the purported downregulation of the cerebellum after anodal stimulation. Specifically, when cerebellar output is degraded by anodal stimulation, the scaffolding

effect the cerebellum provides is reduced, requiring more cortical activation to compensate for the reduced cerebellar output. We believe that the current work provides initial evidence for why there might be a need for greater cortical activation during degraded cerebellar output, such that the cerebellum is helping support cortical processing, through a scaffolding mechanism. This work has a potential to update existing compensatory models, particularly in aging, to include the cerebellum as a structure used to support cognitive processes, which has implications in remediation techniques in a number of clinical populations.

# CHAPTER III

# MODULATED CEREBELLO-CORTICAL CONNECTIVITY FOLLOWING ANODAL TRANSCRANIAL DIRECT CURRENT STIMULATION: A tDCS AND rs-fcMRI STUDY

## Introduction

Classically, the cerebellum has been considered a sensorimotor structure, primarily involved in motor movement (Holmes, 1939) and motor learning (Ballard et al., 2019; Bernard & Seidler, 2013a); however, work from both clinical and basic science disciplines has implicated the cerebellum in non-motor functions (e.g. Buckner, 2013; Desmond, Gabrieli, Wagner, Ginier, & Glover, 1997; Leiner, Leiner, & Dow, 1989; Schmahmann, 2018). These include working memory (Bellebaum & Daum, 2007; Desmond et al., 1997; Hautzel, Mottaghy, Specht, Müller, & Krause, 2009; Hayter, Langdon, & Ramnani, 2007; Stoodley, Valera, & Schmahmann, 2012b), updating (Jahanshahi et al., 2000), inhibition (Neau et al., 2000), shifting (Ravizza & Ivry, 2001; Schall et al., 2003), and planning tasks (Lie et al., 2006). Additionally, activations associated with language processes have been localized to the right posterior cerebellum (Stoodley, 2012; Stoodley et al., 2012b; Stoodley & Schmahmann, 2009). Despite the growing literature on cerebellar function, it remains unclear how the cerebellum interacts with the rest of the cortex during information processing, which could provide a better understanding of cerebellar function.

Viral tract tracing using non-human primates has shown distinct topographical efferent and afferent pathways between the cerebellum and cortex. Specifically, anterior regions such as lobules I-IV and V have projections to the primary motor cortex, whereas posterior lobules such as crus II project to the prefrontal cortex (Kelly & Strick, 2003). Work has also demonstrated projections from the cerebellum to the basil ganglia (Hoshi et al., 2005) and the posterior parietal cortex

(Clower et al., 2005). Further, work has found projections from the motor cortex to the cerebellar vermis (Coffman et al., 2011). This work shows a number of communication circuits between the cerebellum and the cortex, providing a foundation for the interactions between the structures, and support a cerebellar role in multiple domains of function and processing.

One way to examine functional brain networks in humans is through the use of resting-state functional connectivity magnetic resonance imaging (rs-fcMRI). fcMRI can help us understand interactions between the cerebellum and the cerebral cortex. rs-fcMRI works by measuring temporal correlations of the blood oxygen level dependent (BOLD) signal across multiple brain regions when at rest. Critically, regions that perform similar functions have highly correlated signal when at rest (Biswal et al., 2010; Biswal, Zerrin Yetkin, Haughton, & Hyde, 1995) resulting in these functional networks.

Converging evidence in human neuroimaging parallels nicely with the viral tract tracing work in primates (Clower et al., 2005; Coffman et al., 2011; Hoshi et al., 2005; Kelly & Strick, 2003). Specifically, human rs-fcMRI (Krienen & Buckner, 2009) and diffusion-weighted imaging (Salmi et al., 2010) found segregated fronto-cerebellar networks linking the cerebellum to the motor cortex, the dorsal lateral prefrontal cortex, the medial prefrontal cortex, and the anterior prefrontal cortex. O'Reilly and colleagues (2010) have furthered this understanding by demonstrating functional zones in the cerebellum, such that anterior regions of the cerebellum have specific projections to motor, somatosensory, visual, and auditory cortices; whereas, posterior lobes have projections to functional networks with the prefrontal and posterior parietal cortices (Bernard et al., 2012; Diedrichsen et al., 2019; King et al., 2019; O'Reilly et al., 2010). Behaviorally, work has suggested connectivity between the PFC and cerebellum might predict performance on learning executive function tasks (Reineberg et al., 2015), further implicating the

cerebellum in executive functions. Critically, little work has looked to examine how changes in these functional networks might affect cognitive performance and communication between brain regions, though work in aging (Bernard et al., 2013) and disease (Allen et al., 2007; Bai et al., 2009) might begin to provide clues. Specifically, degraded gray and white matter integrity in aging and disease ultimately have behavioral implications as the internal models used by the cerebellum for automaticity may not be utilized as effectively due to disruptions in cerebellar function and network connectivity (Bernard et al., 2013; Bernard & Seidler, 2014; Miller et al., 2013). Therefore, understanding these networks and alterations could be the basis for an improved understanding of cerebellar contributions to behavior.

One commonly used method of neuromodulation is transcranial direct current stimulation (tDCS). tDCS uses a two-electrode pad system in which a positive (anodal) or negative (cathodal) current is sent through the scalp with one electrode pad and a second pad receives the current. Anodal stimulation is thought to increase cortical excitability, while cathodal stimulation decreases cortical excitability (Brunoni et al., 2012; Nitsche & Paulus, 2000; Priori, Berardelli, Rona, Accornero, & Manfredi, 1998). However, anodal stimulation to the cerebellum excites inhibitory Purkinje cells, which ultimately decreases signal to the cortex (Galea et al., 2009; Grimaldi et al., 2016). Cathodal stimulation to the cerebellum inhibits the same cells, resulting in increased signal to the cortex. Cerebellar tDCS has the potential to be particularly informative, as one can increase or decrease the connectivity between brain regions, providing insight into how the cerebellum communicates with the cortex across modulation conditions. The impact of anodal cerebellar tDCS is of particular interest, as it may provide insights into cerebello-cortical interactions that mimic those seen in a variety of neurological and psychiatric illnesses where the cerebellum is impacted (Ferrucci et al., 2016).

Limited work has examined the effects of cerebellar tDCS on cerebello-cortical connectivity, and in this limited literature, the primary focus has been on language processing networks. Specifically, anodal stimulation increased functional connectivity from the cerebellum to cortical areas involved in the motor control of speech (Turkeltaub et al., 2016), language and speech motor regions in the left hemisphere (D'Mello et al., 2017; Turkeltaub et al., 2016), and spelling (Sebastian et al., 2017). Additionally, anodal stimulation reduced cerebellar ataxia symptoms and improved cerebellar output in individuals with cerebellar ataxia (Benussi et al., 2017). Further, anodal stimulation to the cortex also increased cortico-cerebellar connectivity when applied to the dorsal lateral prefrontal cortex (Abellaneda-Pérez et al., 2020), motor cortex (Cummiford et al., 2016) and the right posterior parietal cortex (Callan et al., 2016).

Recent work has also used a lobular based approach to examine static and dynamic connectivity of resting state networks in the absence of a task (Grami et al., 2021). They found anodal stimulation modulated connectivity in a number of networks, including the visual, default-mode, sensorimotor and salience networks. Additionally, temporal variability was greater between crus II and the salience network, but decreased between lobule VII and the default mode and the central executive networks. The authors argued that this provides evidence for a role the cerebellum plays in cognitive processing, and further supports the use of internal models in completing critical motor and non-motor tasks with a high degree of automaticity (Salmi et al., 2010).

Thus, to this point, cerebello-cortical connectivity has been well-documented, and work focused on language networks has indicated that these networks are subject to modulation via cerebellar tDCS (D'Mello et al., 2017; Turkeltaub et al., 2016). However, much of the behavioral work is mixed (Oldrati & Schutter, 2018), such that similar stimulation parameters result in

opposing behavioral effects (Oldrati & Schutter, 2018), but the reason for this discrepancy in results is still unknown. Therefore, the addition of an imaging parameter allows us to understand the functional connectivity changes that occur following stimulation, which can in turn help us to better interpret behavioral changes that also emerge due to stimulation. Here we used tDCS and rs-fcMRI to better understand functional connectivity between the cerebellum and the cortex. This work stands to provide important new insights into the impact of cerebellar tDCS on cerebellar connectivity, and in turn potential impacts on behavior, as well as critical insights into cerebellar networks when function is altered. This latter point may in turn influence our understanding of the cerebellum and cerebello-cortical connectivity in aging, as well as neurological or psychiatric illness.

To this end, participants were placed in one of three stimulation conditions (anodal, cathodal, or sham) and stimulation was applied to the right cerebellum. We used a lobular approach to our analyses (Bernard et al., 2012; Grami et al., 2021) instead of a voxel or seed approach to investigate cerebello-cortical connectivity. In an effort to limit the number of comparisons and in turn false positives, we focused on lobules I-VI, VIIB, crus I and II as these represent areas associated with both motor and prefrontal cortical regions (Bernard et al., 2012; Buckner et al., 2011; King et al., 2019). We also assessed correlations between connectivity and behavior in lobules I-IV and crus I to understand how changes in connectivity might affect behavior. We predict that cathodal stimulation will increase connectivity whereas anodal stimulation will decrease connectivity (Galea et al., 2009; Grimaldi et al., 2016).

## Methods

### Participants

Seventy-five healthy, young adults participated in this study and were provided monetary compensation for their time. This is the same sample used in Chapter 2. Participants were recruited from the broader Texas A&M and Bryan-College Station community via email. Exclusion criteria included left handedness, history of neurological or mood disorders, skin conditions, and history of concussion. Data from one participant was not used because the participant did not wish to finish the experiment after providing consent. Thus, seventy-four right-handed participants (38 female) ages 18 to 30 (M= 22.0 years, SD= 3.45) were included in the analyses. Participants were randomly assigned to either the anodal (n=25), cathodal (n=25), or sham (n=24) stimulation condition. All procedures completed by participants were approved by the Texas A&M University Institutional Review Board and conducted according to the principles expressed in the Declaration of Helsinki.

**Procedure**

Resting state data was collected as part of a larger imaging study which took approximately two hours. However, stimulation was completed and resting state data were collected within 45 minutes, as the resting state scan was the first protocol run in the scanner. Following the completion of the consent form, participants completed a basic demographic survey, followed by tDCS (see below for details). Participants were blind to the stimulation condition and were tDCS naïve, such that participants had not participated in a tDCS study prior to the current experiment. Following stimulation, participants were escorted to the scanner for the brain imaging protocol.

**tDCS Stimulation Parameters**

Participants were fitted with a classic two electrode montage to administer either cathodal, anodal, or sham stimulation using a Soterix 1x1 tES system. One electrode was placed two cm below and four cm lateral of the inion over the right cerebellum (Ferrucci et al., 2015). The second

electrode was placed on the right deltoid. Both electrodes were affixed using elastic bands. Each electrode was placed in a pre-soaked sponge, which had 6 mL of saline solution added on each side.

Once electrodes were placed, stimulation was set to 1.0 mA for thirty seconds to ensure the electrodes made a good connection with the scalp. If contact quality was below 40%, adjustments, such as moving hair to increase the electrode's contact with the scalp, were made and contact quality was rechecked. Following a successful re-check, participants completed a 20-minute stimulation session at 2 mA (Ferrucci et al., 2015; Grimaldi et al., 2014, 2016). During the stimulation conditions, maximum stimulation intensity was reached in 30 seconds and maintained for 20 minutes, and then would return to 0 mA. During sham conditions, maximum stimulation intensity would be reached, but immediately return to 0 mA. There was no additional stimulation during the 20-minute sham session.

**Behavioral Tasks**

The same task parameters used in chapter two are used for this study, but are briefly described below. For more detail, please see the methods section in chapter two.

*Sequence*. Participants completed three learning blocks (early, middle and late) in which participants completed either 18 random trials or 36 sequence trials. During sequence trials, participants had to learn a six-element sequence (1-3-2-3-4-2), which was repeated six times within a block. The order of the task was as follows: R-S-S-S-R-R-S-S-S-R-R-S-S-S-R. Dependent variables used to estimate learning were mean reaction time (RT) for correct trials and average total accuracy.

*Sternberg*. Participants were shown either one, five or seven study letters and were subsequently asked to indicate whether a target letter was one of the original study letters via button press. Dependent variables were average RT for correct trials and accuracy.

**Data Analysis**

*Behavioral*. Statistical analyses are described in chapter two. Correlations between connectivity and behavior were conducted for lobules I-IV and crus I. Correlations were conducted for both RT and accuracy variables for the sequence learning and Sternberg task. Impacts of stimulation on behavior are discussed in chapter two.

**fMRI Data Acquisition**

Resting state fMRI data was collected at the Texas A&M Translational Imaging Center with a 3-T Siemens Magnetom Verio scanner using a 32-channel head coil. Two blood oxygen level dependent (BOLD) whole brain scans with a multiband factor of 4 were collected in the absence of any task (number of volumes = 114, repetition time [TR] = 2000 ms, echo time [TE] = 27 ms; flip angle [FA] = 52°, 3.0 × 3.0 × 3.0 mm3 voxels; 56 slices, interleaved, slice thickness=3.00mm, field of view (FOV) = 300 × 300 mm; time = 4:00 min). The scans were collected in opposite encoding directions (anterior → posterior and posterior → anterior). During the scan participants viewed a centrally located fixation cross and were asked to stay awake while "thinking about nothing in particular". An additional high resolution T1 weighted whole brain anatomical scan was taken (sagittal; GRAPPA with acceleration factor of 2; TR = 2400 ms; TE = 2.07 ms; 0.8 x 0.8 x 0.8 mm3 voxels; 56 slices, interleaved, slice thickness= 0.8mm; FOV = 256 × 256 mm; FA = 8°; time = 7:02 min) for data normalization.

**Rs-fMRI Data Pre-processing**

Both anatomical and functional images were collected using DICOM format but were converted to NIFTI files and organized into a Brain Imaging Data Structure (BIDS) using bidskit (v 2019.8.16; Mike Tyszak, 2016). Functional images were collected using opposite phase encoding directions. For distortion correction, single 4D images were taken for each participant from each phase encoding direction and were merged. Then fieldmap images were created using FSL's topup to unwrap images (Andersson et al., 2003).

FMRI data was pre-processed using FEAT (FMRI Expert Analysis Tool) Version 6.00, part of FSL (FMRIB's Software Library, www.fmrib.ox.ac.uk/fsl). Registration to high resolution structural and/or standard space images was carried out using FLIRT (Jenkinson et al., 2002; Jenkinson & Smith, 2001). Registration from high resolution structural to standard space was then further refined using FNIRT nonlinear registration (Andersson, Jenkinson, & Smith, 2007; Andersson, Jenkinson, & Smith, 2007). The following pre-statistics processing was applied; motion correction using MCFLIRT (Jenkinson et al., 2002); slice-timing correction using Fourier-space time-series phase-shifting; non-brain removal using BET (Smith, 2002); spatial smoothing using a Gaussian kernel of FWHM 5mm; grand-mean intensity normalization of the entire 4D dataset by a single multiplicative factor. ICA was carried out using MELODIC (Beckmann & Smith, 2004), to investigate the possible presence of unexpected artefacts or activation.

Finally, data were subjected to FSL's Motion Outliers tool, which is designed to detect timepoints in the dataset that are corrupted by large motion. Here, the functional files were subjected to a root mean squared head position change intensity difference of volume N to volume N+1 assessment (Power et al., 2012). The resulting confound matrix was submitted to the denoising model in the CONN processing pipeline (www.nitrc.org/projects/conn, RRID:SCR_009550) described below.

## Conn Analysis

Statistical analysis was completed using the CONN (Whitfield-Gabrieli & Nieto-Castanon, 2012) standalone toolbox (v19b). Data that had been preprocessed using FSL were loaded into the toolbox. A band-pass filter (0.008-0.09 Hz) was applied to the resting state data. Subject specific variables included white matter signal, CSF signal, head motion parameters from realignment, and the scrubbing confound matrix created by FSL's motion outlier tool. ROI to ROI analyses, using the Harvard-Oxford cortical and subcortical atlas (Desikan et al., 2006; Frazier et al., 2005; Goldstein et al., 2007; Makris et al., 2006), were conducted using a priori lobular (Bernard et al., 2012; Grami et al., 2021) ROIs (lobule I-IV, V, VI, VIIb, crus I and crus II). For each lobular ROI, connectivity was assessed for anodal, cathodal, and sham stimulation individually. Group level analyses were as follows: anodal >sham, cathodal>sham, anodal>cathodal, cathodal>anodal. All analyses were thresholded at the $p < 0.001$, with an additional FDR $p< 0.05$ correction.

# Results

Networks after sham stimulation (Figure 3.1) were not consistent with past work investigating lobular cerebellar resting state connectivity (Bernard et al., 2012). In brief, for lobules I-IV we primarily see positive connectivity to the cerebellum and some subcortical structures, with no significant connectivity to motor regions in the cortex, as we would expect. In lobules V, VI, and VIIb, we begin to see cortical connectivity to frontal and parietal regions. In crus I and II, we also see positive connectivity to contralateral regions within the frontal, parietal, and occipital regions, and anti-correlations to similar regions in the ipsilateral hemisphere.

## Lobular Connectivity

Tables 3.1-.3.3 (found in Appendix A) display significant ROI to ROI connectivity statistics, while Figure 3.1 visually displays significant (p-FDR < 0.05) connectivity.

*Anodal Stimulation*. Broadly, anodal stimulation (Table 3.2) gave rise to positive connectivity to regions in the left frontal parietal and temporal regions of the cortex, in addition to connectivity to subcortical regions. This was most clearly exhibited in crus I and II. That is, in crus I, anodal stimulation showed positive connectivity to the frontal and parietal lobes, such as the left PFC, left inferior frontal gyrus, and the posterior parietal cortex. Additionally, there was positive connectivity with subcortical regions, such as the left caudate. Similarly, in crus II, anodal stimulation showed positive connectivity to the frontal lobes, such as the left middle frontal gyrus and left prefrontal cortex in the salience network. Similar patterns were seen in lobules VI, and VIIb. In lobules I-IV, anodal stimulation gave rise to connectivity to the right cerebellum, but connectivity outside the cerebellum was limited.

Interestingly, anodal stimulation also seemed to result in anti-correlations to the right cortical regions. This was again clearly demonstrated in crus I and II. In crus I, there were anti-correlations with ipsilateral regions to parietal and frontal lobe, such as the right intraparietal sulcus, right paracingulate gyrus, and the right sensorimotor area. In crus II, anti-correlations with ipsilateral regions to parietal and frontal lobe, such as the paracingulate gyrus and anterior cingulate gyrus were observed. A similar, but less striking, effect was also seen in lobule VI, and VIIb.

*Cathodal stimulation.* Similar to anodal stimulation, cathodal stimulation (Table 3.3) gave rise to connectivity in the frontal parietal and temporal regions of the cortex, in addition to connectivity so subcortical regions. In crus I, cathodal stimulation gave rise to positive connectivity in cortical regions, such as the left inferior, middle and superior frontal gyrus. In crus II, cathodal stimulation resulted in positive connectivity to frontal and temporal regions, such as

the left inferior frontal gyrus, left frontal pole, and the left middle temporal gyrus. Similar patterns were found in Lobule VI and VIIb.

Cathodal stimulation also resulted in anti-correlations. In crus I, cathodal stimulation led to anticorrelations to the posterior and anterior cingulate cortex, and subcortical regions such as the right thalamus. In Crus II, cathodal stimulation led to anti-correlations in frontal and parietal lobe areas, such as the right anterior cingulate gyrus and right juxtapositional lobule cortex. Similar patterns were observed in lobule VIIb.

We did not find any significant contrasts between stimulation conditions. Though we did not find significant contrasts, we did find notable differences in connectivity patterns. These differences were primarily seen following anodal stimulation to crus I and crus II. Broadly, we saw an increase in connectivity to regions in the left frontal and parietal lobes, and anti-correlations to similar regions in the right hemisphere.

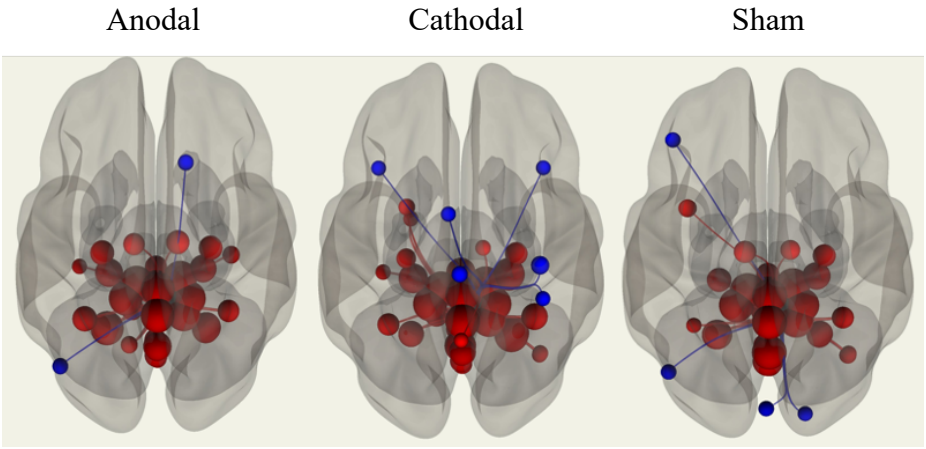

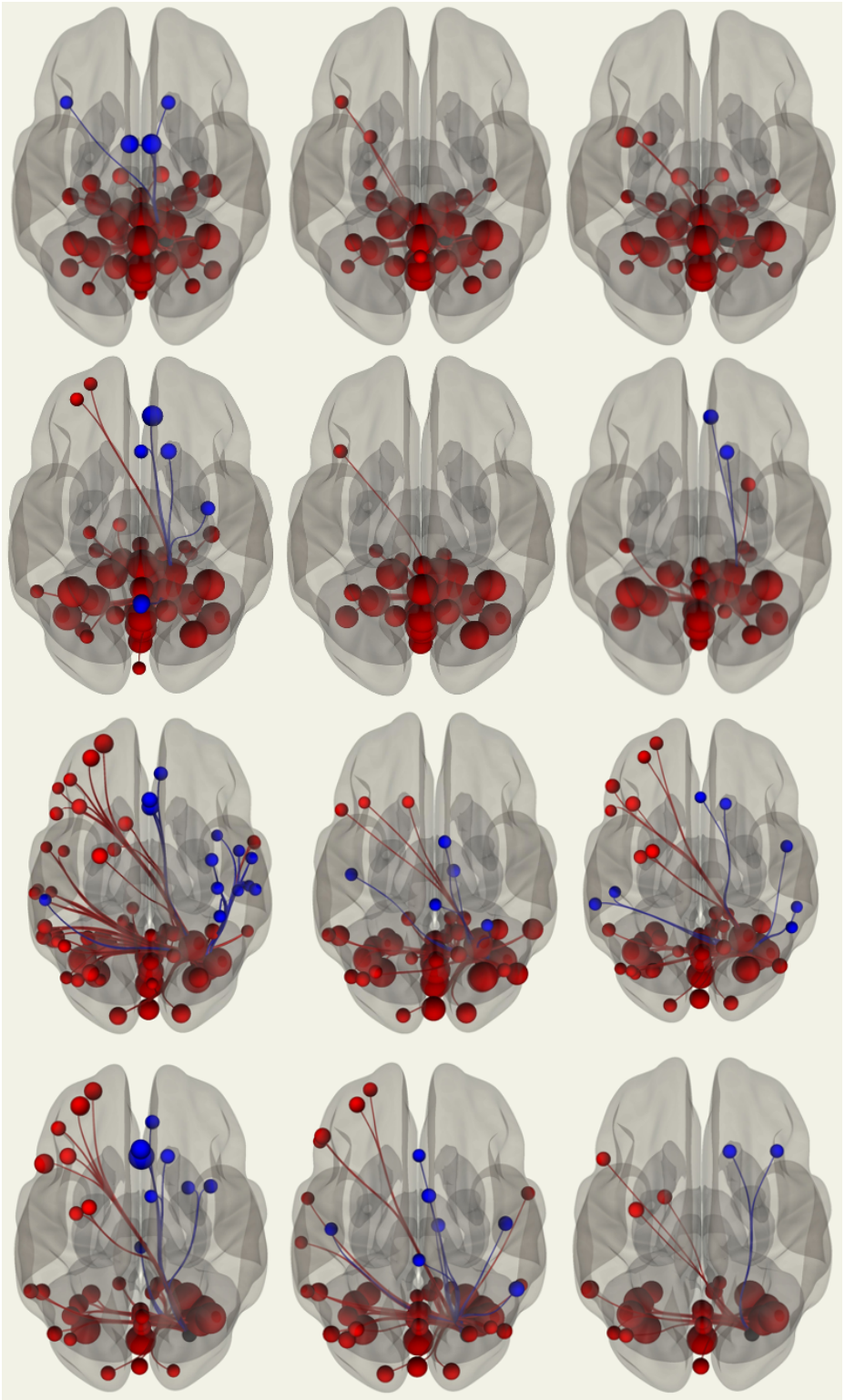

Lobule V

Lobule VI

Crus I

Crus II

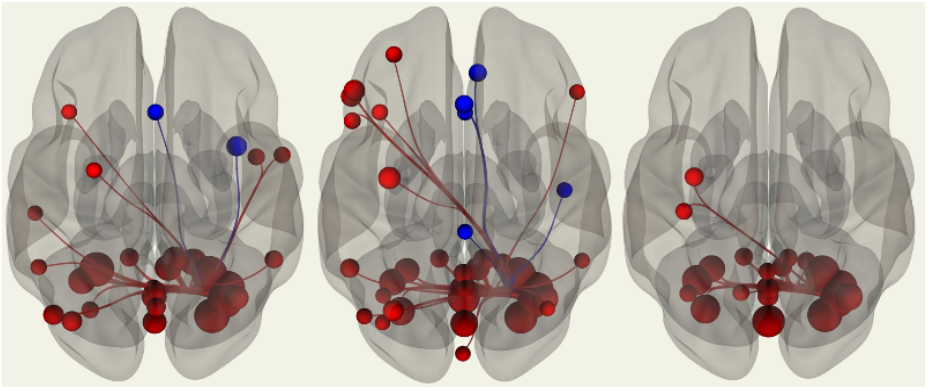

Lobule VIIb

**Figure 3.1 Connectivity by ROI. Superior view. Red indicates positive connectivity and blue indicated negative connectivity.**

**Connectivity Associations with Behavioral Performance**

Here, we examined correlations between connectivity and behavior using a motor (lobules I-IV) and non-motor (crus I) lobular ROI. Correlations were conducted for both reaction time and accuracy variables for the sequence learning and Sternberg task. Behavioral results were reported in chapter 2.

*Sequence Learning*

Table 3.4 (found in Appendix A) displays significant ($p$-FDR < 0.05, cluster level) clusters and Fig. 3.2-3.4 displays these clusters visually.

*Sham.* In lobules I-IV (Figure 3.2), faster reaction times (RT) during sequence learning correlated with connectivity to the left posterior inferior temporal gyrus and slower RT was associated with connectivity with the right posterior inferior temporal gyrus and insular cortex. Better accuracy was associated with lobules I-IV connectivity with bilateral anterior inferior temporal gyrus regions, whereas poor accuracy was associated with the left temporal gyrus.

For the Crus I seed (Figure 3.2), faster RT was associated with connectivity in the frontal and parietal regions, including the right juxapositional lobule cortex, left anterior cingulate gyrus, and the frontal orbital cortex and frontal pole bilaterally. Faster RT was also associated with the

right frontal gyrus and right supplementary motor area. Slower RT was correlated with crus I connectivity to the bilateral inferior temporal gyri and right caudate. Better accuracy was associated with bilateral anterior inferior temporal gyri and poorer accuracy with regions in the left temporal gyrus.

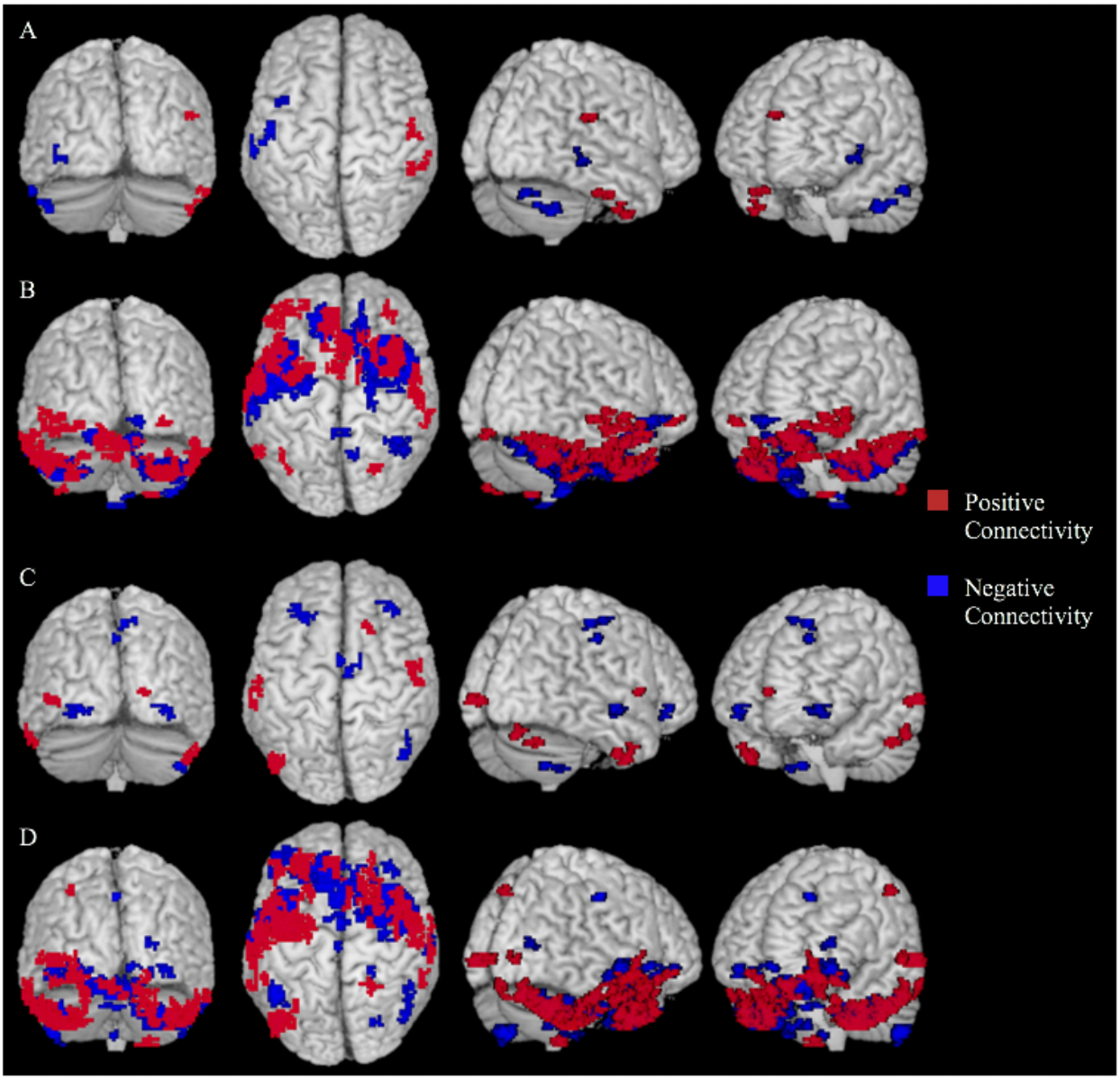


**Figure 3.2 Connectivity associated with performance during sequence learning following sham stimulation. (A) Connectivity from Lobules I-IV associated with reaction time performance following sham stimulation. (B) Connectivity from Lobules I-IV associated with accuracy performance following sham stimulation. (C) Connectivity from Crus I**

**associated with reaction time performance following sham stimulation. (D) Connectivity from Crus I associated with accuracy performance following sham stimulation. Red-Positive Connectivity; Blue-Negative connectivity.**

*Anodal.* In lobule I-IV (Figure 3.3), after anodal stimulation, connectivity to the frontal medial cortex and frontal pole was associated with faster RT. In crus I, anodal stimulation associated increased signal in bilateral temporal poles and anterior frontal pole regions with slower RT, and medial frontal regions, such as the subcallosal cortex bilaterally, with faster RT. Poor accuracy was associated with the right temporal pole.

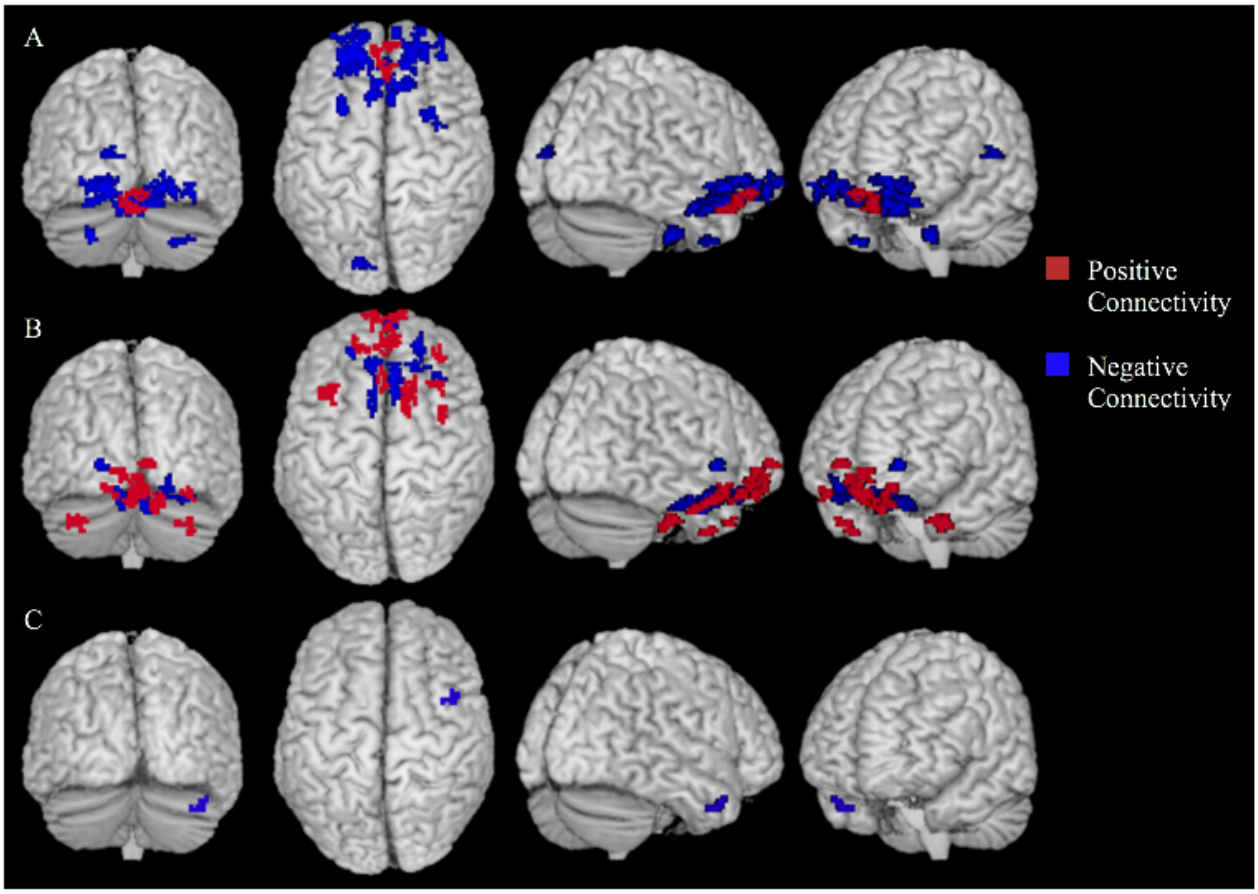


**Figure 3.3 Connectivity associated with performance during sequence learning following anodal stimulation. (A) Connectivity from Lobules I-IV associated with reaction time performance following anodal stimulation. (B) Connectivity from Crus I associated with reaction time performance following anodal stimulation. (C) Connectivity from Crus I associated with accuracy performance following anodal stimulation. Red-Positive Connectivity; Blue-Negative connectivity.**

*Cathodal.* In lobule I-IV (Figure 3.4), slower RT was associated with connectivity to the right frontal pole and middle frontal gyrus after cathodal stimulation. Connectivity with the left frontal and right temporal pole were associated with superior accuracy, whereas poor accuracy was correlated with connectivity to the left precuneus and subcortical regions like the thalamus and lobules VIII and X in the cerebellum.

For the crus I seed (Figure 3.4), slower RT was associated with connectivity to the right temporal pole and right lobule VIII in the cerebellum, but faster RT with connectivity to the left inferior temporal gyrus and left crus II. Superior accuracy was related to connectivity to the right inferior temporal gyrus and lobules VIIb and VIII in the cerebellum, but poorer accuracy with the left inferior, left middle temporal gyrus, and the right lobule VIII in the cerebellum.

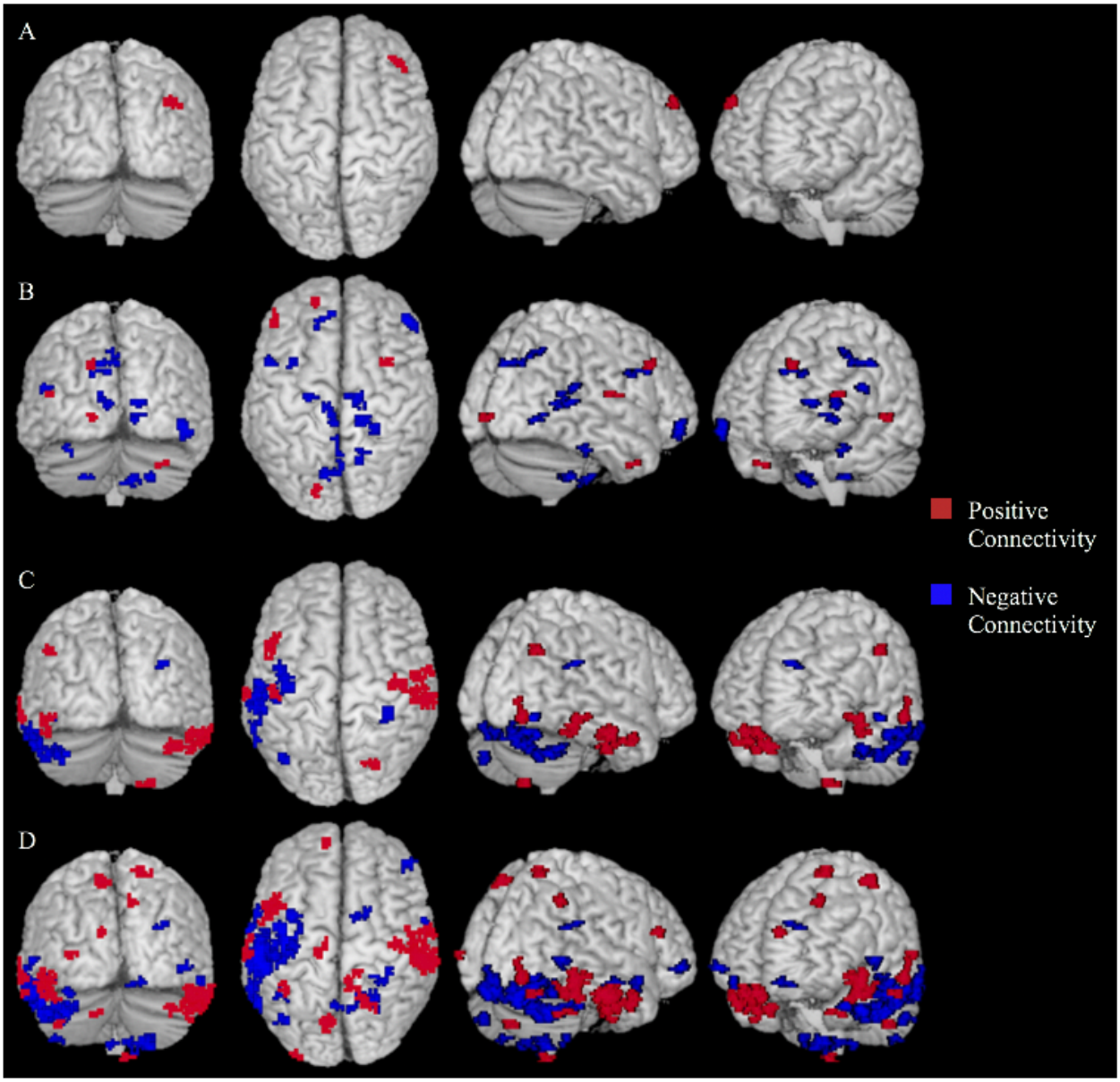


**Figure 3.4 Connectivity associated with performance during sequence learning following cathodal stimulation. (A) Connectivity from Lobules I-IV associated with reaction time performance following cathodal stimulation. (B) Connectivity from Lobules I-IV associated with accuracy performance following cathodal stimulation. (C) Connectivity from Crus I associated with reaction time performance following cathodal stimulation. (D) Connectivity from Crus I associated with accuracy performance following cathodal stimulation. Red-Positive Connectivity; Blue-Negative connectivity.**

Together, we saw connectivity from the cerebellum to frontal and temporal regions were generally related to task performance. For both lobules I-IV and crus I, after cathodal stimulation,

we saw more associations with accuracy than anodal stimulation, perhaps suggesting cathodal stimulation was better at modulating accuracy performance than anodal stimulation. Further anodal stimulation seemed to be particularly associated with faster RT in frontal regions for both lobules I-IV and Crus I.

*Sternberg.*

Table 3.5 (found in Appendix A) displays significant ($p$-FDR < 0.05, cluster level) clusters and Fig. 3.5-3.7 displays these clusters visually.

*Sham.* In lobule I-IV (Figure 3.5), there were no significant correlations between connectivity strength and RT or accuracy. For the crus I seed, poor accuracy correlated with connectivity to parietal regions such as the bilateral supramarginal gyrus and the bilateral postcentral gyrus. No significant correlations between crus I connectivity and RT were found.

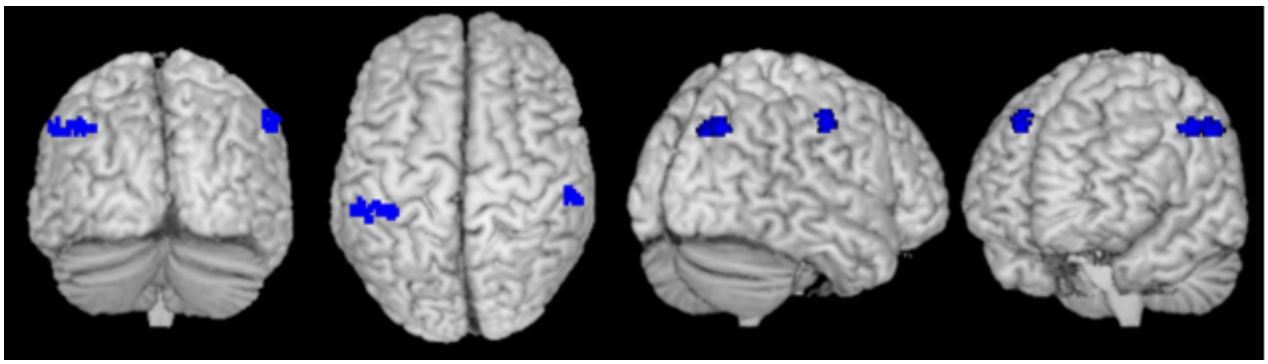

**Figure 3.5 Connectivity from Crus I associated with accuracy performance during working memory following sham stimulation. Blue-Negative connectivity.**

*Anodal.* In lobule I-IV (Figure 3.6), slower RT was associated with connectivity to the left frontal pole and bilaterally in the temporal fusiform cortex and temporal gyrus. Faster RT correlated with connectivity to lateral regions of the temporal pole and anterior inferior temporal gyrus. Better accuracy was associated with connectivity to the left frontal pole and the bilateral

temporal pole and temporal fusiform cortex. Additionally, poor accuracy correlated with connectivity to anterior regions in the bilateral temporal gyrus and temporal fusiform cortex.

In crus I (Figure 3.6), faster RT was associated with connectivity to regions inside the left frontal pole and bilateral temporal pole. Slower RT was associated with connectivity to the right frontal pole and regions within the posterior temporal pole and anterior fusiform gyrus bilaterally. Better accuracy correlated with connectivity to regions inside the right frontal pole and bilateral temporal pole. Poor accuracy was associated with the left frontal pole and regions within the posterior temporal pole bilaterally.

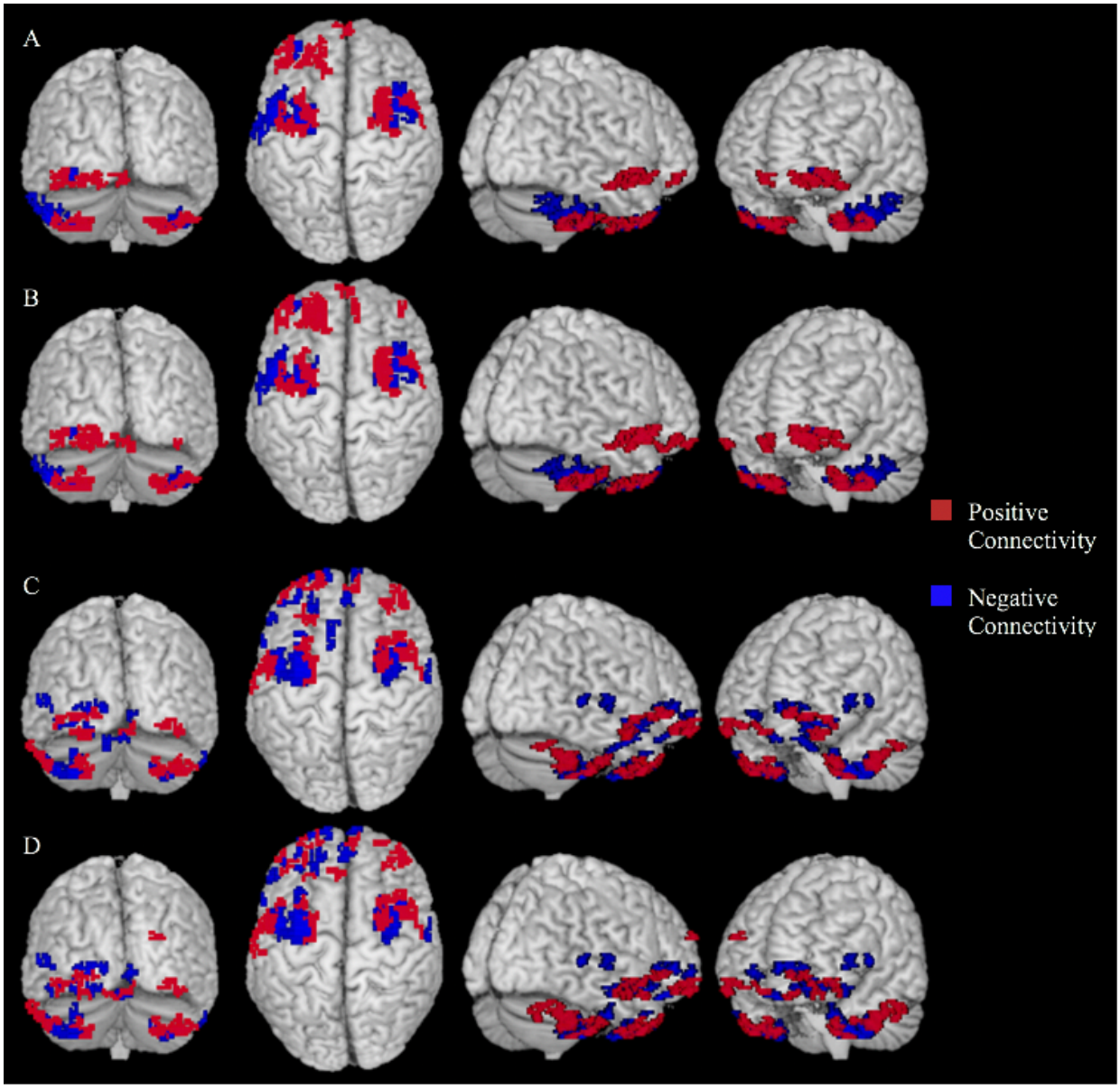


**Figure 3.6 Connectivity associated with performance during working memory following anodal stimulation. (A) Connectivity from Lobules I-IV associated with reaction time performance following anodal stimulation. (B) Connectivity from Lobules I-IV associated with accuracy performance following anodal stimulation. (C) Connectivity from Crus I associated with reaction time performance following anodal stimulation. (D) Connectivity from Crus I associated with accuracy performance following anodal stimulation. Red-Positive Connectivity; Blue-Negative connectivity.**

*Cathodal.* In lobule I-IV (Figure 3.7), faster RT correlated with connectivity to the left lateral occipital cortex. Better accuracy was associated with the left frontal medial cortex, left

frontal pole and the left subcallosal cortex. Poor accuracy was correlated with the left precental and postcentral gyrus, right temporal pole, and left lobule VIII in the cerebellum.

In crus I (Figure 3.7), faster RT correlated with connectivity to the parietal regions such as the right precuneous and right superior parietal lobule. Poor accuracy was related to connectivity with frontal and temporal regions such as the right subcallosal cortex, left temporal pole, and left frontal medial cortex.

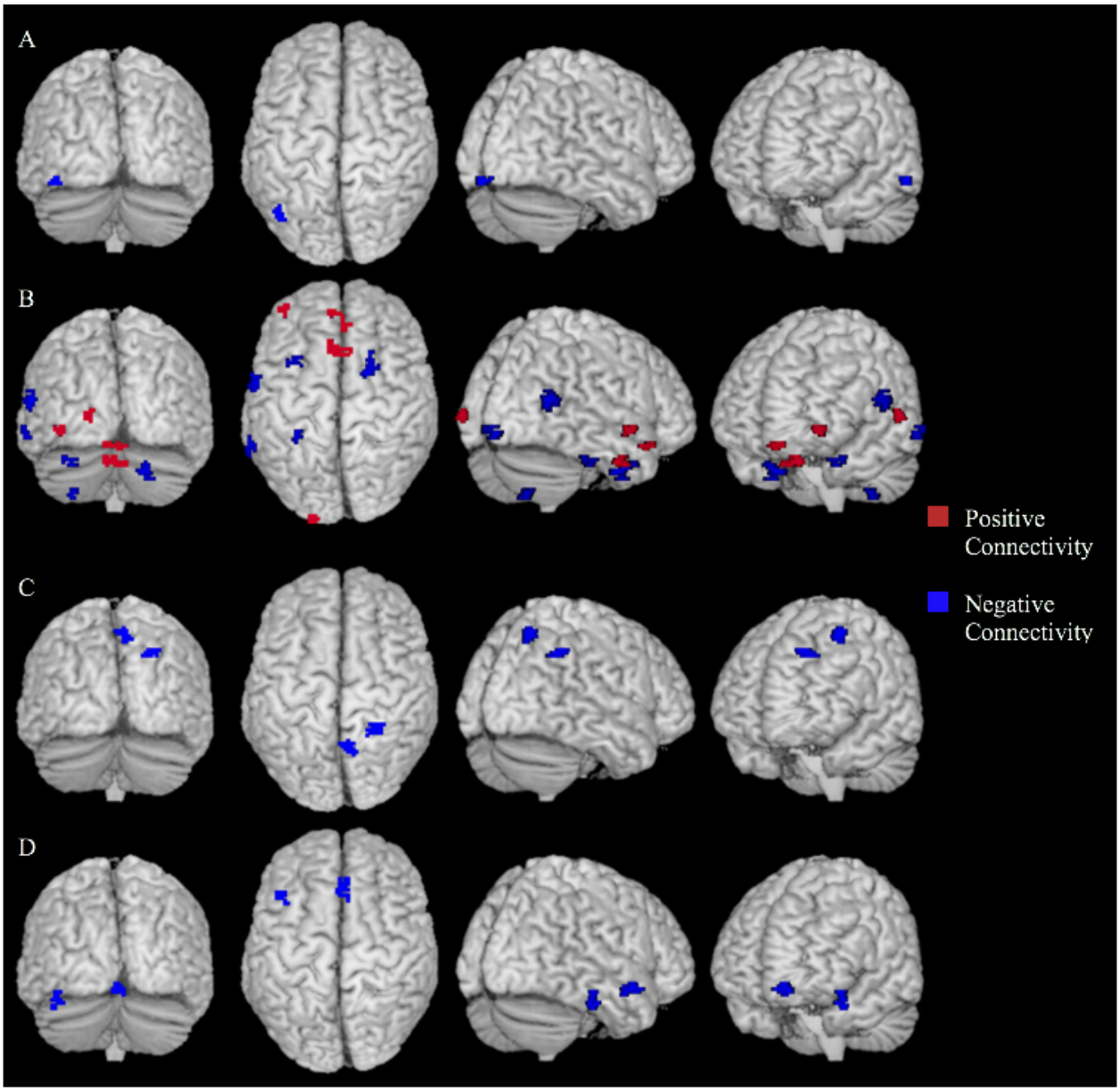

**Figure 3.7 Connectivity associated with performance during working memory following cathodal stimulation. (A) Connectivity from Lobules I-IV associated with reaction time performance following cathodal stimulation. (B) Connectivity from Lobules I-IV associated with accuracy performance following cathodal stimulation. (C) Connectivity from Crus I associated with reaction time performance following cathodal stimulation. (D) Connectivity from Crus I associated with accuracy performance following cathodal stimulation. Red-Positive Connectivity; Blue-Negative connectivity.**

Together, we saw connectivity between the cerebellum and frontal and temporal regions were generally related to verbal working memory task performance. In contrast to sequence learning, after cathodal stimulation, cerebello-cortical connectivity seemed to be associated with faster RT, particularly in frontal regions for both lobule I-IV. Interestingly, anodal stimulation was associated with better accuracy in frontal regions for both lobule I-IV and crus I.

## Discussion

Cerebellar tDCS is an increasingly common technique for modulating cerebellar function, though many of the results to this point have been mixed (Oldrati & Schutter, 2018). Further, tDCS can be used to understand how cerebellar networks with the cortex differ after perturbation, which can in turn provide insights into aging as well as neurological and psychiatric illnesses where the cerebellum and cerebello-cortical networks are impacted (Ferrucci et al., 2016; van Dun & Manto, 2018). To this point however, most work has focused on region of interest analyses and language networks, with little work looking at other nonmotor processing domains using a whole brain approach. The current work used tDCS to better understand whole brain cerebello-cortical connectivity. Broadly, subjective interpretations of connectivity demonstrated that stimulation did not modulate connectivity in lobules I-IV, and V. Alternatively, anodal stimulation increased contralateral connectivity, particularly in crus I and II. Critically, contrasts between stimulation conditions did not show differences in connectivity from lobules within the cerebellum. However, subjective interpretations of connectivity suggested the potential for differences in cerebello-

cortical connectivity, particularly in lobules associated with the prefrontal cortex, following stimulation. Notably of course, these were solely based on within group patterns of activation, and because of these we are limited in our speculations about these patterns. Finally, this work demonstrated differing patterns with respect to the associations between connectivity after stimulation and behavioral performance on both a motor sequence learning and verbal working memory task, which was supported by variability in behavioral performance. This change in performance has methodological implications. Our findings are discussed below, though we should note that much of the interpretation is based on subjective differences in connectivity, which garner the need for further investigation to substantiate evaluations made in the current work.

**Connectivity Patterns and Stimulation**

*Motor Regions.* Broadly, when examining connectivity in the sham stimulation group we did not see the expected cerebello-cortical connectivity patterns one might expect (Buckner et al., 2011; King et al., 2019), though there was connectivity to some subcortical structures like the thalamus and hippocampus. However, we did see lobular connectivity within the cerebellum. Specifically, in lobules I-IV and lobule V we saw connectivity to regions within the cerebellum. Stimulation to cerebellar motor regions did not result in significant connectivity differences compared to sham. This was unexpected in light of previous physiological work that has shown that stimulation alters the M1-cerebellar connection (Galea et al., 2009). Cathodal stimulation resulted in cortical excitability decreases, and anodal stimulation resulted in increases. But, variability in the effect of cerebellar tDCS is not uncommon, particularly when examining motor function and learning (Buch et al., 2017). Continued work is needed to determine why this variability exists, though our work here may provide some initial insights.

There might be several additional reasons for why we did not find any differences in connectivity with stimulation. First, stimulation parameters, such as electrode placement and size might not be conducive to modifying action potentials in lobules I-V in the cerebellum (Rampersad et al., 2014). Indeed, investigation of electric field distributions in the cerebellum suggested anterior regions of the cerebellum, such as lobules I-V, and the vermis were not well stimulated (Rampersad et al., 2014). This was the result of the curvature of the cerebellum and its placement deep within the brain. Further, recent work suggested that stimulating different cerebellar regions can have different behavioral and neural effects (Rice et al., 2021). Specifically, anodal stimulation targeting lobule VIIb improved language task performance and increased activation in cortical regions. However, anodal stimulation targeting lobule V had no impact on task performance, but disrupted task relevant activation increases. This further provides evidence that motor lobules of the cerebellum are difficult to target and modulate and electrode placement is crucial in inducing neural and behavioral change.

Second, the cerebellum is a complex structure and it is difficult to know how the cerebellum might be impacted by stimulation, as the effect depends on current flow direction, relative to axonal position (Chan & Nicholson, 1986). This, coupled with the curvature of the cerebellum, may contribute to the variable effects seen here and elsewhere. This also lends itself to the ongoing discussion about individual differences in the responsiveness of tDCS (Labruna et al., 2019). Third, it is still not clear which cells types are actually influenced by cerebellar tDCS (Grimaldi et al., 2016). Our hypotheses are based on the modulation of Purkinjie fibers, but their activity is not readily captured by fMRI, instead mossy and climbing fibers might drive the fMRI signal. Though optogenetic work suggests Purkinjie cells respond to cerebellar tDCS (Grimaldi et al., 2016), it is unclear whether other cells were also modulated. Though these findings are ultimately null results,

this does provide further data that indicates how cerebellar tDCS might affect cerebello-cortical connectivity, specifically that the impact of stimulation may vary based on region.

*Non-motor regions.* Similar to motor regions, stimulation to non-motor regions did not result in significant connectivity differences when compared to the sham stimulation group. However, subjective interpretations of connectivity patterns suggested anodal stimulation altered connectivity patterns both within the cerebellum and across the left and right hemispheres, particularly in frontal and parietal regions. This was most noticeable in crus I and II, but were also observed in lobule VI and VIIb. In crus I, compared to sham. These results were generally in line with past work from Galea et al. (2009) that suggest anodal stimulation would increase cortical connectivity. Further, this was in line with past cerebellar tDCS and imaging work that found that anodal tDCS to the right cerebellum increased crus I and II activation and connectivity in cortical language centers (D'Mello et al., 2017) and areas involved in the motor control of speech (Turkeltaub et al., 2016). However, this was the first study to suggest changes to frontal and parietal regions associated with non-motor cognitive processing outside of language as a result of cerebellar stimulation using a whole brain approach.

The pattern of results seemed to suggest that anodal stimulation gave rise to anti-correlations with ipsilateral regions in the cortex, possibly suggesting a greater need for cortical scaffolding. That is, down regulation in the cerebellum following anodal stimulation might result in the need for greater connectivity to the contralateral hemisphere to compensate for the degraded communication between the cerebellum and the ipsilateral cortex. As this does not happen following cathodal stimulation, the degraded output of the cerebellum is driving the compensatory connectivity. Interestingly, optogenetic work has suggested that anodal stimulation should degrade connectivity to the cortex (Galea et al., 2009; Grimaldi et al., 2016). Perhaps this degradation is

not widespread, but hemisphere dependent. Perhaps, the anti-correlations in the ipsilateral cortex are forcing the contralateral cortex to carry the majority of the cortical processing, which might have implications during functional task performance.

Alternatively, cathodal stimulation did not seem to meaningfully change connectivity to the cortex. This was again counter to our hypothesis, but was seemingly in line with the cerebellar tDCS resting state literature (D'Mello et al., 2017; Turkeltaub et al., 2016), by default. Critically, this work, to our knowledge, was the first attempt to assess the effect of cathodal stimulation over the right cerebellum on cerebello-cortical connectivity. Perhaps stimulation location might explain the lack of effect. Recent work using anodal stimulation found differential behavioral and neural effects of regional cerebellar tDCS, such that anodal tDCS affected performance and cortical activation when applied to the posterolateral cerebellum, but no effect when applied to the sensorimotor cerebellum (Rice et al., 2021). Though the aforementioned worked used anodal stimulation, cathodal stimulation over the stimulation location in the current work might not be conducive to modulating connectivity.

Therefore, we suggest, in this sample of healthy younger adults, there are changes in cerebellar frontal interactions with stimulation that support degraded cerebellar processing and communication with the cortex is occurring. Research in aging and disease might provide insights into degraded cerebello-cortical interactions. Specifically, disruptions to cerebellar function and network connectivity in aging (Bernard et al., 2013) or disease (Allen et al., 2007; Bai et al., 2009) may negatively impact prefrontal function and processing. Cerebellar resources might be important for supporting cortical processing and provide crucial scaffolding for normative performance and function. However, anodal stimulation might disrupt this scaffolding by perturbing cerebello-cortical connectivity. Existing compensatory scaffolding models broadly

suggest increased activation to compensate for lost ability in advanced age (Cabeza, 2002; Cabeza, Anderson, Locantore, & McIntosh, 2002; Park & Reuter-Lorenz, 2009; Reuter-Lorenz & Campbell, 2008; Reuter-Lorenz & Park, 2014), but these models focused primarily on the prefrontal cortex, and did not involve the cerebellum, though past work suggested the cerebellum might be involved (Bernard et al., 2013). The current work might parallel the perturbed cerebello-cortical connectivity found in advanced age or disease, which would suggest some cerebellar contribution to cortical processing, allowing a better understanding of cerebello-cortical interactions and how these interactions support cortical scaffolding.

**Connectivity and Behavior**

In general, the current work demonstrated a relationship between behavioral task performance and connectivity broadly revolving around connectivity with regions in the frontal and temporal poles following stimulation. These are regions typically active during motor (Dhamala et al., 2003; Newton et al., 2008; Seidler et al., 2005; Wei et al., 2017) and working memory performance (Emch et al., 2019; Jonides et al., 1997, 1998). Though the connectivity patterns were relatively mixed, there are a few notable patterns that we believe are worth discussing as they have implications for polarity specific parameters typically used in cerebellar tDCS (Ferrucci et al., 2015; Galea et al., 2009). First, we found that the cerebello-cortical connectivity in the cathodal group predicted sequence learning accuracy performance, and anodal stimulation was more likely to predict reaction time. This was found for both lobules I-IV and crus I. This might have specific methodological implications, as currently the behavioral literature is largely mixed (Oldrati & Schutter, 2018), but predicts polarity specific outcomes, regardless of the dependent variable (Galea et al., 2009). However, it is possible that modulation of specific

outcome variables might be dependent on specific stimulation parameters, as evidenced by cathodal stimulation predicting sequence learning accuracy performance, but not reaction time.

Second, methodological parameters may also influence how stimulation affects outcome variables across tasks. For example, in the current data set, connectivity in the anodal stimulation group was associated with slower reaction times in a sequence learning task, but faster reaction times in a Sternberg task. Critically, this opposing effect was seen with connectivity in similar regions in the frontal lobe, perhaps indicative of the cognitive component need to complete either task (Doyon et al., 2018; Jonides et al., 1997). Recent work by Maldonado and colleagues found a similar pattern of results in which anodal stimulation negatively affected reaction time during a Sternberg task, but did not alter performance on a sequence learning task (Maldonado & Bernard, 2021). As stated above, the cerebellar tDCS literature is relatively mixed (Oldrati & Schutter, 2018), and stimulation patterns were applied similarly, regardless of task (Galea et al., 2009). However, it is possible that stimulation parameters might affect tasks differently, perhaps by influencing the underlying processes needed to complete the task.

Together, there is a clear relationship between task performance and cerebello-cortical connectivity in frontal and temporal regions of the cortex after cathodal and anodal stimulation. However, specific stimulation parameters might be needed to induce a specific outcome. Though past work has typically been framed in the context of polarity specific hypotheses to predict behavioral change (Galea et al., 2009), it might be necessary to review the polarity specific nature of cerebellar tDCS parameters, such that these parameters become specific to the dependent variable being examined or the task being administered.

**Conclusions**

The current work aimed to better understand cerebello-cortical connectivity after tDCS, using a whole-brain approach. However, while we reported qualitatively different patterns of connectivity between sham, anodal, and cathodal stimulation, there were no significant group differences in the stimulation group contrasts. Further, we found that stimulation alters the relationships between cerebello-cortical connectivity and both sequence learning and verbal working memory task performance. Despite this unexpected finding with respect to group differences, subjective interpretations of connectivity differences between brain regions across stimulation groups provided novel and important insights into the effects of tDCS on cerebellar connectivity and function. Further, this work provided new insights into cerebello-cortical connectivity in the face of perturbation which has implications for aging and both neurological and psychiatric disease. Specifically, initial support for the cerebellum as a component for existing scaffolding models might be evident in the current data, further supporting cerebellar inclusion into models describing frontal lobe activation in health and disease. However, at this point additional work that further considers tDCS stimulation parameters and functional boundaries within the cerebellum is warranted.

# CHAPTER IV

# GENERAL DISCUSSION AND CONCLUSIONS

The literature implicating the cerebellum in motor and non-motor processing is growing (Buckner, 2013; Schmahmann et al., 2019; Stoodley, 2012; Stoodley et al., 2012b). However, little work has looked to understand why the cerebellum might be involved in motor and non-motor processing. Thus, this dissertation used tDCS and neuroimaging techniques to modulate cerebellar output to understand how the cerebellum might support motor and non-motor processing. The first study investigated how tDCS over the right cerebellum modulates behavioral performance and cortical activation. Broadly, the behavioral findings align with the polarity specific nature of cerebellar tDCS (Galea et al., 2009; Grimaldi et al., 2016), such that cathodal stimulation had a benefit on reaction time, whereas anodal stimulation hindered accuracy performance. The effect of anodal stimulation was supported by the functional imaging data, such that there was bilateral cortical activation following anodal stimulation. We speculate that anodal stimulation degraded cerebellar processing and output to the cortex, which ultimately results in greater cortical activation to compensate for the loss of cerebellar resources. The second study examined cerebellar resting state connectivity, in an effort to better understand cerebello-cortical connectivity patterns. Though there were no significant effects of stimulation, subjective interpretations of the data suggest anodal stimulation modulated connectivity patterns, particularly in crus I and II. Additionally, we found correlations between cerebello-cortical connectivity and task performance in frontal and temporal regions of the cortex after cathodal and anodal stimulation. Together, this work further implicates the cerebellum in motor and non-motor processing, indicating an important role for the cerebellum as a component for existing scaffolding models of function and behavior.

## Cerebellum and Working Memory

The literature using tDCS to implicate the cerebellum in working memory is relatively mixed (Oldrati & Schutter, 2018), and has broadly relied on behavioral work to understand the cerebello-cortical relationship (Boehringer et al., 2013; D'Mello et al., 2017; Ferrucci et al., 2008; Küper et al., 2019; Macher et al., 2014; Majidi et al., 2017; Pope & Miall, 2012; Rice et al., 2021; Spielmann et al., 2017; Turkeltaub et al., 2016; van Wessel, Claire Verhage, Holland, Frens, & van der Geest, 2016; Verhage, Avila, Frens, Donchin, & van der Geest, 2017). Thus, there was only a theoretical understanding of how changes in cortical activation might affect working memory task performance. The current work used neuroimaging to better understand how changes in cortical activation might inform our understanding of behavioral changes. Behaviorally, we found that both anodal and cathodal stimulation improved reaction time, but stimulation had no effect on accuracy. Functionally, when examining activation following cathodal stimulation under high load, we found activations in frontal, parietal and cerebellar regions associated with verbal working memory (Jonides et al., 1997; Stoodley, 2012), likely resulting in the improved reaction time performance following cathodal stimulation. However, when contrasting high and low load following anodal stimulation, we found greater frontal activations to the inferior, middle and superior frontal regions, which are also regions implicated in verbal working memory task performance (Emch et al., 2019; Jonides et al., 1997, 1998). We believe this increase in activation also contributed to the improved reaction time performance following anodal stimulation.

We propose this effect of anodal stimulation is of significance, as the increased cortical activation may be compensation as a result of diminished cerebellar output, given what is known about the impact of anodal stimulation on the cerebellum (Galea et al., 2009; Grimaldi et al., 2016). Interestingly, working memory activations are thought to be relatively lateralized in young adults,

such that activations seem to primarily emerge in the left hemisphere (Reuter-Lorenz et al., 2000). In advanced age, purportedly as a way to compensate for neural and functional integrity decline, older adults exhibit bilateral frontal activations to complete the same task as young adults (Cabeza et al., 2018; Reuter-Lorenz & Cappell, 2008; Reuter-Lorenz & Park, 2014). However, when the compensatory mechanism is not enough, older adults experience deficits in cognitive performance (Reuter-Lorenz & Park, 2014). In the current work, it is possible that connectivity to the frontal lobes was attenuated following anodal stimulation, as might be predicted by Grimaldi et al (2016), resulting in the need for more cortical processing to ensure successful task completion. That is, when the cerebellum was not processing information from the cortex adequately, more cortical resources were needed to make up for this, resulting in increased cortical activation. Further, the internal models stored in the cerebellum and used to help support cortical processing might have been negatively impacted following anodal stimulation, hindering task performance (Bernard & Seidler, 2014; Filip et al., 2019; Ito, 2008). Therefore, in this specific data set, cathodal stimulation resulted in a behavioral boost manifesting as improved reaction time during a verbal working memory task. But we might also be observing an effective compensatory reaction in frontal lobes, such that when anodal stimulation diminished cerebellar output and degraded internal models during high cognitive load tasks, the cortex was able to successfully recruit more neural resources bilaterally in the frontal lobes, which ultimately improved reaction time following anodal stimulation. Taken together, the cerebellum plays an important role in working memory, such that the cerebellum provides resources to the cortex, especially when processing demands are high.

### Cerebellum and Sequence Learning

Similar to the working memory literature, the sequence learning literature is also mixed with respect to the impact of cerebellar tDCS, and there is little imaging work to help interpret the

mixed results (Buch et al., 2017). We found that cathodal stimulation helps improve reaction time, but anodal stimulation hinders accuracy, particularly during late learning. This effect of accuracy might be of note, as the cerebellum was particularly active during early learning when procedural memories were created (Imamizu et al., 2000), but was less active during late learning when the cortex relied on the internal models that were created during early learning phases (Doyon et al., 2018). However, if these internal models were not adequately formed during early learning due to anodal stimulation disrupting communication with the cortex, this could negatively affect performance during late learning. It is possible that anodal stimulation was disrupting the formation of these models, particularly in early learning, which had an adverse impact on accuracy in late learning as the brain cannot rely on these models.

Our imaging data suggested anodal stimulation increased cortical activations, in key frontal (Emch et al., 2019; Jonides et al., 1997), parietal (Honda et al., 1998; Lissek et al., 2013) and cerebellar (Stoodley, 2012) regions associated with non-motor cognition. Critically, the activations in parietal regions were greater following anodal stimulation when compared to cathodal, suggesting that this may be extensive compensatory activation. Unlike in the working memory task, this increased bilateral activation was not enough to compensate for the loss of cerebellar function, which resulted in poor performance in late learning. We propose that the internal models that should have been created during early learning (Imamizu et al., 2000), were not developed adequately, such that in late learning we saw poor accuracy as a result of degraded output from the cerebellum, and poorly formed internal models. This would result in a greater need for cortical processing, but it might also explain why accuracy still suffered, as not enough cortical resources were brought on. Since the cerebellum was no longer able to provide resources to the cortex, cortical activations increased to complete a task efficiently (Bernard et al., 2013; Filip et al., 2019).

Critically, cortical activation during a sequence learning task indicated parietal activation was important for recall of the sequence (Honda et al., 1998), likely the process needed to complete the sequence task during later learning. This provides further evidence to suggest that the cerebellum plays a supporting role in mon-motor cognitive processing and degradation of cerebellar output has functional and behavioral consequences.

## Cerebellum and Resting State Networks

The cerebellar resting state literature is relatively consistent, in that anodal stimulation seems to benefit language processing (D'Mello et al., 2017) and production (Turkeltaub et al., 2016). However little work has examined cerebello-cortical connectivity as it relates to non-motor processing following cerebellar tDCS using a lobular approach. Therefore, we used cerebellar tDCS to better understand whole brain cerebello-cortical connectivity to regions implicated in non-motor processing. We did not find significant effects of stimulation, but subjective interpretations of the results did show notable patterns that were worth considering. Broadly, when examining connectivity in motor regions (Lobules I-IV and V) of the cerebellum following stimulation, we did not see the expected cerebello-cortical connectivity patterns one might to expect (Buckner et al., 2011; King et al., 2019), though methodological considerations during active stimulation such as electrode placement and size (Rampersad et al., 2014), and cytoarchitecture (Chan & Nicholson, 1986; Grimaldi et al., 2016) might influence these results. Alternatively, connectivity in non-motor regions did show the expected connectivity patterns, and this was most noticeable in crus I and II. Lastly, we assessed the relationships between behavioral task performance and connectivity which broadly demonstrated associations between connectivity to frontal and temporal lobes and behavior. Critically, specific stimulation parameters might be needed to induce a specific behavioral outcome. Though past work has typically been framed in the context of polarity specific

hypotheses to predict behavioral change (Galea et al., 2009), it might be necessary to review the polarity specific nature of cerebellar tDCS parameters, such that these parameters may be specific to the dependent variable being examined or the task being administered.

Together, these findings provide further data that indicates how cerebellar tDCS might affect cerebello-cortical connectivity and interactions, specifically that the impact of stimulation may vary based on region and dependent variable assessed. Further, this was the first study to suggest changes to frontal and parietal regions associated with non-motor cognitive processing outside of language as a result of cerebellar stimulation using a whole brain approach. Similar to the functional work provided above, we suggest that in this sample of healthy young adults, there were changes in cerebello-frontal interactions following anodal stimulation that indicated a negative impact on cerebellar processing had occurred. Cerebellar resources were important for supporting cortical processing and provided crucial scaffolding for normative performance and function. However, anodal stimulation disrupted this scaffolding by perturbing cerebello-cortical connectivity, negatively affecting cortical processing. The current work might parallel the perturbed cerebello-cortical connectivity found in advanced age (Bernard et al., 2013) and disease (Allen et al., 2007; Bai et al., 2009), which would suggest some cerebellar contribution to cortical processing, allowing for a better understanding of cerebello-cortical interactions and how these interactions support cortical scaffolding.

## The Cerebellum as a Scaffolding Structure

The main goal for this dissertation was to better understand the functional importance of cerebello-cortical interactions during non-motor cognitive processing. It is well understood that the cerebellum is active during non-motor processing (Buckner, 2013; Schmahmann et al., 2019; Stoodley, 2012; Stoodley et al., 2012b), but little work has examined the relative contributions of

the cerebellum. In behavioral (Ballard et al., 2019; Cantarero et al., 2015; Ferrucci et al., 2008; Ferrucci et al., 2013; Hardwick & Celnik, 2014; Jongkees et al., 2019; Maldonado & Bernard, 2021), functional (Macher et al., 2014), and resting state data (D'Mello et al., 2017; Turkeltaub et al., 2016) we see anodal stimulation modulate behavioral performance, cortical activation and connectivity networks. The current work consistently demonstrates increased cortical activation following anodal stimulation, or increased connectivity to contralateral hemispheres during resting state, perhaps as a compensatory mechanism.

Optogenetic work has suggested that anodal stimulation to the cerebellum excites inhibitory Purkinje cells, which decreases signal to the cortex (Grimaldi et al., 2016). The current work broadly demonstrated cortical compensation for lost cerebellar input and processing following anodal stimulation, indicating the supporting role the cerebellum played in task performance. Of note, these changes in cortical activation occurred when cognitive processing demands were high, which was evident during high load trials in a Sternberg task. This might indicate that the cerebellum was relied upon when cortical regions were taxed. That is, some offloading of processing via internal models may occur when tasks get more difficult. Critically, the increase in activation was beneficial in regard to behavioral performance, providing an example of a successful compensatory response to degraded cerebellar output. Additionally, the current work might also suggest anodal stimulation negatively impacted the creation of internal models. That is, in sequence learning we saw poor accuracy during late learning following anodal stimulation, which was when the task was well learned and task completion should be more automatic (Doyon et al., 2018; Imamizu et al., 2000). However, the decrease in performance might be the result of poorly created models, as anodal stimulation disrupted creation of the internal model needed by the cortex during late learning. In this instance, the compensatory response was

not successful, though the expected cortical response was present. Together, degraded output of the cerebellum demonstrates the importance of the cerebellum during motor and non-motor processing. That is, the cerebellum places a supporting role in cortical processing, providing resources when the cortex is taxed, or support when internal models are not implemented effectively.

This new insight has particularly strong implications in a number of existing compensatory models (Cabeza, 2002; Cabeza et al., 2018; Park & Reuter-Lorenz, 2009; Reuter-Lorenz & Park, 2014). Briefly, as a result of neural degeneration, such as decreases in cortical volume (Raz et al., 2005), white matter changes (Head et al., 2004; Wen & Sachdev, 2004), and changes in neurotransmitters (Li et al., 2001; Yang et al., 2003), older adults experience functional deterioration, resulting in decreased behavioral performance. However, a growing line of work indicated there were several mechanisms by which neural degradation was overcome. One of the most prominent findings was increased cortical activation, or "overactivation" (Reuter-Lorenz & Cappell, 2008), with most models indicating this increase was bilateral (Cabeza et al., 2018; Reuter-Lorenz & Cappell, 2008; Reuter-Lorenz & Park, 2014). That is, in young adults, activation was typically lateralized, but became bilateral in advanced age. This was thought to be compensatory in nature and was able to help maintain performance (Cabeza et al., 2018; Reuter-Lorenz & Park, 2014). Critically, these models and much of the work that supported this model has focused on the frontal and parietal lobes, and ignored the cerebellum. However, the current work would suggest that cerebellum should be involved, as degraded cerebellar output mimicked degraded cortical output, suggesting that the cerebellum supported cortical processing, and without cerebellar output, the brain needed to compensate for the lack of resources.

In regard to the cerebellum, it is generally understood that in advanced age cerebellar volume declines (Bernard & Seidler, 2013b; Han et al., 2020; Hoogendam et al., 2012; Koppelmans et al., 2015) and there is a decrease in connectivity with the cortex (Bernard et al., 2013; Ferreira & Busatto, 2013). This degradation is behaviorally relevant as internal models for procedures are formed in the cerebellum and are used to guide behavior (Ito, 2008; Ramnani, 2006). Critically, if these models are not created properly, or the ability to follow these models is degraded, there are performance consequences (Bernard & Seidler, 2014). The current work would suggest that the cerebellum should be integrated into these models (Bernard & Seidler, 2014; Filip et al., 2019), and should be considered an integral support system for cortical processing. That is, degraded cerebellar output and graded cortical function both result in the same compensatory mechanisms. This would indicate that the cerebellum is needed for cortical processing, and should be considered in these models. Therefore, we propose that the cerebellum plays a supporting role in cortical processing, particularly in motor and non-motor processing. That is, we suggest that the cerebellum provides resources to help execute cortical processing, particularly when cognitive demand is high, or when internal models created in the cerebellum are degraded.

## Limitations and Future Directions

Several methodological limitations were already outlined in chapter two. First, electrode size and location were considered (Horvath et al., 2014). Future work might look to incorporate HD-tDCS which allows for more focal targeting of brain regions (Datta et al., 2009; Datta et al., 2016; Dmochowski et al., 2011; Huang et al., 2017; Villamar et al., 2013). An HD approach might be particularly useful when targeting lobules I-IV, which are tucked beneath the cortex and are difficult to reach, but are critical in understanding functional differences within the cerebellum. Second, task difficulty was possibly a limitation, as behavioral data indicate accuracy was

relatively close to ceiling. Future work may look to increase task difficulty, but also to vary task type. While there was a growing literature to indicate cerebellar activation during verbal working memory (Stoodley, 2012), there are a number of task domains that would also benefit further investigation. Particularly, other executive functions such as set shifting and inhibition might also benefit from further examination.

Future work may also look to extend this work in older adults. Outcomes from this future work would further highlight the role the cerebellum plays in cortical processing, but also might open up avenues to examine remediation techniques to optimize compensatory mechanisms. Maintaining cognitive ability is key in maintaining independence in advanced age. tDCS is a relatively simple way of improving and maintaining cognitive ability. Thus, therapeutic techniques involving tDCS might be a cheap, and effective way of maintaining cognitive ability, and ultimately independence in advanced age. Work has begun to use tDCS in clinical populations with relatively high success (Hsu et al., 2015; Leggio et al., 2020; van Dun & Manto, 2018). This work stands to provide further insights into how tDCS might improve compensatory mechanisms in advanced age and disease.

Lastly, in regard to resting state, we used a lobular approach (Bernard et al., 2012; Grami et al., 2021) that might overlook functional boundaries within the cerebellum (Bernard & Seidler, 2014; King et al., 2019). Future work may look to apply functional masks to further assess how connectivity might change, particularly if the networks assessed were diversified.

## Conclusions

The current work looked to better understand cerebello-cortical interactions during non-motor cognitive performance, by applying anodal, cathodal, and sham stimulation over the right cerebellum prior to completing a motor and non-motor task in the neuroimaging environment.

Broadly, we found cathodal stimulation resulted in a performance boost, and anodal stimulation hindered task performance. This effect of anodal stimulation also resulted in increased cortical activation and connectivity, presumably a result of a compensatory mechanism. Specifically, when cerebellar output is degraded by anodal stimulation, the scaffolding effect the cerebellum provides is reduced, requiring more cortical activation to compensate for the reduced cerebellar output. We believe that the current work provides initial evidence for why there might be a need for greater cortical activation, such that the cerebellum is helping support cortical processing, through a scaffolding mechanism, which ultimately helps the cortex in task processing. This work has the potential to update existing compensatory models to include the cerebellum as a structure use to support cognitive processes, which has implications in remediation techniques in a number of clinical populations.

# REFERENCES


Abellaneda-Pérez, K., Vaqué-Alcázar, L., Perellón-Alfonso, R., Bargalló, N., Kuo, M. F., Pascual-Leone, A., Nitsche, M. A., & Bartrés-Faz, D. (2020). Differential tDCS and tACS Effects on Working Memory-Related Neural Activity and Resting-State Connectivity. *Frontiers in Neuroscience*, *13*, 1440. https://doi.org/10.3389/fnins.2019.01440

Aizenstein, H. J., Stenger, V. A., Cochran, J., Clark, K., Johnson, M., Nebes, R. D., & Carter, C. S. (2004). Regional Brain Activation during Concurrent Implicit and Explicit Sequence Learning. *Cerebral Cortex*, *14*(2), 199–208. https://doi.org/10.1093/cercor/bhg119

Allen, G., Barnard, H., McColl, R., Hester, A. L., Fields, J. A., Weiner, M. F., Ringe, W. K., Lipton, A. M., Brooker, M., McDonald, E., Rubin, C. D., & Cullum, C. M. (2007). Reduced hippocampal functional connectivity in Alzheimer disease. *Archives of Neurology*, *64*(10), 1482–1487. https://doi.org/10.1001/archneur.64.10.1482

Ambrus, G. G., Chaieb, L., Stilling, R., Rothkegel, H., Antal, A., & Paulus, W. (2016). Monitoring transcranial direct current stimulation induced changes in cortical excitability during the serial reaction time task. *Neuroscience Letters*, *616*, 98–104. https://doi.org/10.1016/j.neulet.2016.01.039

Andersson, J.L.R., Jenkinson, M., & Smith, S. M. (2007). Non-linear optimisation. *FMRIB Technical Report TR07JA1*.

Andersson, Jesper L R, Jenkinson, M., & Smith, S. (2007). *Non-linear registration aka Spatial normalisation FMRIB Technial Report TR07JA2*.

Andersson, Jesper L R, Skare, S., & Ashburner, J. (2003). How to correct susceptibility distortions in spin-echo echo-planar images: application to diffusion tensor imaging.

*NeuroImage*, *20*(2), 870–888. https://doi.org/https://doi.org/10.1016/S1053-8119(03)00336-7

Anguera, J. A., Bernard, J. A., Jaeggi, S. M., Buschkuehl, M., Benson, B. L., Jennett, S., Humfleet, J., Reuter-Lorenz, P. A., Jonides, J., & Seidler, R. D. (2012). The effects of working memory resource depletion and training on sensorimotor adaptation. *Behavioural Brain Research*, *228*(1), 107–115. https://doi.org/10.1016/j.bbr.2011.11.040

Anguera, J. A., Reuter-Lorenz, P. A., Willingham, D. T., & Seidler, R. D. (2010). Contributions of spatial working memory to visuomotor learning. *Journal of Cognitive Neuroscience*, *22*(9), 1917–1930. https://doi.org/10.1162/jocn.2009.21351

Antal, A., Terney, D., Poreisz, C., & Paulus, W. (2007). Towards unravelling task-related modulations of neuroplastic changes induced in the human motor cortex. *European Journal of Neuroscience*, *26*(9), 2687–2691. https://doi.org/10.1111/j.1460-9568.2007.05896.x

Bai, F., Zhang, Z., Watson, D. R., Yu, H., Shi, Y., Yuan, Y., Zang, Y., Zhu, C., & Qian, Y. (2009). Abnormal Functional Connectivity of Hippocampus During Episodic Memory Retrieval Processing Network in Amnestic Mild Cognitive Impairment. *Biological Psychiatry*, *65*(11), 951–958. https://doi.org/10.1016/j.biopsych.2008.10.017

Ballard, H. K., Goen, J. R. M., Maldonado, T., & Bernard, J. A. (2019). Effects of cerebellar transcranial direct current stimulation on the cognitive stage of sequence learning. *Journal of Neurophysiology*, *122*(2), 490–499. https://doi.org/10.1152/jn.00036.2019

Bates, D., Mächler, M., Bolker, B., & Walker, S. (2015). Fitting Linear Mixed-Effects Models Using **lme4**. *Journal of Statistical Software*, *67*(1). https://doi.org/10.18637/jss.v067.i01

Beckmann, C. F., & Smith, S. M. (2004). Probabilistic Independent Component Analysis for Functional Magnetic Resonance Imaging. *IEEE Transactions on Medical Imaging*, *23*(2),

137–152. https://doi.org/10.1109/TMI.2003.822821

Bellebaum, C., & Daum, I. (2007). Cerebellar involvement in executive control. *The Cerebellum*, *6*(3), 184–192. https://doi.org/10.1080/14734220601169707

Benussi, A., Dell'Era, V., Cotelli, M. S., Turla, M., Casali, C., Padovani, A., & Borroni, B. (2017). Long term clinical and neurophysiological effects of cerebellar transcranial direct current stimulation in patients with neurodegenerative ataxia. *Brain Stimulation*, *10*(2), 242–250. https://doi.org/10.1016/J.BRS.2016.11.001

Bernard, J. A., Nguyen, A. D., Hausman, H. K., Maldonado, T., Ballard, H. K., Jackson, T. B., Eakin, S. M., Lokshina, Y., & Goen, J. R. M. (2020). Shaky scaffolding: Age differences in cerebellar activation revealed through activation likelihood estimation meta-analysis. *Human Brain Mapping*, *41*(18), 5255–5281. https://doi.org/10.1002/hbm.25191

Bernard, J. A., Orr, J. M., & Mittal, V. A. (2015). Abnormal hippocampal-thalamic white matter tract development and positive symptom course in individuals at ultra-high risk for psychosis. *Npj Schizophrenia*, *1*(1), 15009. https://doi.org/10.1038/npjschz.2015.9

Bernard, J. A., Orr, J. M., & Mittal, V. A. (2016). Differential motor and prefrontal cerebello-cortical network development: Evidence from multimodal neuroimaging. *NeuroImage*, *124*(Pt A), 591–601. https://doi.org/10.1016/j.neuroimage.2015.09.022

Bernard, J. A., Peltier, S. J., Wiggins, J. L., Jaeggi, S. M., Buschkuehl, M., Fling, B. W., Kwak, Y., Jonides, J., Monk, C. S., & Seidler, R. D. (2013). Disrupted cortico-cerebellar connectivity in older adults. *NeuroImage*, *83*(734), 103–119. https://doi.org/10.1016/j.neuroimage.2013.06.042

Bernard, J. A., & Seidler, R. D. (2013a). Cerebellar contributions to visuomotor adaptation and motor sequence learning: an ALE meta-analysis. *Frontiers in Human Neuroscience*,

*7*(February), 1–14. https://doi.org/10.3389/fnhum.2013.00027

Bernard, J. A., & Seidler, R. D. (2013b). Relationships between regional cerebellar volume and sensorimotor and cognitive function in young and older adults. *Cerebellum*, *12*(5), 721–737. https://doi.org/10.1007/s12311-013-0481-z

Bernard, J. A., & Seidler, R. D. (2014). Moving forward: Age effects on the cerebellum underlie cognitive and motor declines. *Neuroscience and Biobehavioral Reviews*, *42*, 193–207. https://doi.org/10.1016/j.neubiorev.2014.02.011

Bernard, J. A., Seidler, R. D., Hassevoort, K. M., Benson, B. L., Welsh, R. C., Wiggins, J. L., Jaeggi, S. M., Buschkuehl, M., Monk, C. S., Jonides, J., & Peltier, S. J. (2012). Resting state cortico-cerebellar functional connectivity networks: a comparison of anatomical and self-organizing map approaches. *Frontiers in Neuroanatomy*, *6*(August), 1–19. https://doi.org/10.3389/fnana.2012.00031

Berryhill, M. E., & Olson, I. R. (2008). Is the posterior parietal lobe involved in working memory retrieval? Evidence from patients with bilateral parietal lobe damage. *Neuropsychologia*, *46*(7), 1767–1774. https://doi.org/10.1016/j.neuropsychologia.2008.01.009

Bischoff-Grethe, A., Goedert, K. M., Willingham, D. T., & Grafton, S. T. (2004). Neural Substrates of Response-based Sequence Learning using fMRI. *Journal of Cognitive Neuroscience*, *16*(1), 127–138. https://doi.org/10.1162/089892904322755610

Biswal, B. B., Mennes, M., Zuo, X. N., Gohel, S., Kelly, C., Smith, S. M., Beckmann, C. F., Adelstein, J. S., Buckner, R. L., Colcombe, S., Dogonowski, A. M., Ernst, M., Fair, D., Hampson, M., Hoptman, M. J., Hyde, J. S., Kiviniemi, V. J., Kötter, R., Li, S. J., … Milham, M. P. (2010). Toward discovery science of human brain function. *Proceedings of*

*the National Academy of Sciences of the United States of America*, *107*(10), 4734–4739. https://doi.org/10.1073/pnas.0911855107

Biswal, B., Zerrin Yetkin, F., Haughton, V. M., & Hyde, J. S. (1995). Functional connectivity in the motor cortex of resting human brain using echo-planar mri. *Magnetic Resonance in Medicine*, *34*(4), 537–541. https://doi.org/10.1002/mrm.1910340409

Blakemore, Sarah J., Wolpert, D. M., & Frith, C. D. (1998). Central cancellation of self-produced tickle sensation. *Nature Neuroscience*, *1*(7), 635–640. https://doi.org/10.1038/2870

Blakemore, Sarah Jayne, Wolpert, D., & Frith, C. (2000). Why can't you tickle yourself? In *NeuroReport* (Vol. 11, Issue 11, pp. R11–R16). Neuroreport. https://doi.org/10.1097/00001756-200008030-00002

Block, H., & Celnik, P. (2013). Stimulating the Cerebellum Affects Visuomotor Adaptation but not Intermanual Transfer of Learning. *Cerebellum*, *12*, 781–793. https://doi.org/10.1007/s12311-013-0486-7

Bo, J., & Seidler, R. D. (2009). Visuospatial Working Memory Capacity Predicts the Organization of Acquired Explicit Motor Sequences. *Journal of Neurophysiology*, *101*(6), 3116–3125. https://doi.org/10.1152/jn.00006.2009

Boehringer, A., Macher, K., Dukart, J., Villringer, A., & Pleger, B. (2013). Cerebellar transcranial direct current stimulation modulates verbal working memory. *Brain Stimulation*, *6*(4), 649–653. https://doi.org/10.1016/j.brs.2012.10.001

Bolognini, N., Fregni, F., Casati, C., Olgiati, E., & Vallar, G. (2010). Brain polarization of parietal cortex augments training-induced improvement of visual exploratory and attentional skills. *Brain Research*, *1349*, 76–89.

https://doi.org/10.1016/j.brainres.2010.06.053

Bolognini, N., Olgiati, E., Rossetti, A., & Maravita, A. (2010). Enhancing multisensory spatial orienting by brain polarization of the parietal cortex. *European Journal of Neuroscience*, *31*(10), 1800–1806. https://doi.org/10.1111/j.1460-9568.2010.07211.x

Brunoni, A. R., Nitsche, M. A., Bolognini, N., Bikson, M., Wagner, T., Merabet, L., Edwards, D. J., Valero-Cabre, A., Rotenberg, A., Pascual-Leone, A., Ferrucci, R., Priori, A., Boggio, P. S., & Fregni, F. (2012). Clinical research with transcranial direct current stimulation (tDCS): Challenges and future directions. *Brain Stimulation*, *5*(3), 175–195. https://doi.org/10.1016/j.brs.2011.03.002

Buch, E. R., Santarnecchi, E., Antal, A., Born, J., Celnik, P. A., Classen, J., Gerloff, C., Hallett, M., Hummel, F. C., Nitsche, M. A., Pascual-Leone, A., Paulus, W. J., Reis, J., Robertson, E. M., Rothwell, J. C., Sandrini, M., Schambra, H. M., Wassermann, E. M., Ziemann, U., & Cohen, L. G. (2017). Effects of tDCS on motor learning and memory formation: A consensus and critical position paper. In *Clinical Neurophysiology* (Vol. 128, Issue 4, pp. 589–603). Elsevier Ireland Ltd. https://doi.org/10.1016/j.clinph.2017.01.004

Buckner, R. L. (2013). The Cerebellum and Cognitive Function: 25 Years of Insight from Anatomy and Neuroimaging. *Neuron*, *80*(3), 807–815. https://doi.org/10.1016/J.NEURON.2013.10.044

Buckner, R. L., Krienen, F. M., Castellanos, A., Diaz, J. C., & Thomas Yeo, B. T. (2011). The organization of the human cerebellum estimated by intrinsic functional connectivity. *J Neurophysiol*, *106*(5), 2322–2345. https://doi.org/10.1152/jn.00339.2011.-The

Cabeza, R. (2002). Hemispheric Asymmetry Reduction in Older Adults: The HAROLD model. *Psychology and Aging*, *17*(1), 85–100. https://doi.org/10.1037/0882-7974.17.1.85

Cabeza, R., Albert, M., Belleville, S., Craik, F. I. M., Duarte, A., Grady, C. L., Lindenberger, U., Nyberg, L., Park, D. C., Reuter-Lorenz, P. A., Rugg, M. D., Steffener, J., & Rajah, M. N. (2018). Maintenance, reserve and compensation: the cognitive neuroscience of healthy ageing. In *Nature Reviews Neuroscience* (Vol. 19, Issue 11, pp. 701–710). Nature Publishing Group. https://doi.org/10.1038/s41583-018-0068-2

Cabeza, R., Anderson, N. D., Locantore, J. K., & McIntosh, A. R. (2002). Aging gracefully: Compensatory brain activity in high-performing older adults. *NeuroImage*, *17*(3), 1394–1402. https://doi.org/10.1006/nimg.2002.1280

Callan, D. E., Falcone, B., Wada, A., & Parasuraman, R. (2016). Simultaneous tDCS-fMRI Identifies Resting State Networks Correlated with Visual Search Enhancement. *Frontiers in Human Neuroscience*, *10*(MAR2016), 72. https://doi.org/10.3389/fnhum.2016.00072

Cantarero, G., Spampinato, D., Reis, J., Ajagbe, L., Thompson, T., Kulkarni, K., & Celnik, P. (2015). Cerebellar direct current stimulation enhances on-line motor skill acquisition through an effect on accuracy. *Journal of Neuroscience*, *35*(7), 3285–3290. https://doi.org/10.1523/JNEUROSCI.2885-14.2015

Cappell, K. A., Gmeindl, L., & Reuter-Lorenz, P. A. (2010). Age differences in prefontal recruitment during verbal working memory maintenance depend on memory load. *Cortex*, *46*(4), 462–473. https://doi.org/10.1016/j.cortex.2009.11.009

Chan, C. Y., & Nicholson, C. (1986). Modulation by applied electric fields of Purkinje and stellate cell activity in the isolated turtle cerebellum. *The Journal of Physiology*, *371*(1), 89–114. https://doi.org/10.1113/jphysiol.1986.sp015963

Chen, S. H. A., & Desmond, J. E. (2005). Temporal dynamics of cerebro-cerebellar network recruitment during a cognitive task. *Neuropsychologia*, *43*(9), 1227–1237.

https://doi.org/10.1016/J.NEUROPSYCHOLOGIA.2004.12.015

Clower, D. M., Dum, R. P., & Strick, P. L. (2005). Basal ganglia and cerebellar inputs to "AIP." *Cerebral Cortex*, *15*(7), 913–920. https://doi.org/10.1093/cercor/bhh190

Coffman, B. A., Clark, V. P., & Parasuraman, R. (2014). Battery powered thought: Enhancement of attention, learning, and memory in healthy adults using transcranial direct current stimulation. *NeuroImage*, *85*, 895–908. https://doi.org/10.1016/J.NEUROIMAGE.2013.07.083

Coffman, B. A., Trumbo, M. C., & Clark, V. P. (2012). Enhancement of object detection with transcranial direct current stimulation is associated with increased attention. *BMC Neuroscience*, *13*(1), 1–8. https://doi.org/10.1186/1471-2202-13-108

Coffman, K. A., Dum, R. P., & Strick, P. L. (2011). Cerebellar vermis is a target of projections from the motor areas in the cerebral cortex. *Proceedings of the National Academy of Sciences of the United States of America*, *108*(38), 16068–16073. https://doi.org/10.1073/pnas.1107904108

Cowan, N. (2001). The magical number 4 in short-term memory: A reconsideration of mental storage capacity. *Behavioral and Brain Sciences*, *24*(1), 87–114. https://doi.org/10.1017/S0140525X01003922

Cummiford, C. M., Nascimento, T. D., Foerster, B. R., Clauw, D. J., Zubieta, J. K., Harris, R. E., & DaSilva, A. F. (2016). Changes in resting state functional connectivity after repetitive transcranial direct current stimulation applied to motor cortex in fibromyalgia patients. *Arthritis Research and Therapy*, *18*(1), 1–12. https://doi.org/10.1186/s13075-016-0934-0

D'Mello, A. M., Turkeltaub, P. E., & Stoodley, C. J. (2017). Cerebellar tDCS Modulates Neural Circuits during Semantic Prediction: A Combined tDCS-fMRI Study. *The Journal of*

*Neuroscience*, *37*(6), 1604 –1613. https://doi.org/10.1523/JNEUROSCI.2818-16.2017

Datta, Abhishek, Bansal, V., Diaz, J., Patel, J., Reato, D., & Bikson, M. (2009). Gyri-precise head model of transcranial direct current stimulation: improved spatial focality using a ring electrode versus conventional rectangular pad. *Brain Stimulation*, *2*(4), 201–207, 207.e1. https://doi.org/10.1016/j.brs.2009.03.005

Datta, Anupam, Sen, S., & Zick, Y. (2016). Algorithmic transparency via quantitative input influence: Theory and experiments with learning systems. *2016 IEEE Symposium on Security and Privacy (SP)*, 598–617. https://doi.org/10.1109/SP.2016.42

Desikan, R. S., Ségonne, F., Fischl, B., Quinn, B. T., Dickerson, B. C., Blacker, D., Buckner, R. L., Dale, A. M., Maguire, R. P., Hyman, B. T., Albert, M. S., & Killiany, R. J. (2006). An automated labeling system for subdividing the human cerebral cortex on MRI scans into gyral based regions of interest. *NeuroImage*, *31*(3), 968–980. https://doi.org/10.1016/j.neuroimage.2006.01.021

Desmond, J. E., Chen, S. H. A., & Shieh, P. B. (2005). Cerebellar transcranial magnetic stimulation impairs verbal working memory. *Annals of Neurology*, *58*(4), 553–560. https://doi.org/10.1002/ana.20604

Desmond, J. E., Gabrieli, J. D., Wagner, A. D., Ginier, B. L., & Glover, G. H. (1997). Lobular patterns of cerebellar activation in verbal working-memory and finger-tapping tasks as revealed by functional MRI. *The Journal of Neuroscience : The Official Journal of the Society for Neuroscience*, *17*(24), 9675–9685. https://doi.org/10.1523/JNEUROSCI.17-24-09675.1997

Dhamala, M., Pagnoni, G., Wiesenfeld, K., Zink, C. F., Martin, M., & Berns, G. S. (2003). Neural correlates of the complexity of rhythmic finger tapping. *NeuroImage*, *20*(2), 918–

926. https://doi.org/10.1016/S1053-8119(03)00304-5

Diedrichsen, J., King, M., Hernandez-Castillo, C., Sereno, M., & Ivry, R. B. (2019). Universal Transform or Multiple Functionality? Understanding the Contribution of the Human Cerebellum across Task Domains. *Neuron*, *102*(5), 918–928. https://doi.org/10.1016/j.neuron.2019.04.021

Dmochowski, J. P., Datta, A., Bikson, M., Su, Y., & Parra, L. C. (2011). Optimized multi-electrode stimulation increases focality and intensity at target. *Journal of Neural Engineering*, *8*(4), 046011. https://doi.org/10.1088/1741-2560/8/4/046011

Doppelmayr, M., Pixa, N. H., & Steinberg, F. (2016). Cerebellar, but not Motor or Parietal, High-Density Anodal Transcranial Direct Current Stimulation Facilitates Motor Adaptation. *Journal of the International Neuropsychological Society*, *22*, 928–936. https://doi.org/10.1017/S1355617716000345

Doyon, J., Gabitov, E., Vahdat, S., Lungu, O., & Boutin, A. (2018). Current issues related to motor sequence learning in humans. *Current Opinion in Behavioral Sciences*, *20*, 89–97. https://doi.org/10.1016/j.cobeha.2017.11.012

Doyon, Julien, Gaudreau, D., Laforce, R. L., Castonguay, M., Bédard, P. J., Bédard, F., & Bouchard, J. P. (1997). Role of the striatum, cerebellum, and frontal lobes in the learning of a visuomotor sequence. *Brain and Cognition*, *34*(2), 218–245. https://doi.org/10.1006/brcg.1997.0899

Dum, R. P., & Strick, P. L. (2003). An unfolded map of the cerebellar dentate nucleus and its projections to the cerebral cortex. *Journal of Neurophysiology*, *89*(1), 634–639. https://doi.org/10.1152/jn.00626.2002

Ehsani, F., Bakhtiary, A. H., Jaberzadeh, S., Talimkhani, A., & Hajihasani, A. (2016).

Differential effects of primary motor cortex and cerebellar transcranial direct current stimulation on motor learning in healthy individuals: A randomized double-blind sham-controlled study. *Neuroscience Research*, *112*, 10–19. https://doi.org/10.1016/j.neures.2016.06.003

Eliassen, J. C., Souza, T., & Sanes, J. N. (2001). Human brain activation accompanying explicitly directed movement sequence learning. *Experimental Brain Research*, *141*(3), 269–280. https://doi.org/10.1007/s002210100822

Emch, M., von Bastian, C. C., & Koch, K. (2019). Neural correlates of verbal working memory: An fMRI meta-analysis. In *Frontiers in Human Neuroscience* (Vol. 13, p. 180). Frontiers Media S.A. https://doi.org/10.3389/fnhum.2019.00180

Ferreira, L. K., & Busatto, G. F. (2013). Resting-state functional connectivity in normal brain aging. *Neuroscience & Biobehavioral Reviews*, *37*(3), 384–400. https://doi.org/10.1016/J.NEUBIOREV.2013.01.017

Ferrucci, R., Marceglia, S., Vergari, M., Cogiamanian, F., Mrakic-Sposta, S., Mameli, F., Zago, S., Barbieri, S., & Priori, A. (2008). Cerebellar Transcranial Direct Current Stimulation Impairs the Practice-dependent Proficiency Increase in Working Memory. *Journal of Cognitive Neuroscience*, *20*(9), 1687–1697. https://doi.org/10.1162/jocn.2008.20112

Ferrucci, Roberta, Bocci, T., Cortese, F., Ruggiero, F., & Priori, A. (2016). Cerebellar transcranial direct current stimulation in neurological disease. *Cerebellum & Ataxias*, *3*(1), 16. https://doi.org/10.1186/s40673-016-0054-2

Ferrucci, Roberta, Brunoni, A. R., Parazzini, M., Vergari, M., Rossi, E., Fumagalli, M., Mameli, F., Rosa, M., Giannicola, G., Zago, S., & Priori, A. (2013). Modulating Human Procedural Learning by Cerebellar Transcranial Direct Current Stimulation. *The Cerebellum*, *12*(4),

485–492. https://doi.org/10.1007/s12311-012-0436-9

Ferrucci, Roberta, Cortese, F., & Priori, A. (2015). Cerebellar tDCS: How to Do It. *Cerebellum*, *14*(1), 27–30. https://doi.org/10.1007/s12311-014-0599-7

Filip, P., Gallea, C., Lehéricy, S., Lungu, O., & Bareš, M. (2019). Neural Scaffolding as the Foundation for Stable Performance of Aging Cerebellum. *The Cerebellum*, *18*(3), 500–510. https://doi.org/10.1007/s12311-019-01015-7

Frazier, J. A., Chiu, S., Breeze, J. L., Makris, N., Lange, N., Kennedy, D. N., Herbert, M. R., Bent, E. K., Koneru, V. K., Dieterich, M. E., Hodge, S. M., Rauch, S. L., Grant, P. E., Cohen, B. M., Seidman, L. J., Caviness, V. S., & Biederman, J. (2005). Structural brain magnetic resonance imaging of limbic and thalamic volumes in pediatric bipolar disorder. *American Journal of Psychiatry*, *162*(7), 1256–1265. https://doi.org/10.1176/appi.ajp.162.7.1256

Galea, J. M., Jayaram, G., Ajagbe, L., & Celnik, P. (2009). Modulation of cerebellar excitability by polarity-specific noninvasive direct current stimulation. *Journal of Neuroscience*, *29*(28), 9115–9122. https://doi.org/10.1523/JNEUROSCI.2184-09.2009

Galea, J. M., Vazquez, A., Pasricha, N., Orban De Xivry, J.-J., & Celnik, P. (2011). Dissociating the Roles of the Cerebellum and Motor Cortex during Adaptive Learning: The Motor Cortex Retains What the Cerebellum Learns. *Cerebral Cortex August*, *21*, 1761–1770. https://doi.org/10.1093/cercor/bhq246

Ghez, C. (1991). The Cerebellum. In E.R. Kandel, J. H. Schwartz, & T. M. Jessell (Eds.), *Principles of neural science* (pp. 626–646). Appleton & Lange.

Goldstein, J. M., Seidman, L. J., Makris, N., Ahern, T., O'Brien, L. M., Caviness, V. S., Kennedy, D. N., Faraone, S. V., & Tsuang, M. T. (2007). Hypothalamic Abnormalities in

Schizophrenia: Sex Effects and Genetic Vulnerability. *Biological Psychiatry*, *61*(8), 935–945. https://doi.org/10.1016/j.biopsych.2006.06.027

Grami, F., Marco, G. de, Bodranghien, F., Manto, M., & Habas, C. (2021). Cerebellar transcranial direct current stimulation reconfigurates static and dynamic functional connectivity of the resting-state networks. *Cerebellum & Ataxias*, *8*(1), 1–12. https://doi.org/https://doi.org/10.1186/s40673-021-00132-6

Grimaldi, G., Argyropoulos, G. P., Bastian, A., Cortes, M., Davis, N. J., Edwards, D. J., Ferrucci, R., Fregni, F., Galea, J. M., Hamada, M., Manto, M., Miall, R. C., Morales-Quezada, L., Pope, P. A., Priori, A., Rothwell, J., Tomlinson, S. P., & Celnik, P. (2016). Cerebellar Transcranial Direct Current Stimulation (ctDCS): A Novel Approach to Understanding Cerebellar Function in Health and Disease. *The Neuroscientist*, *22*(1), 83–97. https://doi.org/10.1177/1073858414559409

Grimaldi, G., Argyropoulos, G. P., Boehringer, A., Celnik, P., Edwards, M. J., Ferrucci, R., Galea, J. M., Groiss, S. J., Hiraoka, K., Kassavetis, P., Lesage, E., Manto, M., Miall, R. C., Priori, A., Sadnicka, A., Ugawa, Y., & Ziemann, U. (2014). Non-invasive cerebellar stimulation - a consensus paper. *The Cerebellum*, *13*(1), 121–138. https://doi.org/10.1007/s12311-013-0514-7

Habas, C., Kamdar, N., Nguyen, D., Prater, K., Beckmann, C. F., Menon, V., & Greicius, M. D. (2009). *Behavioral/Systems/Cognitive Distinct Cerebellar Contributions to Intrinsic Connectivity Networks*. https://doi.org/10.1523/JNEUROSCI.1868-09.2009

Han, S., An, Y., Carass, A., Prince, J. L., & Resnick, S. M. (2020). Longitudinal analysis of regional cerebellum volumes during normal aging. *NeuroImage*, *220*, 117062. https://doi.org/10.1016/j.neuroimage.2020.117062

Hardwick, R. M., & Celnik, P. A. (2014). Cerebellar direct current stimulation enhances motor learning inolder adults. *Neurobiology of Aging*, *35*(10), 2217–2221. https://doi.org/10.1016/j.neurobiolaging.2014.03.030

Hautzel, H., Mottaghy, F. M., Specht, K., Müller, H.-W., & Krause, B. J. (2009). Evidence of a modality-dependent role of the cerebellum in working memory? An fMRI study comparing verbal and abstract n-back tasks. *NeuroImage*, *47*(4), 2073–2082. https://doi.org/10.1016/J.NEUROIMAGE.2009.06.005

Hayter, A. L., Langdon, D. W., & Ramnani, N. (2007). Cerebellar contributions to working memory. *NeuroImage*, *36*(3), 943–954. https://doi.org/10.1016/J.NEUROIMAGE.2007.03.011

Head, D., Buckner, R. L., Shimony, J. S., Williams, L. E., Akbudak, E., Conturo, T. E., McAvoy, M., Morris, J. C., & Snyder, A. Z. (2004). Differential Vulnerability of Anterior White Matter in Nondemented Aging with Minimal Acceleration in Dementia of the Alzheimer Type: Evidence from Diffusion Tensor Imaging. *Cerebral Cortex*, *14*(4), 410–423. https://doi.org/10.1093/cercor/bhh003

Holmes, G. (1939). The Cerebellum of Man. *Brain*, *62*(1), 1–30. https://doi.org/10.1093/brain/62.1.1

Honda, M., Deiber, M. P., Ibáñez, V., Pascual-Leone, A., Zhuang, P., & Hallett, M. (1998). Dynamic cortical involvement in implicit and explicit motor sequence learning. A PET study. *Brain*, *121*(11), 2159–2173. https://doi.org/10.1093/brain/121.11.2159

Hoogendam, Y. Y., van der Geest, J. N., van der Lijn, F., van der Lugt, A., Niessen, W. J., Krestin, G. P., Hofman, A., Vernooij, M. W., Breteler, M. M. B., & Ikram, M. A. (2012). Determinants of cerebellar and cerebral volume in the general elderly population.

*Neurobiology of Aging*, *33*(12), 2774–2781. https://doi.org/10.1016/J.NEUROBIOLAGING.2012.02.012

Horvath, J. C., Carter, O., & Forte, J. D. (2014). Transcranial direct current stimulation: Five important issues we aren't discussing (but probably should be). In *Frontiers in Systems Neuroscience* (Vol. 8, Issue JAN, p. 2). Frontiers. https://doi.org/10.3389/fnsys.2014.00002

Hoshi, E., Tremblay, L., Féger, J., Carras, P. L., & Strick, P. L. (2005). The cerebellum communicates with the basal ganglia. *Nature Neuroscience*, *8*(11), 1491–1493. https://doi.org/10.1038/nn1544

Hsu, W. Y., Ku, Y., Zanto, T. P., & Gazzaley, A. (2015). Effects of noninvasive brain stimulation on cognitive function in healthy aging and Alzheimer's disease: A systematic review and meta-analysis. *Neurobiology of Aging*, *36*(8), 2348–2359. https://doi.org/10.1016/j.neurobiolaging.2015.04.016

Huang, Y., Liu, A. A., Lafon, B., Friedman, D., Dayan, M., Wang, X., Bikson, M., Doyle, W. K., Devinsky, O., & Parra, L. C. (2017). Measurements and models of electric fields in the in vivo human brain during transcranial electric stimulation. *ELife*, *6*. https://doi.org/10.7554/eLife.18834

Ilg, W., Christensen, A., Mueller, O. M., Goericke, S. L., Giese, M. A., & Timmann, D. (2013). Effects of cerebellar lesions on working memory interacting with motor tasks of different complexities. *Journal of Neurophysiology*, *110*(10), 2337–2349. https://doi.org/10.1152/jn.00062.2013

Imamizu, H., Miyauchi, S., Tamada, T., Sasaki, Y., Takino, R., Pütz, B., Yoshioka, T., & Kawato, M. (2000a). Human cerebellar activity reflecting an acquired internal model of a new tool. *Nature*, *403*(6766), 192–195. https://doi.org/10.1038/35003194

Imamizu, H., Miyauchi, S., Tamada, T., Sasaki, Y., Takino, R., Pütz, B., Yoshioka, T., & Kawato, M. (2000b). Human cerebellar activity reflecting an acquired internal model of a new tool. *Nature*, *403*(6766), 192–195. https://doi.org/10.1038/35003194

Ito, M. (2008). Control of Mental Activities by Internal Models in the Cerebellum. *Nature Reviews Neuroscience*, *9*(4), 304–313. https://doi.org/10.1038/nrn2332

Jahanshahi, M., Dirnberger, G., Fuller, R., & Frith, C. D. (2000). The Role of the Dorsolateral Prefrontal Cortex in Random Number Generation: A Study with Positron Emission Tomography. *NeuroImage*, *12*(6), 713–725. https://doi.org/10.1006/NIMG.2000.0647

Jenkinson, M., Bannister, P., Brady, M., & Smith, S. (2002). Improved Optimization for the Robust and Accurate Linear Registration and Motion Correction of Brain Images. *NeuroImage*, *17*(2), 825–841. https://doi.org/10.1006/NIMG.2002.1132

Jenkinson, M., & Smith, S. (2001). A global optimisation method for robust affine registration of brain images. *Medical Image Analysis*, *5*(2), 143–156. https://doi.org/10.1016/S1361-8415(01)00036-6

Jongkees, B. J., Immink, M. A., Boer, O. D., Yavari, F., Nitsche, M. A., & Colzato, L. S. (2019). The Effect of Cerebellar tDCS on Sequential Motor Response Selection. *Cerebellum*, *18*(4), 738–749. https://doi.org/10.1007/s12311-019-01029-1

Jonides, J., Schumacher, E. H., Smith, E. E., Koeppe, R. A., Awh, E., Reuter-Lorenz, P. A., Marshuetz, C., & Willis, C. R. (1998). The role of parietal cortex in verbal working memory. *Journal of Neuroscience*, *18*(13), 5026–5034. https://doi.org/10.1523/jneurosci.18-13-05026.1998

Jonides, J., Schumacher, E. H., Smith, E. E., Lauber, E. J., Awh, E., Minoshima, S., & Koeppe, R. A. (1997). Verbal working memory load affects regional brain activation as measured by

PET. *Journal of Cognitive Neuroscience*, *9*(4), 462–475. https://doi.org/10.1162/jocn.1997.9.4.462

Karni, A., Meyer, G., Rey-Hipolito, C., Jezzard, P., Adams, M. M., Turner, R., & Ungerleider, L. G. (1998). The acquisition of skilled motor performance: Fast and slow experience-driven changes in primary motor cortex. *Proceedings of the National Academy of Sciences of the United States of America*, *95*(3), 861–868. https://doi.org/10.1073/pnas.95.3.861

Kelly, R. M., & Strick, P. L. (2000). Rabies as a transneuronal tracer of circuits in the central nervous system. In *Journal of Neuroscience Methods* (Vol. 103). www.elsevier.com/locate/jneumeth

Kelly, R. M., & Strick, P. L. (2003). Cerebellar loops with motor cortex and prefrontal cortex of a nonhuman primate. *Journal of Neuroscience*, *23*(23), 8432–8444. https://doi.org/10.1523/jneurosci.23-23-08432.2003

King, M., Hernandez-Castillo, C. R., Poldrack, R. A., Ivry, R. B., & Diedrichsen, J. (2019). Functional boundaries in the human cerebellum revealed by a multi-domain task battery. *Nature Neuroscience*, *22*(8), 1371–1378. https://doi.org/10.1038/s41593-019-0436-x

Koppelmans, V., Hirsiger, S., Mérillat, S., Jäncke, L., & Seidler, R. D. (2015). Cerebellar gray and white matter volume and their relation with age and manual motor performance in healthy older adults. *Human Brain Mapping*, *36*(6), 2352–2363. https://doi.org/10.1002/hbm.22775

Krienen, F. M., & Buckner, R. L. (2009). Segregated Fronto-Cerebellar Circuits Revealed by Intrinsic Functional Connectivity. *Cerebral Cortex*, *19*(10), 2485–2497. https://doi.org/10.1093/cercor/bhp135

Küper, M., Mallick, J. S., Ernst, T., Kraff, O., Thürling, M., Stefanescu, M. R., Göricke, S.,

Nitsche, M. A., & Timmann, D. (2019). Cerebellar transcranial direct current stimulation modulates the fMRI signal in the cerebellar nuclei in a simple motor task. *Brain Stimulation*. https://doi.org/10.1016/J.BRS.2019.04.002

Kuznetsova, A., Brockhoff, P. B., & Christensen, R. H. B. (2017). **lmerTest** Package: Tests in Linear Mixed Effects Models. *Journal of Statistical Software*, *82*(13). https://doi.org/10.18637/jss.v082.i13

Kwak, Y., Müller, M. L. T. M., Bohnen, N. I., Dayalu, P., & Seidler, R. D. (2012). L-DOPA changes ventral striatum recruitment during motor sequence learning in Parkinson's disease. *Behavioural Brain Research*, *230*(1), 116–124. https://doi.org/10.1016/j.bbr.2012.02.006

Labruna, L., Stark-Inbar, A., Breska, A., Dabit, M., Vanderschelden, B., Nitsche, M. A., & Ivry, R. B. (2019). Individual differences in TMS sensitivity influence the efficacy of tDCS in facilitating sensorimotor adaptation. *Brain Stimulation*, *12*(4), 992–1000. https://doi.org/10.1016/j.brs.2019.03.008

Leggio, M., Olivito, G., Lupo, M., & Clausi, S. (2020). The Cerebellum: A Therapeutic Target in Treating Speech and Language Disorders. In *Translational Neuroscience of Speech and Language Disorders* (pp. 141–175). Springer International Publishing. https://doi.org/10.1007/978-3-030-35687-3_8

Leiner, H. C., Leiner, A. L., & Dow, R. S. (1989). Reappraising the cerebellum: What does the hindbrain contribute to the forebrain? *Behavioral Neuroscience*, *103*(5), 998–1008. https://doi.org/10.1037/0735-7044.103.5.998

Leiner, H. C., Leiner, A. L., & Dow, R. S. (1991). The human cerebro-cerebellar system: its computing, cognitive, and language skills. *Behavioural Brain Research*, *44*(2), 113–128. https://doi.org/10.1016/S0166-4328(05)80016-6

Lenth, R., Singmann, H., Love, J., Buerkner, P., & Herve, M. (2018). Emmeans: Estimated marginal means, aka least-squares means. *R Package Version*, *1*(1). https://doi.org/10.1080/00031305.1980.10483031

Li, S. C., Lindenberger, U., & Sikström, S. (2001). Aging cognition: From neuromodulation to representation. In *Trends in Cognitive Sciences* (Vol. 5, Issue 11, pp. 479–486). Elsevier Current Trends. https://doi.org/10.1016/S1364-6613(00)01769-1

Lie, C.-H., Specht, K., Marshall, J. C., & Fink, G. R. (2006). Using fMRI to decompose the neural processes underlying the Wisconsin Card Sorting Test. *Neuroimage*, *30*(3), 1038–1049. https://doi.org/10.1016/J.NEUROIMAGE.2005.10.031

Liebrand, M., Karabanov, A., Antonenko, D., Flöel, A., Siebner, H. R., Classen, J., Krämer, U. M., & Tzvi, E. (2020a). Beneficial effects of cerebellar tDCS on motor learning are associated with altered putamen-cerebellar connectivity: A simultaneous tDCS-fMRI study. *NeuroImage*, *223*, 117363. https://doi.org/10.1016/j.neuroimage.2020.117363

Liebrand, M., Karabanov, A., Antonenko, D., Flöel, A., Siebner, H. R., Classen, J., Krämer, U. M., & Tzvi, E. (2020b). Beneficial effects of cerebellar tDCS on motor learning are associated with altered putamen-cerebellar connectivity: A simultaneous tDCS-fMRI study. *NeuroImage*, *223*, 117363. https://doi.org/10.1016/j.neuroimage.2020.117363

Lissek, S., Vallana, G. S., Güntürkün, O., Dinse, H., & Tegenthoff, M. (2013). Brain Activation in Motor Sequence Learning Is Related to the Level of Native Cortical Excitability. *PLoS ONE*, *8*(4), 61863. https://doi.org/10.1371/journal.pone.0061863

Loewenstein, D. A., Czaja, S. J., Bowie, C. R., & Harvey, P. D. (2012). Age-Associated Differences in Cognitive Performance in Older Patients With Schizophrenia: A Comparison With Healthy Older Adults. *The American Journal of Geriatric Psychiatry*, *20*(1), 29–40.

https://doi.org/10.1097/JGP.0b013e31823bc08c

Macher, K., Böhringer, A., Villringer, A., & Pleger, B. (2014). Cerebellar-parietal connections underpin phonological storage. *Journal of Neuroscience*, *34*(14), 5029–5037. https://doi.org/10.1523/JNEUROSCI.0106-14.2014

Majidi, S. N., Verhage, M. C., Donchin, O., Holland, P., Frens, M. A., & van der Geest, J. N. (2017). Cerebellar tDCS does not improve performance in probabilistic classification learning. *Experimental Brain Research*, *235*(2), 421–428. https://doi.org/10.1007/s00221-016-4800-8

Makris, N., Goldstein, J. M., Kennedy, D., Hodge, S. M., Caviness, V. S., Faraone, S. V., Tsuang, M. T., & Seidman, L. J. (2006). Decreased volume of left and total anterior insular lobule in schizophrenia. *Schizophrenia Research*, *83*(2–3), 155–171. https://doi.org/10.1016/j.schres.2005.11.020

Maldonado, T., & Bernard, J. A. (2021). The Polarity-Specific Nature of Single-Session High-definition Transcranial Direct Current Stimulation to the Cerebellum and Prefrontal Cortex on Motor and Non-motor Task Performance. *Cerebellum*. https://doi.org/10.1007/s12311-021-01235-w

Maldonado, T., Goen, J. R. M., Imburgio, M. J., Eakin, S. M., & Bernard, J. A. (2019). Single session high definition transcranial direct current stimulation to the cerebellum does not impact higher cognitive function. *PLoS ONE*, *14*(10). https://doi.org/10.1371/journal.pone.0222995

Maldonado, Ted, Goen, J., Eakin, S. M., & Bernard, J. A. (2019). High definition transcranial direct current stimulation to the cerebellum does not impact higher cognitive function. *PloS One*, *14*(10). https://doi.org/none

Mannarelli, D., Pauletti, C., Currà, A., Marinelli, L., Corrado, A., Delle Chiaie, R., & Fattapposta, F. (2019). The Cerebellum Modulates Attention Network Functioning: Evidence from a Cerebellar Transcranial Direct Current Stimulation and Attention Network Test Study. *Cerebellum*, *18*(3), 457–468. https://doi.org/10.1007/s12311-019-01014-8

Mannarelli, D., Pauletti, C., Petritis, A., Delle Chiaie, R., Currà, A., Trompetto, C., & Fattapposta, F. (2020). Effects of Cerebellar tDCS on Inhibitory Control: Evidence from a Go/NoGo Task. *Cerebellum*, *19*(6), 788–798. https://doi.org/10.1007/s12311-020-01165-z

Miall, R. C., Antony, J., Goldsmith-Sumner, A., Harding, S. R., McGovern, C., & Winter, J. L. (2016). Modulation of linguistic prediction by TDCS of the right lateral cerebellum. *Neuropsychologia*, *86*, 103–109. https://doi.org/10.1016/j.neuropsychologia.2016.04.022

Middleton, F. A., & Strick, P. L. (2001). Cerebellar projections to the prefrontal cortex of the primate. *Journal of Neuroscience*, *21*(2), 700–712. https://doi.org/10.1523/jneurosci.21-02-00700.2001

Miller, T. D., Ferguson, K. J., Reid, L. M., Wardlaw, J. M., Starr, J. M., Seckl, J. R., Deary, I. J., & MacLullich, A. M. J. (2013). Cerebellar Vermis Size and Cognitive Ability in Community-Dwelling Elderly Men. *The Cerebellum*, *12*(1), 68–73. https://doi.org/10.1007/s12311-012-0397-z

Minks, E., Kopickova, M., Marecek, R., Streitova, H., & Bares, M. (2010). Transcranial magnetic stimulation of the cerebellum. *Biomedical Papers*, *154*(2), 133–139. https://doi.org/10.5507/bp.2010.020

Moos, K., Vossel, S., Weidner, R., Sparing, R., & Fink, G. R. (2012). Modulation of top-down control of visual attention by cathodal tDCS over right IPS. *Journal of Neuroscience*, *32*(46), 16360–16368. https://doi.org/10.1523/JNEUROSCI.6233-11.2012

Neau, J.-P., Anllo, E. A., Bonnaud, V., Ingrand, P., & Gil, R. (2000). Neuropsychological disturbances in cerebellar infarcts. *Acta Neurologica Scandinavica*, *102*(6), 363–370. https://doi.org/10.1034/j.1600-0404.2000.102006363.x

Newton, J. M., Dong, Y., Hidler, J., Plummer-D'Amato, P., Marehbian, J., Albistegui-DuBois, R. M., Woods, R. P., & Dobkin, B. H. (2008). Reliable assessment of lower limb motor representations with fMRI: Use of a novel MR compatible device for real-time monitoring of ankle, knee and hip torques. *NeuroImage*, *43*(1), 136–146. https://doi.org/10.1016/j.neuroimage.2008.07.001

Nguemeni, C., Stiehl, A., Hiew, S., & Zeller, D. (2021). No Impact of Cerebellar Anodal Transcranial Direct Current Stimulation at Three Different Timings on Motor Learning in a Sequential Finger-Tapping Task. *Frontiers in Human Neuroscience*, *15*, 33. https://doi.org/10.3389/fnhum.2021.631517

Nitsche, M. A., & Paulus, W. (2000). Excitability changes induced in the human motor cortex by weak transcranial direct current stimulation. *The Journal of Physiology*, *527*(3), 633–639. https://doi.org/10.1111/j.1469-7793.2000.t01-1-00633.x

Nitsche, Michael A., & Paulus, W. (2001). Sustained excitability elevations induced by transcranial DC motor cortex stimulation in humans. *Neurology*, *57*(10), 1899–1901. https://doi.org/10.1212/WNL.57.10.1899

Nitsche, Michael A., Seeber, A., Frommann, K., Klein, C. C., Rochford, C., Nitsche, M. S., Fricke, K., Liebetanz, D., Lang, N., Antal, A., Paulus, W., & Tergau, F. (2005). Modulating parameters of excitability during and after transcranial direct current stimulation of the human motor cortex. *Journal of Physiology*, *568*(1), 291–303. https://doi.org/10.1113/jphysiol.2005.092429

O'Reilly, J. X., Beckmann, C. F., Tomassini, V., Ramnani, N., & Johansen-Berg, H. (2010). Distinct and overlapping functional zones in the cerebellum defined by resting state functional connectivity. *Cerebral Cortex*, *20*(4), 953–965. https://doi.org/10.1093/cercor/bhp157

Oberman, L., Edwards, D., Eldaief, M., & Pascual-Leone, A. (2011). Safety of theta burst transcranial magnetic stimulation: A systematic review of the literature. In *Journal of Clinical Neurophysiology* (Vol. 28, Issue 1, pp. 67–74). NIH Public Access. https://doi.org/10.1097/WNP.0b013e318205135f

Oldrati, V., & Schutter, D. J. L. G. (2018). Targeting the Human Cerebellum with Transcranial Direct Current Stimulation to Modulate Behavior : a Meta-Analysis. *The Cerebellum* , *17*(2), 228–236. https://doi.org/10.1007/s12311-017-0877-2

Palesi, F., Tournier, J.-D., Calamante, F., Muhlert, N., Castellazzi, G., Chard, D., D'Angelo, E., & Wheeler-Kingshott, C. A. M. (2015). Contralateral cerebello-thalamo-cortical pathways with prominent involvement of associative areas in humans in vivo. *Brain Structure and Function*, *220*(6), 3369–3384. https://doi.org/10.1007/s00429-014-0861-2

Park, D. C., & Reuter-Lorenz, P. (2009). The Adaptive Brain: Aging and Neurocognitive Scaffolding. *Annual Review of Psychology*, *60*(1), 173–196. https://doi.org/10.1146/annurev.psych.59.103006.093656

Peirce, J., Gray, J. R., Simpson, S., MacAskill, M., Höchenberger, R., Sogo, H., Kastman, E., & Lindeløv, J. K. (2019). PsychoPy2: Experiments in behavior made easy. *Behavior Research Methods*, *51*(1), 195–203. https://doi.org/10.3758/s13428-018-01193-y

Peirce, J. W. (2007). PsychoPy—Psychophysics software in Python. *Journal of Neuroscience Methods*, *162*(1–2), 8–13. https://doi.org/10.1016/J.JNEUMETH.2006.11.017

Penhune, V. B., & Steele, C. J. (2012). Parallel contributions of cerebellar, striatal and M1 mechanisms to motor sequence learning. In *Behavioural Brain Research* (Vol. 226, Issue 2, pp. 579–591). Elsevier. https://doi.org/10.1016/j.bbr.2011.09.044

Pope, P. A., & Miall, R. C. (2012). Task-specific facilitation of cognition by cathodal transcranial direct current stimulation of the cerebellum. *Brain Stimulation*, *5*(2), 84–94. https://doi.org/10.1016/j.brs.2012.03.006

Power, J. D., Barnes, K. A., Snyder, A. Z., Schlaggar, B. L., & Petersen, S. E. (2012). Spurious but systematic correlations in functional connectivity MRI networks arise from subject motion. *NeuroImage*, *59*(3), 2142–2154. https://doi.org/https://doi.org/10.1016/j.neuroimage.2011.10.018

Priori, A. (2003). Brain polarization in humans: A reappraisal of an old tool for prolonged non-invasive modulation of brain excitability. In *Clinical Neurophysiology* (Vol. 114, Issue 4, pp. 589–595). Elsevier Ireland Ltd. https://doi.org/10.1016/S1388-2457(02)00437-6

Priori, A., Berardelli, A., Rona, S., Accornero, N., & Manfredi, M. (1998). Polarization of the human motor cortex through the scalp. *NeuroReport*, *9*(10), 2257–2260. https://doi.org/10.1097/00001756-199807130-00020

Quartarone, A., Morgante, F., Bagnato, S., Rizzo, V., Sant'Angelo, A., Aiello, E., Reggio, E., Battaglia, F., Messina, C., & Girlanda, P. (2004). Long lasting effects of transcranial direct current stimulation on motor imagery. *NeuroReport*, *15*(8), 1287–1291. https://doi.org/10.1097/01.wnr.0000127637.22805.7c

Rami, L., Gironell, A., Kulisevsky, J., García-Sánchez, C., Berthier, M., & Estévez-González, A. (2003). Effects of repetitive transcranial magnetic stimulation on memory subtypes: a controlled study. *Neuropsychologia*, *41*(14), 1877–1883. https://doi.org/10.1016/S0028-

3932(03)00131-3

Ramnani, N. (2006). The primate cortico-cerebellar system: anatomy and function. *Nature Reviews Neuroscience*, *7*(7), 511–522. https://doi.org/10.1038/nrn1953

Ramnani, N. (2014). Automatic and Controlled Processing in the Corticocerebellar System. In *Progress in Brain Research* (Vol. 210, pp. 255–285). Elsevier B.V. https://doi.org/10.1016/B978-0-444-63356-9.00010-8

Rampersad, S. M., Janssen, A. M., Lucka, F., Aydin, U., Lanfer, B., Lew, S., Wolters, C. H., Stegeman, D. F., & Oostendorp, T. F. (2014). Simulating transcranial direct current stimulation with a detailed anisotropic human head model. *IEEE Transactions on Neural Systems and Rehabilitation Engineering*, *22*(3), 441–452. https://doi.org/10.1109/TNSRE.2014.2308997

Ravizza, S. M., & Ivry, R. B. (2001). *Comparison of the Basal Ganglia and Cerebellum in Shifting Attention*. https://doi.org/10.1162/08989290151137340

Raz, N., Lindenberger, U., Rodrigue, K. M., Kennedy, K. M., Head, D., Williamson, A., Dahle, C., Gerstorf, D., & Acker, J. D. (2005). Regional brain changes in aging healthy adults: General trends, individual differences and modifiers. *Cerebral Cortex*, *15*(11), 1676–1689. https://doi.org/10.1093/cercor/bhi044

Reineberg, A. E., Andrews-Hanna, J. R., Depue, B. E., Friedman, N. P., & Banich, M. T. (2015). Resting-state networks predict individual differences in common and specific aspects of executive function. *NeuroImage*, *104*(1), 69–78. https://doi.org/10.1016/J.NEUROIMAGE.2014.09.045

Reis, J., & Fritsch, B. (2011). Modulation of motor performance and motor learning by transcranial direct current stimulation. *Current Opinion in Neurology*, *24*(6), 590–596.

https://doi.org/10.1097/WCO.0b013e32834c3db0

Reuter-Lorenz, P.A., & Campbell, K. A. (2008). Neurocognitive ageing and the compensation hypothesis. *Current Directions in Psychological Science*, *17*(3), 177–182. https://doi.org/10.1111/j.1467-8721.2008.00570.x

Reuter-Lorenz, Patricia A., & Cappell, K. A. (2008). Neurocognitive aging and the compensation hypothesis. In *Current Directions in Psychological Science* (Vol. 17, Issue 3, pp. 177–182). SAGE PublicationsSage CA: Los Angeles, CA. https://doi.org/10.1111/j.1467-8721.2008.00570.x

Reuter-Lorenz, Patricia A., Jonides, J., Smith, E. E., Hartley, A., Miller, A., Marshuetz, C., & Koeppe, R. A. (2000). Age differences in the frontal lateralization of verbal and spatial working memory revealed by PET. *Journal of Cognitive Neuroscience*, *12*(1), 174–187. https://doi.org/10.1162/089892900561814

Reuter-Lorenz, Patricia A., & Park, D. C. (2014). How Does it STAC Up? Revisiting the Scaffolding Theory of Aging and Cognition. *Neuropsychology Review*, *24*(3), 355–370. https://doi.org/10.1007/s11065-014-9270-9

Rice, L. C., D'Mello, A. M., & Stoodley, C. J. (2021). Differential Behavioral and Neural Effects of Regional Cerebellar tDCS. *Neuroscience*, *462*, 288–302. https://doi.org/10.1016/j.neuroscience.2021.03.008

Richter, S., Gerwig, M., Aslan, B., Wilhelm, H., Schoch, B., Dimitrova, A., Gizewski, E. R., Ziegler, W., Karnath, H. O., & Timmann, D. (2007). Cognitive functions in patients with MR-defined chronic focal cerebellar lesions. *Journal of Neurology*. https://doi.org/10.1007/s00415-006-0500-9

Roy, L. B., Sparing, R., Fink, G. R., & Hesse, M. D. (2015). Modulation of attention functions

by anodal tDCS on right PPC. *Neuropsychologia*, *74*, 96–107. https://doi.org/10.1016/j.neuropsychologia.2015.02.028

Sakai, K., Hikosaka, O., Miyauchi, S., Takino, R., Sasaki, Y., & Pütz, B. (1998). Transition of brain activation from frontal to parietal areas in visuomotor sequence learning. *Journal of Neuroscience*, *18*(5), 1827–1840. https://doi.org/10.1523/jneurosci.18-05-01827.1998

Salmi, J., Pallesen, K. J., Neuvonen, T., Brattico, E., Korvenoja, A., Salonen, O., & Carlson, S. (2010). Cognitive and motor loops of the human cerebro-cerebellar system. *Journal of Cognitive Neuroscience*, *22*(11), 2663–2676. https://doi.org/10.1162/jocn.2009.21382

Samaei, A., Ehsani, F., Zoghi, M., Hafez Yosephi, M., & Jaberzadeh, S. (2017). Online and offline effects of cerebellar transcranial direct current stimulation on motor learning in healthy older adults: a randomized double-blind sham-controlled study. *European Journal of Neuroscience*, *45*(9), 1177–1185. https://doi.org/10.1111/ejn.13559

Sarmiento, C. I., San-Juan, D., & Prasath, V. B. S. (2016). Letter to the Editor: Brief history of transcranial direct current stimulation (tDCS): From electric fishes to microcontrollers. In *Psychological Medicine* (Vol. 46, Issue 15, pp. 3259–3261). Cambridge University Press. https://doi.org/10.1017/S0033291716001926

Schall, U., Johnston, P., Lagopoulos, J., Jüptner, M., Jentzen, W., Thienel, R., Dittmann-Balçar, A., Bender, S., & Ward, P. B. (2003). Functional brain maps of Tower of London performance: a positron emission tomography and functional magnetic resonance imaging study. *NeuroImage*, *20*(2), 1154–1161. https://doi.org/10.1016/S1053-8119(03)00338-0

Schendan, H. E., Searl, M. M., Melrose, R. J., & Stern, C. E. (2003). An fMRI study of the role of the medial temporal lobe in implicit and explicit sequence learning. *Neuron*, *37*(6), 1013–1025. https://doi.org/10.1016/S0896-6273(03)00123-5

Schmahmann, J. D. (2018). The cerebellum and cognition. *Neuroscience Letters*, 62–75. https://doi.org/10.1016/J.NEULET.2018.07.005

Schmahmann, J. D., Guell, X., Stoodley, C. J., & Halko, M. A. (2019). The Theory and Neuroscience of Cerebellar Cognition. *Annual Review of Neuroscience*, *42*(1), 337–364. https://doi.org/10.1146/annurev-neuro-070918-050258

Schmahmann, J., & Sherman, J. C. (1998). The cerebellar cognitive affective syndrome. *Brain*, *121*(4), 561–579. https://doi.org/10.1093/brain/121.4.561

Sebastian, R., Saxena, S., Tsapkini, K., Faria, A. V., Long, C., Wright, A., Davis, C., Tippett, D. C., Mourdoukoutas, A. P., Bikson, M., Celnik, P., & Hillis, A. E. (2017). Cerebellar tDCS: A Novel Approach to Augment Language Treatment Post-stroke. *Frontiers in Human Neuroscience*, *10*, 695. https://doi.org/10.3389/fnhum.2016.00695

Seidler, R. D., Purushotham, A., Kim, S. G., Ugurbil, K., Willingham, D., & Ashe, J. (2005). Neural correlates of encoding and expression in implicit sequence learning. *Experimental Brain Research*, *165*(1), 114–124. https://doi.org/10.1007/s00221-005-2284-z

Seidler, Rachael D., Bo, J., & Anguera, J. A. (2012). Neurocognitive Contributions to Motor Skill Learning: The Role of Working Memory. *Journal of Motor Behavior*, *44*(6), 445–453. https://doi.org/10.1080/00222895.2012.672348

Sen, S., Kawaguchi, A., Truong, Y., Lewis, M. M., & Huang, X. (2010). Dynamic changes in cerebello-thalamo-cortical motor circuitry during progression of Parkinson's disease. *Neuroscience*, *166*(2), 712–719. https://doi.org/10.1016/J.NEUROSCIENCE.2009.12.036

Sereno, M. I., Diedrichsen, J. rn, Tachrount, M., Testa-Silva, G., D Arceuil, H., & De Zeeuw, C. (2020). The human cerebellum has almost 80% of the surface area of the neocortex. *Proceedings of the National Academy of Sciences of the United States of America*, *117*(32),

19538–19543. https://doi.org/10.1073/pnas.2002896117

Shah, B., Nguyen, T. T., & Madhavan, S. (2013). Polarity independent effects of cerebellar tDCS on short term ankle visuomotor learning. *Brain Stimulation*, *6*(6), 966–968. https://doi.org/10.1016/j.brs.2013.04.008

Shimizu, R. E., Wu, A. D., Samra, J. K., & Knowlton, B. J. (2017). The impact of cerebellar transcranial direct current stimulation (tDCS) on learning fine-motor sequences. *Philosophical Transactions of the Royal Society B: Biological Sciences*, *372*(1711). https://doi.org/http://dx.doi.org/10.1098/rstb.2016.0050

Shirer, W. R., Ryali, S., Rykhlevskaia, E., Menon, V., & Greicius, M. D. (2012). Decoding subject-driven cognitive states with whole-brain connectivity patterns. *Cerebral Cortex*, *22*(1), 158–165. https://doi.org/10.1093/cercor/bhr099

Smith, S. M. (2002). Fast robust automated brain extraction. *Human Brain Mapping*, *17*(3), 143–155. https://doi.org/10.1002/hbm.10062

Spielmann, K., van der Vliet, R., van de Sandt-Koenderman, W. M. E., Frens, M. A., Ribbers, G. M., Selles, R. W., van Vugt, S., van der Geest, J. N., & Holland, P. (2017). Cerebellar Cathodal Transcranial Direct Stimulation and Performance on a Verb Generation Task: A Replication Study. *Neural Plasticity*, *2017*, 1–12. https://doi.org/10.1155/2017/1254615

Steiner, K. M., Enders, A., Thier, W., Batsikadze, G., Ludolph, N., Ilg, W., & Timmann, D. (2016). Cerebellar tDCS Does Not Improve Learning in a Complex Whole Body Dynamic Balance Task in Young Healthy Subjects. *PLOS ONE*, *11*(9), e0163598. https://doi.org/10.1371/journal.pone.0163598

Sternberg, S. (1966). High-speed scanning in human memory. *Science*, *153*(3736), 652–654. https://doi.org/10.1126/SCIENCE.153.3736.652

Stoodley, C. J. (2012). The cerebellum and cognition: Evidence from functional imaging studies. *Cerebellum*, *11*(2), 352–365. https://doi.org/10.1007/s12311-011-0260-7

Stoodley, C. J., & Schmahmann, J. D. (2010). Evidence for topographic organization in the cerebellum of motor control versus cognitive and affective processing. *CORTEX*, *46*(7), 831–844. https://doi.org/10.1016/j.cortex.2009.11.008

Stoodley, C. J., Valera, E. M., & Schmahmann, J. D. (2012a). Functional topography of the cerebellum for motor and cognitive tasks: An fMRI study. *NeuroImage*, *59*(2), 1560–1570. https://doi.org/10.1016/j.neuroimage.2011.08.065

Stoodley, C. J., Valera, E., & Schmahmann, J. (2012b). Functional topography of the cerebellum for cognitive and motor tasks. *Neuron*, *59*(2), 1560–1570. https://doi.org/10.1016/j.neuroimage.2011.08.065.Functional

Stoodley, C., & Schmahmann, J. (2009). Functional topography in the human cerebellum: A meta-analysis of neuroimaging studies. *NeuroImage*, *44*(2), 489–501. https://doi.org/10.1016/j.neuroimage.2008.08.039

Team, R. C. (2018). *R: A Language and Environment for Statistical Computing*. R Foundation for Statistical Computing.

Timmann, D., Brandauer, B., Hermsdörfer, J., Ilg, W., Konczak, J., Gerwig, M., Gizewski, E. R., & Schoch, B. (2008). Lesion-Symptom Mapping of the Human Cerebellum. *The Cerebellum*, *7*(4), 602–606. https://doi.org/10.1007/s12311-008-0066-4

Timmann, D., Konczak, J., Ilg, W., Donchin, O., Hermsdörfer, J., Gizewski, E. R., & Schoch, B. (2009). Current advances in lesion-symptom mapping of the human cerebellum. *Neuroscience*, *162*(3), 836–851. https://doi.org/10.1016/j.neuroscience.2009.01.040

Tremblay, S., Austin, D., Hannah, R., & Rothwell, J. C. (2016). Non-invasive brain stimulation

as a tool to study cerebellar-M1 interactions in humans. In *Cerebellum and Ataxias* (Vol. 3, Issue 1, pp. 1–23). BioMed Central Ltd. https://doi.org/10.1186/s40673-016-0057-z

Turkeltaub, P. E., Swears, M. K., D'Mello, A. M., & Stoodley, C. J. (2016). Cerebellar tDCS as a novel treatment for aphasia? Evidence from behavioral and resting-state functional connectivity data in healthy adults. *Restorative Neurology and Neuroscience*, *34*(4), 491–505. https://doi.org/10.3233/RNN-150633

Valero-Cabré, A., Amengual, J. L., Stengel, C., Pascual-Leone, A., & Coubard, O. A. (2017). Transcranial magnetic stimulation in basic and clinical neuroscience: A comprehensive review of fundamental principles and novel insights. In *Neuroscience and Biobehavioral Reviews* (Vol. 83, pp. 381–404). Elsevier Ltd. https://doi.org/10.1016/j.neubiorev.2017.10.006

van Dun, K., & Manto, M. (2018). Non-invasive Cerebellar Stimulation: Moving Towards Clinical Applications for Cerebellar and Extra-Cerebellar Disorders. In *Cerebellum* (Vol. 17, Issue 3, pp. 259–263). Springer New York LLC. https://doi.org/10.1007/s12311-017-0908-z

van Wessel, B. W. V., Claire Verhage, M., Holland, P., Frens, M. A., & van der Geest, J. N. (2016). Cerebellar tDCS does not affect performance in the N-back task. *Journal of Clinical and Experimental Neuropsychology*, *38*(3), 319–326. https://doi.org/10.1080/13803395.2015.1109610

Verhage, M. C., Avila, E. O., Frens, M. A., Donchin, O., & van der Geest, J. N. (2017). Cerebellar tDCS Does Not Enhance Performance in an Implicit Categorization Learning Task. *Frontiers in Psychology*, *8*, 476. https://doi.org/10.3389/fpsyg.2017.00476

Villamar, M. F., Volz, M. S., Bikson, M., Datta, A., DaSilva, A. F., & Fregni, F. (2013).

Technique and Considerations in the Use of 4x1 Ring High-definition Transcranial Direct Current Stimulation (HD-tDCS). *Journal of Visualized Experiments*, *77*, e50309. https://doi.org/10.3791/50309

Wei, P., Zhang, Z., Lv, Z., & Jing, B. (2017). Strong functional connectivity among homotopic brain areas is vital for motor control in unilateral limb movement. *Frontiers in Human Neuroscience*, *11*, 366. https://doi.org/10.3389/fnhum.2017.00366

Wen, W., & Sachdev, P. (2004). The topography of white matter hyperintensities on brain MRI in healthy 60- to 64-year-old individuals. *NeuroImage*, *22*(1), 144–154. https://doi.org/10.1016/j.neuroimage.2003.12.027

Whitfield-Gabrieli, S., & Nieto-Castanon, A. (2012). *Conn* : A Functional Connectivity Toolbox for Correlated and Anticorrelated Brain Networks. *Brain Connectivity*, *2*(3), 125–141. https://doi.org/10.1089/brain.2012.0073

Woolrich, M. W., Ripley, B. D., Brady, M., & Smith, S. M. (2001). Temporal autocorrelation in univariate linear modeling of FMRI data. *NeuroImage*, *14*(6), 1370–1386. https://doi.org/10.1006/nimg.2001.0931

Worsley, K. J. (2001). Statistical analysis of activation images. In Peter Jezzard, Paul M. Matthews, & Stephen M. Smith (Eds.), *Functional MRI—An Introduction to Methods* (pp. 251–270). Oxford University Press. https://pdfs.semanticscholar.org/ef6b/6c4f7701f433a5804a4e8408179d91d94e44.pdf#page=266

Wynn, S. C., Driessen, J. M. A., Glennon, J. C., Brazil, I. A., & Schutter, D. J. L. G. (2019). Cerebellar Transcranial Direct Current Stimulation Improves Reactive Response Inhibition in Healthy Volunteers. *Cerebellum*, *18*(6), 983–988. https://doi.org/10.1007/s12311-019-

01047-z

Yang, Y. K., Chiu, N. T., Chen, C. C., Chen, M., Yeh, T. L., & Lee, I. H. (2003). Correlation between fine motor activity and striatal dopamine D2 receptor density in patients with schizophrenia and healthy controls. *Psychiatry Research - Neuroimaging*, *123*(3), 191–197. https://doi.org/10.1016/S0925-4927(03)00066-0

APPENDIX A

CHAPTER III TABLES

**Table A.1 Significant ROI connectivity by cerebellar ROI following sham stimulation.**

| Targets | beta | T(24) | p-FDR |
|---|---|---|---|
| Lobule I-IV | | | |
| Right Lobule IV & V, Cerebellum | 0.91 | 16.56 | 0.000 |
| Right Lobule III, Cerebellum | 0.72 | 15.06 | 0.000 |
| Vermis III, Cerebellum | 0.59 | 14 | 0.000 |
| Vermis IV & V, Cerebellum | 0.67 | 13.66 | 0.000 |
| Right Lobule V, Cerebellum | 0.59 | 12.25 | 0.000 |
| Left Lobule IV & V, Cerebellum | 0.59 | 12.1 | 0.000 |
| Left Lobule III, Cerebellum | 0.38 | 10.47 | 0.000 |
| Vermis I & II, Cerebellum | 0.34 | 10.23 | 0.000 |
| Vermis VI, Cerebellum | 0.31 | 8.97 | 0.000 |
| Vermis X, Cerebellum | 0.25 | 8.48 | 0.000 |
| Vermis VI, Cerebellum | 0.23 | 7.28 | 0.000 |
| Left Lobule IV, Cerebellum | 0.23 | 7.25 | 0.000 |
| Right Parahippocampal Gyrus | 0.24 | 6.59 | 0.000 |
| Anterior Cerebellar Network (0,-63,-30) | 0.23 | 6.48 | 0.000 |
| Right Lobule VI, Cerebellum | 0.24 | 5.95 | 0.000 |
| Right Lobule V, Cerebellum | 0.23 | 5.61 | 0.000 |
| Left Parahippocampal Gyrus | 0.22 | 5.53 | 0.000 |
| Vermis VII, Cerebellum | 0.21 | 5.47 | 0.000 |
| Brain Stem | 0.24 | 5.07 | 0.000 |
| Right Hippocampus | 0.12 | 5.07 | 0.000 |
| Left Thalamus | 0.16 | 4.89 | 0.001 |
| Right Temporal Occipital Fusiform Gyrus | 0.18 | 4.8 | 0.001 |
| Right Thalamus | 0.14 | 4.22 | 0.003 |
| Vermis VIII, Cerebellum | 0.18 | 3.98 | 0.004 |
| Vermis VIIb, Cerebellum | 0.17 | 3.8 | 0.007 |
| Left Insular Cortex | 0.13 | 3.74 | 0.007 |
| Vermis IX, Cerebellum | 0.13 | 3.56 | 0.011 |
| Right Crus I, Cerebellum | 0.09 | 3.44 | 0.014 |
| Right Lobule IX, Cerebellum | 0.11 | 3.15 | 0.027 |
| Right Crus I, Cerebellum | 0.09 | 3.14 | 0.027 |
| Occipital Visual Network (0,-93,-4) | -0.1 | -2.98 | 0.038 |
| Left Lateral Occipital Cortex | -0.09 | -2.97 | 0.038 |

| | | | |
|---|---|---|---|
| FrontoParietal Network (Left Lateral Prefrontal Cortex; -43,33,28) | -0.09 | -2.94 | 0.039 |
| Left Temporal Occipital Fusiform Gyrus | 0.1 | 2.85 | 0.047 |
| Right Occipital Pole | -0.11 | -2.82 | 0.049 |
| Lobule V | | | |
| Right Lobule IV & V, Cerebellum | 1.3 | 26.92 | 0.000 |
| Right Lobule V, Cerebellum | 0.6 | 16.09 | 0.000 |
| Right Lobule VI, Cerebellum | 0.62 | 15.96 | 0.000 |
| Left Lobule IV & V, Cerebellum | 0.72 | 14.97 | 0.000 |
| Vermis VI, Cerebellum | 0.72 | 14.66 | 0.000 |
| Left Lobule IV, Cerebellum | 0.53 | 13.29 | 0.000 |
| Vermis IV & V, Cerebellum | 0.6 | 13.03 | 0.000 |
| Right Lobule I-IV, Cerebellum | 0.59 | 12.25 | 0.000 |
| Anterior Cerebellar Network (0,-63,-30) | 0.38 | 10.36 | 0.000 |
| Right Temporal Occipital Fusiform Gyrus | 0.39 | 9.49 | 0.000 |
| Vermis VI, Cerebellum | 0.5 | 9.27 | 0.000 |
| Vermis III, Cerebellum | 0.3 | 6.94 | 0.000 |
| Vermis VII, Cerebellum | 0.35 | 6.93 | 0.000 |
| Left Lobule III, Cerebellum | 0.24 | 6.86 | 0.000 |
| Right Lobule III, Cerebellum | 0.24 | 6.48 | 0.000 |
| Left Temporal Occipital Fusiform Gyrus | 0.22 | 6 | 0.000 |
| Vermis VIII, Cerebellum | 0.25 | 5.28 | 0.000 |
| Left Insular Cortex | 0.13 | 5.28 | 0.000 |
| Left Parahippocampal Gyrus | 0.22 | 4.95 | 0.001 |
| Right Lingual Gyrus | 0.22 | 4.82 | 0.001 |
| Right Lobule VIII, Cerebellum | 0.13 | 4.57 | 0.001 |
| Vermis VIIb, Cerebellum | 0.2 | 4.26 | 0.002 |
| Right Parahippocampal Gyrus | 0.22 | 4.26 | 0.002 |
| Left Thalamus | 0.15 | 4.2 | 0.003 |
| Vermis X, Cerebellum | 0.13 | 4.15 | 0.003 |
| Left Lobule VIII, Cerebellum | 0.14 | 3.8 | 0.006 |
| Vermis VIII, Cerebellum | 0.16 | 3.79 | 0.006 |
| Right Temporal Fusiform Cortex | 0.16 | 3.49 | 0.012 |
| Brain Stem | 0.14 | 3.48 | 0.012 |
| Vermis I & II, Cerebellum | 0.11 | 3.42 | 0.014 |
| Right Lobule VIIb, Cerebellum | 0.11 | 3.38 | 0.015 |
| Left Lingual Gyrus | 0.18 | 3.36 | 0.015 |
| Right Thalamus | 0.12 | 3.18 | 0.023 |
| Left Crus I, Cerebellum | 0.11 | 3.13 | 0.025 |
| Left Putamen | 0.09 | 3.08 | 0.027 |

| | | | |
|---|---|---|---|
| Right Crus I, Cerebellum | 0.11 | 2.96 | 0.035 |
| Right Crus I, Cerebellum | 0.11 | 2.91 | 0.038 |
| Left Temporal Fusiform Cortex | 0.1 | 2.87 | 0.040 |
| Right Lobule X, Cerebellum | 0.1 | 2.8 | 0.046 |
| Lobule VI | | | |
| Right Lobule VI, Cerebellum | 2.54 | 41.17 | 0.000 |
| Right Lobule V, Cerebellum | 0.6 | 16.09 | 0.000 |
| Left Lobule IV, Cerebellum | 0.73 | 15.09 | 0.000 |
| Anterior Cerebellar Network (0,-63,-30) | 0.81 | 14.98 | 0.000 |
| Right Temporal Occipital Fusiform Gyrus | 0.63 | 12.83 | 0.000 |
| Vermis VI, Cerebellum | 0.5 | 12.44 | 0.000 |
| Vermis VI, Cerebellum | 0.54 | 11.73 | 0.000 |
| Right Lobule IV & V, Cerebellum | 0.47 | 11.43 | 0.000 |
| Right Crus I, Cerebellum | 0.43 | 9.59 | 0.000 |
| Right Crus I, Cerebellum | 0.45 | 9.47 | 0.000 |
| Left Temporal Occipital Fusiform Gyrus | 0.35 | 8.79 | 0.000 |
| Left Crus I, Cerebellum | 0.33 | 7.97 | 0.000 |
| Left Lobule IV & V, Cerebellum | 0.35 | 7.4 | 0.000 |
| Vermis VII, Cerebellum | 0.45 | 7.36 | 0.000 |
| Right Lobule VIII, Cerebellum | 0.26 | 6.01 | 0.000 |
| Right Lobule I-IV, Cerebellum | 0.23 | 5.61 | 0.000 |
| Vermis VIII, Cerebellum | 0.26 | 5.23 | 0.000 |
| Vermis IV & V, Cerebellum | 0.24 | 4.96 | 0.001 |
| Right Occipital Fusiform Gyrus | 0.28 | 4.66 | 0.001 |
| Vermis VIII, Cerebellum | 0.21 | 4.62 | 0.001 |
| Posterior Cerebellar Network (0,-79,-32) | 0.25 | 4.33 | 0.002 |
| Vermis III, Cerebellum | 0.15 | 4.24 | 0.002 |
| Left Lobule VIII, Cerebellum | 0.22 | 4.24 | 0.002 |
| Vermis VIIb, Cerebellum | 0.21 | 4.02 | 0.004 |
| Vermis X, Cerebellum | 0.15 | 3.89 | 0.005 |
| Right Lobule X, Cerebellum | 0.14 | 3.55 | 0.012 |
| Left Temporal Fusiform Cortex | 0.11 | 3.4 | 0.016 |
| Right Paracingulate Gyrus | -0.13 | -3.37 | 0.017 |
| Right Superior Frontal Gyrus | -0.12 | -3.18 | 0.025 |
| Right Putamen | 0.12 | 3.14 | 0.027 |
| Right Lobule V, CerebellumIIa | 0.12 | 3.07 | 0.031 |
| Right Lingual Gyrus | 0.16 | 3.06 | 0.031 |
| Left Lobule VIIb, Cerebellum | 0.14 | 2.99 | 0.035 |
| Vermis IX, Cerebellum | 0.12 | 2.98 | 0.035 |

| | | | |
|---|---|---|---|
| Right Parahippocampal Gyrus | 0.12 | 2.87 | 0.044 |
| Lobule VIIb | | | |
| Right Lobule VIII, Cerebellum | 0.74 | 15.56 | 0.000 |
| Right Lobule VIIb, Cerebellum | 1.18 | 14.96 | 0.000 |
| Right Lobule V, CerebellumIIa | 0.58 | 11.27 | 0.000 |
| Right Crus I, CerebellumI | 0.61 | 11.02 | 0.000 |
| Right Crus II, Cerebellum | 0.56 | 10.78 | 0.000 |
| Posterior Cerebellar Network (0,-79,-32) | 0.33 | 7.95 | 0.000 |
| Left Lobule VIIb, Cerebellum | 0.42 | 7.27 | 0.000 |
| Left Crus II, Cerebellum | 0.31 | 6.96 | 0.000 |
| Right Crus I, Cerebellum | 0.26 | 6.28 | 0.000 |
| Left Lobule VIII, Cerebellum | 0.34 | 6.25 | 0.000 |
| Right Crus I, Cerebellum | 0.25 | 5.62 | 0.000 |
| Vermis VIII, Cerebellum | 0.2 | 4.73 | 0.001 |
| Vermis VIII, Cerebellum | 0.22 | 4.5 | 0.002 |
| Right Lobule IX, Cerebellum | 0.22 | 4.22 | 0.004 |
| Left Precentral Gyrus | 0.12 | 3.94 | 0.008 |
| Right Lobule IX, Cerebellum | 0.2 | 3.81 | 0.010 |
| Right Lobule VIIb, Cerebellum | 0.16 | 3.8 | 0.010 |
| Left Lobule IX, Cerebellum | 0.17 | 3.74 | 0.011 |
| Vermis VIII, Cerebellum | 0.18 | 3.56 | 0.016 |
| Left Crus I, Cerebellum | 0.17 | 3.53 | 0.016 |
| Vermis IX, Cerebellum | 0.12 | 3.42 | 0.020 |
| Left Postcentral Gyrus | 0.08 | 3.37 | 0.021 |
| Left Lingual Gyrus | 0.11 | 3.32 | 0.023 |
| Crus I | | | |
| Right Crus I, Cerebellum | 2.3 | 40.43 | 0.000 |
| Posterior Cerebellar Network (0,-79,-32) | 1.09 | 17.3 | 0.000 |
| Right Crus II, Cerebellum | 0.83 | 14.72 | 0.000 |
| Right Crus I, CerebellumI | 0.69 | 13.41 | 0.000 |
| Anterior Cerebellar Network (0,-63,-30) | 0.56 | 11.06 | 0.000 |
| Left Crus I, Cerebellum | 0.55 | 10.69 | 0.000 |
| Right Lobule VI, Cerebellum | 0.47 | 10.45 | 0.000 |
| Right Lobule VIIb, Cerebellum | 0.32 | 9.84 | 0.000 |
| Right Lobule V, Cerebellum | 0.43 | 9.59 | 0.000 |
| Left Crus II, Cerebellum | 0.45 | 9.33 | 0.000 |
| Right Occipital Fusiform Gyrus | 0.3 | 7.27 | 0.000 |
| Right Lobule VIII, Cerebellum | 0.28 | 6.31 | 0.000 |
| Right Lobule V, CerebellumIb | 0.26 | 6.28 | 0.000 |

| | | | |
|---|---|---|---|
| Vermis VI, Cerebellum | 0.3 | 6.16 | 0.000 |
| Vermis VII, Cerebellum | 0.38 | 5.88 | 0.000 |
| Left Lobule VIII, Cerebellum | 0.22 | 5.75 | 0.000 |
| Occipital Visual Network (0,-93,-4) | 0.3 | 5.64 | 0.000 |
| Right Temporal Occipital Fusiform Gyrus | 0.2 | 5.32 | 0.000 |
| Left Lobule VIIb, Cerebellum | 0.21 | 5.27 | 0.000 |
| Vermis VI, Cerebellum | 0.19 | 4.81 | 0.001 |
| Vermis VIII, Cerebellum | 0.22 | 4.74 | 0.001 |
| Left Lobule IV, Cerebellum | 0.2 | 4.39 | 0.002 |
| Vermis VIII, Cerebellum | 0.16 | 4.19 | 0.003 |
| Right Lateral Occipital Cortex | 0.19 | 4.02 | 0.004 |
| Vermis VIII, Cerebellum | 0.2 | 4 | 0.004 |
| Right Lingual Gyrus | 0.15 | 3.95 | 0.004 |
| Left Middle Frontal Gyrus | 0.18 | 3.94 | 0.004 |
| Left Occipital Fusiform Gyrus | 0.21 | 3.87 | 0.005 |
| Right Occipital Pole | 0.18 | 3.78 | 0.006 |
| Left Inferior Frontal Gyrus | 0.13 | 3.67 | 0.007 |
| Vermis VIIb, Cerebellum | 0.17 | 3.67 | 0.007 |
| Right Lobule IX, Cerebellum | 0.14 | 3.65 | 0.007 |
| Right Lobule V, CerebellumIIa | 0.17 | 3.64 | 0.007 |
| Dorsal Attentional Network (Left Frontal Eye Field; -27,-9,64) | 0.15 | 3.61 | 0.008 |
| Left Precentral Gyrus | 0.15 | 3.46 | 0.011 |
| Right Lobule I-IV, Cerebellum | 0.09 | 3.44 | 0.011 |
| Left Frontal Pole | 0.14 | 3.42 | 0.011 |
| Left Occipital Pole | 0.18 | 3.38 | 0.012 |
| Left Inferior Temporal Gyrus | 0.15 | 3.35 | 0.013 |
| Salience Network (Left Rostal Prefrontal Cortex; -32,45,27) | 0.13 | 3.19 | 0.018 |
| Salience Network (Left Supramarginal Gyrus; -60,-39,31) | -0.11 | -3.1 | 0.022 |
| Vermis IX, Cerebellum | 0.11 | 2.98 | 0.028 |
| Right Lobule V, Cerebellum | 0.11 | 2.96 | 0.029 |
| Right Central Opercular Cortex | -0.12 | -2.91 | 0.032 |
| Right Lobule IX, Cerebellum | 0.13 | 2.86 | 0.035 |
| Right Superior Frontal Gyrus | -0.13 | -2.85 | 0.035 |
| Left Lingual Gyrus | 0.1 | 2.8 | 0.038 |
| Left Lateral Occipital Cortex | 0.13 | 2.76 | 0.041 |
| FrontoParietal Network (Right Posterior Parietal Cortex; 52,-52,45) | -0.1 | -2.76 | 0.041 |
| Left Inferior Frontal Gyrus | 0.09 | 2.75 | 0.041 |
| Default Mode Network (Left Lateral Parietal Cortex; -39,-77,33) | 0.13 | 2.71 | 0.042 |

| | | | |
|---|---|---|---|
| Left Parietal Operculum Cortex | -0.1 | -2.71 | 0.042 |
| Right Supramarginal Gyrus | -0.1 | -2.71 | 0.042 |
| Right Lobule IV & V, Cerebellum | 0.09 | 2.68 | 0.044 |
| Left Lateral Visual Network (-37,-79,10) | 0.11 | 2.65 | 0.046 |
| Salience Network (Anterior Cingulate Cortex; 0,22,35) | -0.11 | -2.62 | 0.049 |
| Crus II | | | |
| Right Crus II, Cerebellum | 2.29 | 22.66 | 0.000 |
| Posterior Cerebellar Network (0,-79,-32) | 0.86 | 16.31 | 0.000 |
| Right Crus I, Cerebellum | 0.69 | 13.41 | 0.000 |
| Left Crus II, Cerebellum | 0.54 | 13.13 | 0.000 |
| Right Lobule VIIb, Cerebellum | 0.8 | 12.91 | 0.000 |
| Right Crus I, Cerebellum | 0.65 | 11.91 | 0.000 |
| Right Lobule V, CerebellumIb | 0.61 | 11.02 | 0.000 |
| Right Lobule VIII, Cerebellum | 0.36 | 10.39 | 0.000 |
| Left Lobule VIIb, Cerebellum | 0.33 | 9.17 | 0.000 |
| Left Crus I, Cerebellum | 0.32 | 7.82 | 0.000 |
| Left Lobule VIII, Cerebellum | 0.25 | 5.94 | 0.000 |
| Vermis VIII, Cerebellum | 0.26 | 5.01 | 0.001 |
| Anterior Cerebellar Network (0,-63,-30) | 0.26 | 4.9 | 0.001 |
| Vermis VIII, Cerebellum | 0.27 | 4.77 | 0.001 |
| Left Middle Temporal Gyrus | 0.16 | 4.42 | 0.002 |
| Right Lobule V, CerebellumIIa | 0.22 | 4.4 | 0.002 |
| Right Lobule IX, Cerebellum | 0.19 | 4.21 | 0.004 |
| Vermis VII, Cerebellum | 0.24 | 4.15 | 0.004 |
| Vermis VIII, Cerebellum | 0.2 | 4.02 | 0.005 |
| Occipital Visual Network (0,-93,-4) | 0.2 | 3.85 | 0.007 |
| Left Precentral Gyrus | 0.18 | 3.62 | 0.012 |
| Left Pallidum | 0.11 | 3.34 | 0.023 |
| Default Mode Network (Left Lateral Parietal Cortex; -39,-77,33) | 0.14 | 3.2 | 0.031 |
| Left Inferior Frontal Gyrus | 0.1 | 3.18 | 0.031 |
| Left Lateral Occipital Cortex | 0.13 | 3.11 | 0.035 |
| Right Superior Frontal Gyrus | -0.11 | -3.05 | 0.039 |
| Right Lobule IX, Cerebellum | 0.14 | 2.97 | 0.046 |
| Vermis VI, Cerebellum | 0.17 | 2.95 | 0.046 |
| Right Middle Frontal Gyrus | -0.11 | -2.93 | 0.046 |

**Table A.2 Significant ROI connectivity by cerebellar ROI following anodal stimulation.**

| Target | beta | T(24) | p-FDR |
|---|---|---|---|
| Lobule I-IV | | | |
| Right Lobule III, Cerebellum | 0.64 | 18.83 | 0.000 |
| Right Lobule IV & V, Cerebellum | 0.92 | 16.81 | 0.000 |
| Vermis IV & V, Cerebellum | 0.61 | 14.89 | 0.000 |
| Vermis III, Cerebellum | 0.67 | 14.31 | 0.000 |
| Left Lobule IV & V, Cerebellum | 0.6 | 12.64 | 0.000 |
| Right Lobule V, Cerebellum | 0.59 | 11.99 | 0.000 |
| Left Lobule III, Cerebellum | 0.41 | 9.84 | 0.000 |
| Left Lobule IV, Cerebellum | 0.29 | 8.35 | 0.000 |
| Vermis I & II, Cerebellum | 0.33 | 7.87 | 0.000 |
| Right Lobule VI, Cerebellum | 0.28 | 7.05 | 0.000 |
| Vermis VI, Cerebellum | 0.29 | 6.84 | 0.000 |
| Left Parahippocampal Gyrus | 0.26 | 6.67 | 0.000 |
| Right Lobule V, Cerebellum | 0.27 | 6.57 | 0.000 |
| Right Parahippocampal Gyrus | 0.3 | 6.42 | 0.000 |
| Left Temporal Occipital Fusiform Gyrus | 0.2 | 5.67 | 0.000 |
| Left Hippocampus | 0.17 | 5.57 | 0.000 |
| Right Hippocampus | 0.18 | 5.45 | 0.000 |
| Right Thalamus | 0.18 | 5.31 | 0.000 |
| Left Lobule IX, Cerebellum | 0.18 | 5.2 | 0.000 |
| Vermis VI, Cerebellum | 0.23 | 5.18 | 0.000 |
| Anterior Cerebellar Network (0,-63,-30) | 0.23 | 4.94 | 0.000 |
| Brain Stem | 0.18 | 4.92 | 0.000 |
| Right Temporal Occipital Fusiform Gyrus | 0.2 | 4.86 | 0.000 |
| Left Thalamus | 0.17 | 4.81 | 0.000 |
| Vermis VII, Cerebellum | 0.19 | 3.9 | 0.005 |
| Vermis X, Cerebellum | 0.17 | 3.82 | 0.006 |
| Right Temporal Fusiform Cortex | 0.14 | 3.61 | 0.009 |
| Left Lingual Gyrus | 0.13 | 3.5 | 0.012 |
| Left Lateral Occipital Cortex | -0.09 | -3.17 | 0.025 |
| Right Superior Frontal Gyrus | -0.1 | -3.11 | 0.028 |
| Right Lobule IX, Cerebellum | 0.12 | 3.01 | 0.035 |
| Vermis VIII, Cerebellum | 0.13 | 2.98 | 0.036 |
| Left Temporal Fusiform Cortex | 0.09 | 2.9 | 0.042 |
| Vermis IX, Cerebellum | 0.13 | 2.89 | 0.042 |
| Lobule V | | | |
| Right Lobule IV & V, Cerebellum | 1.23 | 30.87 | 0.000 |

| | | | |
|---|---|---|---|
| Vermis IV & V, Cerebellum | 0.65 | 15.92 | 0.000 |
| Vermis VI, Cerebellum | 0.73 | 15.63 | 0.000 |
| Right Lobule VI, Cerebellum | 0.64 | 14.61 | 0.000 |
| Left Lobule IV, Cerebellum | 0.58 | 14.06 | 0.000 |
| Left Lobule IV & V, Cerebellum | 0.76 | 13.35 | 0.000 |
| Right Lobule V, Cerebellum | 0.6 | 13.25 | 0.000 |
| Right Lobule I-IV, Cerebellum | 0.59 | 11.99 | 0.000 |
| Vermis VI, Cerebellum | 0.47 | 9.81 | 0.000 |
| Anterior Cerebellar Network (0,-63,-30) | 0.41 | 8.19 | 0.000 |
| Vermis III, Cerebellum | 0.29 | 7.75 | 0.000 |
| Left Lobule III, Cerebellum | 0.3 | 7.18 | 0.000 |
| Left Parahippocampal Gyrus | 0.23 | 6.95 | 0.000 |
| Right Parahippocampal Gyrus | 0.27 | 6.92 | 0.000 |
| Right Temporal Occipital Fusiform Gyrus | 0.34 | 6.74 | 0.000 |
| Vermis VII, Cerebellum | 0.34 | 6.64 | 0.000 |
| Left Temporal Occipital Fusiform Gyrus | 0.29 | 6.47 | 0.000 |
| Left Lingual Gyrus | 0.32 | 6.21 | 0.000 |
| Right Lingual Gyrus | 0.36 | 5.94 | 0.000 |
| Right Temporal Fusiform Cortex | 0.23 | 5.9 | 0.000 |
| Vermis VIII, Cerebellum | 0.25 | 5.5 | 0.000 |
| Left Lobule IX, Cerebellum | 0.19 | 5.17 | 0.000 |
| Right Juxtapositional Lobule Cortex | -0.14 | -4.91 | 0.000 |
| Right Lobule III, Cerebellum | 0.2 | 4.69 | 0.001 |
| Left Hippocampus | 0.2 | 4.53 | 0.001 |
| Brain Stem | 0.14 | 4.48 | 0.001 |
| Left Crus I, Cerebellum | 0.19 | 4.4 | 0.001 |
| Left Juxtapositional Lobule Cortex | -0.16 | -4.3 | 0.002 |
| Right Crus I, Cerebellum | 0.15 | 4.21 | 0.002 |
| Right Hippocampus | 0.19 | 4.21 | 0.002 |
| Right Lobule VIIb, Cerebellum | 0.11 | 3.97 | 0.003 |
| Left Temporal Fusiform Cortex | 0.16 | 3.97 | 0.003 |
| Right Crus I, Cerebellum | 0.13 | 3.88 | 0.004 |
| Right Thalamus | 0.17 | 3.87 | 0.004 |
| Left Thalamus | 0.17 | 3.81 | 0.004 |
| Vermis IX, Cerebellum | 0.19 | 3.79 | 0.004 |
| Vermis VIIb, Cerebellum | 0.18 | 3.73 | 0.005 |
| Right Lobule IX, Cerebellum | 0.15 | 3.62 | 0.006 |
| Vermis IX, Cerebellum | 0.15 | 3.59 | 0.007 |
| Right Occipital Fusiform Gyrus | 0.15 | 3.43 | 0.010 |

| | | | |
|---|---|---|---|
| Right Lobule VIII, Cerebellum | 0.14 | 3.16 | 0.019 |
| Right Superior Frontal Gyrus | -0.12 | -3.07 | 0.022 |
| Left Lobule VIII, Cerebellum | 0.14 | 3.02 | 0.024 |
| Vermis X, Cerebellum | 0.15 | 3.02 | 0.024 |
| Vermis VIII, Cerebellum | 0.14 | 2.85 | 0.035 |
| Posterior Cerebellar Network (0,-79,-32) | 0.1 | 2.76 | 0.042 |
| Left Middle Frontal Gyrus | -0.1 | -2.75 | 0.042 |
| Vermis VIII, Cerebellum | 0.11 | 2.74 | 0.042 |
| Left Occipital Fusiform Gyrus | 0.11 | 2.69 | 0.047 |
| Lobule VI | | | |
| Right Lobule VI, Cerebellum | 2.64 | 48.41 | 0.000 |
| Left Lobule IV, Cerebellum | 0.77 | 14.49 | 0.000 |
| Right Lobule V, Cerebellum | 0.6 | 13.25 | 0.000 |
| Anterior Cerebellar Network (0,-63,-30) | 0.81 | 13.14 | 0.000 |
| Vermis VI, Cerebellum | 0.44 | 10.77 | 0.000 |
| Left Lobule IV & V, Cerebellum | 0.42 | 10.62 | 0.000 |
| Right Crus I, Cerebellum | 0.53 | 10.24 | 0.000 |
| Right Lobule IV & V, Cerebellum | 0.5 | 10.02 | 0.000 |
| Right Crus I, Cerebellum | 0.5 | 9.62 | 0.000 |
| Right Temporal Occipital Fusiform Gyrus | 0.47 | 9.42 | 0.000 |
| Vermis VI, Cerebellum | 0.47 | 8.7 | 0.000 |
| Vermis III, Cerebellum | 0.21 | 8.67 | 0.000 |
| Left Temporal Occipital Fusiform Gyrus | 0.29 | 8.65 | 0.000 |
| Vermis VII, Cerebellum | 0.42 | 7.9 | 0.000 |
| Left Crus I, Cerebellum | 0.4 | 7.7 | 0.000 |
| Right Occipital Fusiform Gyrus | 0.3 | 7.2 | 0.000 |
| Right Lobule I-IV, Cerebellum | 0.27 | 6.57 | 0.000 |
| Posterior Cerebellar Network (0,-79,-32) | 0.32 | 6.18 | 0.000 |
| Vermis IV & V, Cerebellum | 0.21 | 6.16 | 0.000 |
| Left Lobule III, Cerebellum | 0.2 | 5.94 | 0.000 |
| Right Lingual Gyrus | 0.28 | 5.53 | 0.000 |
| Right Paracingulate Gyrus | -0.12 | -5.09 | 0.000 |
| Left Lingual Gyrus | 0.19 | 4.41 | 0.001 |
| Precuneous Cortex | -0.14 | -3.98 | 0.004 |
| Right Lobule III, Cerebellum | 0.17 | 3.97 | 0.004 |
| Right Temporal Fusiform Cortex | 0.19 | 3.88 | 0.005 |
| Brain Stem | 0.14 | 3.83 | 0.005 |
| Vermis VIIb, Cerebellum | 0.17 | 3.8 | 0.006 |
| Right Superior Frontal Gyrus | -0.12 | -3.66 | 0.007 |

| | | | |
|---|---|---|---|
| Right Lobule VIII, Cerebellum | 0.19 | 3.66 | 0.007 |
| Left Crus II, Cerebellum | 0.15 | 3.58 | 0.009 |
| Left Parahippocampal Gyrus | 0.11 | 3.3 | 0.017 |
| Left Lobule VIII, Cerebellum | 0.16 | 3.22 | 0.020 |
| Default Mode Network (Posterior Cingulate Cortex; 1,-61,38) | -0.11 | -3.21 | 0.020 |
| Vermis VIII, Cerebellum | 0.15 | 3.18 | 0.020 |
| Right Crus II, Cerebellum | 0.13 | 3.1 | 0.024 |
| Right Precentral Gyrus | -0.08 | -3.08 | 0.024 |
| Left Thalamus | 0.12 | 2.97 | 0.031 |
| Left Occipital Fusiform Gyrus | 0.11 | 2.94 | 0.032 |
| Anterior Cingulate Gyrus | -0.11 | -2.93 | 0.032 |
| Vermis I & II, Cerebellum | 0.13 | 2.88 | 0.036 |
| Salience Network (Left Rostal Prefrontal Cortex; -32,45,27) | 0.12 | 2.84 | 0.038 |
| Left Inferior Temporal Gyrus | 0.11 | 2.81 | 0.040 |
| Right Lobule X, Cerebellum | 0.08 | 2.78 | 0.042 |
| Left Frontal Pole | 0.11 | 2.77 | 0.042 |
| Left Hippocampus | 0.1 | 2.71 | 0.047 |
| Occipital Visual Network (0,-93,-4) | 0.18 | 2.7 | 0.047 |
| Right Parahippocampal Gyrus | 0.13 | 2.68 | 0.049 |
| Lobule VIIb | | | |
| Right Lobule VIII, Cerebellum | 0.76 | 15.5 | 0.000 |
| Right Lobule VIIb, Cerebellum | 1.14 | 13.18 | 0.000 |
| Right Crus II, Cerebellum | 0.5 | 13.08 | 0.000 |
| Right Crus I, CerebellumI | 0.52 | 12.85 | 0.000 |
| Right Lobule V, CerebellumIIa | 0.59 | 11.85 | 0.000 |
| Left Lobule VIII, Cerebellum | 0.33 | 9.26 | 0.000 |
| Right Lobule VIIb, Cerebellum | 0.27 | 6.12 | 0.000 |
| Left Lobule VIIb, Cerebellum | 0.33 | 6.07 | 0.000 |
| Right Lobule IX, Cerebellum | 0.22 | 5.99 | 0.000 |
| Vermis VIII, Cerebellum | 0.24 | 5.41 | 0.000 |
| Right Lobule IX, Cerebellum | 0.23 | 5.31 | 0.000 |
| Right Crus I, Cerebellum | 0.26 | 5.2 | 0.000 |
| Posterior Cerebellar Network (0,-79,-32) | 0.27 | 5.15 | 0.000 |
| Right Crus I, Cerebellum | 0.24 | 4.4 | 0.002 |
| Left Lateral Occipital Cortex | 0.15 | 4.28 | 0.003 |
| Right Insular Cortex | -0.12 | -4.26 | 0.003 |
| Left Lateral Visual Network (-37,-79,10) | 0.15 | 4.22 | 0.003 |
| Vermis VII, Cerebellum | 0.12 | 3.84 | 0.008 |
| Left Lobule IX, Cerebellum | 0.16 | 3.82 | 0.008 |

| | | | |
|---|---|---|---|
| Right Inferior Temporal Gyrus | 0.14 | 3.67 | 0.011 |
| Vermis VIII, Cerebellum | 0.16 | 3.66 | 0.011 |
| Vermis VIII, Cerebellum | 0.16 | 3.6 | 0.012 |
| Left Crus II, Cerebellum | 0.19 | 3.4 | 0.018 |
| Right Inferior Temporal Gyrus | 0.1 | 3.35 | 0.020 |
| Right Middle Temporal Gyrus | 0.13 | 3.25 | 0.024 |
| Anterior Cingulate Gyrus | -0.12 | -3.17 | 0.028 |
| Left Inferior Temporal Gyrus | 0.14 | 3.13 | 0.030 |
| Dorsal Attentional Network (Left Frontal Eye Field; -27,-9,64) | 0.13 | 3.03 | 0.037 |
| Left Middle Frontal Gyrus | 0.12 | 2.94 | 0.044 |
| Left Inferior Temporal Gyrus | 0.1 | 2.9 | 0.046 |
| Crus I | | | |
| Right Crus I, Cerebellum | 2.2 | 41.48 | 0.000 |
| Posterior Cerebellar Network (0,-79,-32) | 1 | 20.39 | 0.000 |
| Anterior Cerebellar Network (0,-63,-30) | 0.67 | 12.85 | 0.000 |
| Right Crus II, Cerebellum | 0.66 | 12.32 | 0.000 |
| Left Crus I, Cerebellum | 0.6 | 10.42 | 0.000 |
| Right Crus I, CerebellumI | 0.56 | 10.15 | 0.000 |
| Right Lobule VI, Cerebellum | 0.52 | 9.9 | 0.000 |
| Right Lobule V, Cerebellum | 0.5 | 9.62 | 0.000 |
| Left Crus II, Cerebellum | 0.47 | 7.92 | 0.000 |
| Vermis VII, Cerebellum | 0.36 | 7.37 | 0.000 |
| Right Lobule VIII, Cerebellum | 0.33 | 6.9 | 0.000 |
| Occipital Visual Network (0,-93,-4) | 0.33 | 5.85 | 0.000 |
| Vermis VIIb, Cerebellum | 0.21 | 5.84 | 0.000 |
| Left Lobule IV, Cerebellum | 0.27 | 5.76 | 0.000 |
| Vermis VIII, Cerebellum | 0.26 | 5.65 | 0.000 |
| Left Inferior Temporal Gyrus | 0.2 | 5.57 | 0.000 |
| Left Lobule VIII, Cerebellum | 0.27 | 5.49 | 0.000 |
| Right Occipital Fusiform Gyrus | 0.3 | 5.36 | 0.000 |
| Vermis VIII, Cerebellum | 0.23 | 5.36 | 0.000 |
| Vermis VI, Cerebellum | 0.26 | 5.23 | 0.000 |
| Right Lobule V, CerebellumIb | 0.26 | 5.2 | 0.000 |
| Left Frontal Pole | 0.23 | 5.08 | 0.000 |
| Right Occipital Pole | 0.26 | 4.99 | 0.000 |
| Vermis VI, Cerebellum | 0.18 | 4.65 | 0.001 |
| Right Lobule VIIb, Cerebellum | 0.27 | 4.64 | 0.001 |
| Left Occipital Pole | 0.23 | 4.6 | 0.001 |
| Left Lateral Occipital Cortex | 0.18 | 4.4 | 0.001 |

| | | | |
|---|---|---|---|
| Salience Network (Left Rostal Prefrontal Cortex; -32,45,27) | 0.22 | 4.4 | 0.001 |
| Anterior Cingulate Gyrus | -0.17 | -4.39 | 0.001 |
| Left Lobule VIIb, Cerebellum | 0.21 | 4.32 | 0.001 |
| Dorsal Attentional Network (Left Frontal Eye Field; -27,-9,64) | 0.17 | 4.05 | 0.003 |
| Right Temporal Occipital Fusiform Gyrus | 0.19 | 3.95 | 0.003 |
| Right Lobule V, Cerebellum | 0.13 | 3.88 | 0.004 |
| Salience Network (Anterior Cingulate Cortex; 0,22,35) | -0.15 | -3.87 | 0.004 |
| Left Middle Temporal Gyrus | 0.16 | 3.84 | 0.004 |
| Left Middle Frontal Gyrus | 0.21 | 3.83 | 0.004 |
| Left Caudate | 0.11 | 3.69 | 0.005 |
| Language Network (Posterior Superior Temporal Gyrus; -57,-47,15) | 0.11 | 3.61 | 0.007 |
| Left Temporal Occipital Fusiform Gyrus | 0.16 | 3.55 | 0.007 |
| Right Lobule IX, Cerebellum | 0.15 | 3.45 | 0.009 |
| Left Lobule IX, Cerebellum | 0.14 | 3.43 | 0.010 |
| Right Lobule IX, Cerebellum | 0.14 | 3.4 | 0.010 |
| Right Lingual Gyrus | 0.15 | 3.35 | 0.011 |
| Left Pallidum | 0.13 | 3.33 | 0.011 |
| Right Paracingulate Gyrus | -0.14 | -3.25 | 0.014 |
| Left Inferior Frontal Gyrus | 0.13 | 3.21 | 0.014 |
| Right Lobule VIIa, Cerebellum | 0.13 | 3.2 | 0.015 |
| Default Mode Network (Left Lateral Parietal Cortex; -39,-77,33) | 0.17 | 3.18 | 0.015 |
| FrontoParietal Network (Left Lateral Prefrontal Cortex; -43,33,28) | 0.15 | 3.12 | 0.017 |
| Right Precentral Gyrus | -0.13 | -3.07 | 0.019 |
| FrontoParietal Network (Left Posterior Parietal Cortex; -46,-58,49) | 0.12 | 3.02 | 0.021 |
| Right Middle Temporal Gyrus | 0.1 | 2.96 | 0.023 |
| Right Superior Temporal Gyrus | 0.09 | 2.94 | 0.024 |
| Right Postcentral Gyrus | -0.16 | -2.93 | 0.024 |
| Vermis IX, Cerebellum | 0.18 | 2.93 | 0.024 |
| Vermis VIII, Cerebellum | 0.13 | 2.92 | 0.024 |
| Vermis IV & V, Cerebellum | 0.08 | 2.91 | 0.024 |
| Left Superior Temporal Gyrus | 0.11 | 2.91 | 0.024 |
| Left Lateral Occipital Cortex | 0.14 | 2.9 | 0.024 |
| Dorsal Attentional Network (Intraparietal cortex; 39,-42,54) | -0.16 | -2.84 | 0.027 |
| Right Supramarginal Gyrus | -0.14 | -2.79 | 0.029 |
| Left Lobule III, Cerebellum | 0.1 | 2.79 | 0.029 |
| Left Middle Temporal Gyrus | 0.1 | 2.76 | 0.031 |

| | | | |
|---|---|---|---|
| Vermis IX, Cerebellum | 0.16 | 2.75 | 0.031 |
| Left Supramarginal Gyrus | -0.12 | -2.73 | 0.032 |
| SensoriMotor Network (Right Sensory Motor Network; 56,-10,29) | -0.12 | -2.71 | 0.033 |
| Right Inferior Temporal Gyrus | 0.13 | 2.7 | 0.033 |
| Left Inferior Frontal Gyrus | 0.11 | 2.63 | 0.039 |
| Left Lobule IV & V, Cerebellum | 0.08 | 2.62 | 0.039 |
| Right Lobule VIIb, Cerebellum | 0.08 | 2.61 | 0.039 |
| Right Central Opercular Cortex | -0.1 | -2.59 | 0.040 |
| Right Parietal Operculum Cortex | -0.11 | -2.56 | 0.043 |
| Left Occipital Fusiform Gyrus | 0.13 | 2.54 | 0.043 |
| Left Inferior Temporal Gyrus | 0.07 | 2.54 | 0.043 |
| Left Angular Gyrus | 0.1 | 2.54 | 0.043 |
| Left Planum Polare | 0.07 | 2.52 | 0.044 |
| Right Insular Cortex | -0.09 | -2.51 | 0.044 |
| Medial Visual Network (2,-79,12) | 0.09 | 2.48 | 0.047 |
| Right Planum Temporale | -0.1 | -2.47 | 0.047 |
| Left Superior Temporal Gyrus | 0.08 | 2.45 | 0.049 |
| Crus II | | | |
| Right Crus II, Cerebellum | 1.99 | 20.62 | 0.000 |
| Right Lobule V, CerebellumIb | 0.52 | 12.85 | 0.000 |
| Right Lobule VIIb, Cerebellum | 0.68 | 10.86 | 0.000 |
| Posterior Cerebellar Network (0,-79,-32) | 0.77 | 10.77 | 0.000 |
| Right Crus I, Cerebellum | 0.56 | 10.15 | 0.000 |
| Right Crus I, Cerebellum | 0.5 | 9.6 | 0.000 |
| Right Lobule VIII, Cerebellum | 0.39 | 9.1 | 0.000 |
| Left Crus II, Cerebellum | 0.5 | 8.31 | 0.000 |
| Anterior Cingulate Gyrus | -0.24 | -7.08 | 0.000 |
| Right Lobule V, CerebellumIIa | 0.22 | 5.98 | 0.000 |
| Left Inferior Frontal Gyrus | 0.19 | 5 | 0.001 |
| Salience Network (Anterior Cingulate Cortex; 0,22,35) | -0.2 | -4.99 | 0.001 |
| Left Lobule VIIb, Cerebellum | 0.27 | 4.95 | 0.001 |
| Salience Network (Left Rostal Prefrontal Cortex; -32,45,27) | 0.18 | 4.82 | 0.001 |
| Left Crus I, Cerebellum | 0.23 | 4.66 | 0.001 |
| Left Lobule VIII, Cerebellum | 0.22 | 4.63 | 0.001 |
| Left Frontal Pole | 0.17 | 4.45 | 0.002 |
| Vermis VII, Cerebellum | 0.2 | 4.42 | 0.002 |
| Vermis VIII, Cerebellum | 0.2 | 4.38 | 0.002 |
| Right Lobule VIIb, Cerebellum | 0.14 | 4.32 | 0.002 |

| | | | |
|---|---|---|---|
| Anterior Cerebellar Network (0,-63,-30) | 0.23 | 4.17 | 0.003 |
| Left Middle Frontal Gyrus | 0.13 | 4.09 | 0.003 |
| Occipital Visual Network (0,-93,-4) | 0.25 | 4.09 | 0.003 |
| Left Inferior Temporal Gyrus | 0.14 | 3.97 | 0.004 |
| Vermis VI, Cerebellum | 0.13 | 3.62 | 0.010 |
| Dorsal Attentional Network (Left Frontal Eye Field; -27,-9,64) | 0.14 | 3.6 | 0.010 |
| Left Lateral Occipital Cortex | 0.18 | 3.59 | 0.010 |
| Right Lobule IX, Cerebellum | 0.18 | 3.58 | 0.010 |
| Vermis VI, Cerebellum | 0.1 | 3.5 | 0.011 |
| Left Middle Temporal Gyrus | 0.12 | 3.5 | 0.011 |
| Right Lobule IX, Cerebellum | 0.18 | 3.46 | 0.012 |
| FrontoParietal Network (Left Lateral Prefrontal Cortex; -43,33,28) | 0.11 | 3.42 | 0.012 |
| Left Occipital Pole | 0.19 | 3.38 | 0.013 |
| Right Superior Frontal Gyrus | -0.12 | -3.33 | 0.015 |
| Right Insular Cortex | -0.14 | -3.23 | 0.018 |
| Left Precentral Gyrus | 0.14 | 3.21 | 0.018 |
| Right Paracingulate Gyrus | -0.15 | -3.19 | 0.019 |
| Vermis VIII, Cerebellum | 0.16 | 3.13 | 0.021 |
| Left Lobule IX, Cerebellum | 0.15 | 3.07 | 0.024 |
| Right Putamen | -0.1 | -3.04 | 0.025 |
| Left Lateral Visual Network (-37,-79,10) | 0.13 | 2.88 | 0.035 |
| Brain Stem | -0.1 | -2.8 | 0.041 |
| Right Occipital Pole | 0.16 | 2.8 | 0.041 |
| Right Juxtapositional Lobule Cortex | -0.09 | -2.79 | 0.041 |

**Table A.3 Significant ROI connectivity by cerebellar ROI following cathodal stimulation.**

| Targets | beta | T(24) | p-FDR |
|---|---|---|---|
| Lobule I-IV | | | |
| Right Lobule III, Cerebellum | 0.75 | 21.92 | 0.000 |
| Right Lobule IV & V, Cerebellum | 0.96 | 20.36 | 0.000 |
| Right Lobule V, Cerebellum | 0.63 | 15.51 | 0.000 |
| Left Lobule III, Cerebellum | 0.49 | 14.69 | 0.000 |
| Vermis III, Cerebellum | 0.63 | 13.35 | 0.000 |
| Vermis IV & V, Cerebellum | 0.59 | 13.19 | 0.000 |
| Left Lobule IV & V, Cerebellum | 0.59 | 11.18 | 0.000 |
| Right Lobule VI, Cerebellum | 0.29 | 10.84 | 0.000 |
| Right Lobule V, Cerebellum | 0.29 | 10.29 | 0.000 |
| Right Parahippocampal Gyrus | 0.35 | 7.89 | 0.000 |
| Vermis I & II, Cerebellum | 0.31 | 7.66 | 0.000 |
| Anterior Cerebellar Network (0,-63,-30) | 0.28 | 7.61 | 0.000 |
| Vermis IX, Cerebellum | 0.24 | 7 | 0.000 |
| Left Parahippocampal Gyrus | 0.27 | 6.96 | 0.000 |
| Brain Stem | 0.26 | 6.92 | 0.000 |
| Vermis VI, Cerebellum | 0.27 | 6.31 | 0.000 |
| Right Temporal Occipital Fusiform Gyrus | 0.21 | 6.07 | 0.000 |
| Vermis IX | 0.19 | 5.98 | 0.000 |
| Left Lobule IV, Cerebellum | 0.23 | 5.94 | 0.000 |
| Left Lobule IX, Cerebellum | 0.17 | 5.54 | 0.000 |
| Right Hippocampus | 0.17 | 5.01 | 0.000 |
| Vermis VI, Cerebellum | 0.2 | 4.86 | 0.000 |
| Left Temporal Occipital Fusiform Gyrus | 0.15 | 4.83 | 0.001 |
| Right Lobule IX, Cerebellum | 0.17 | 4.44 | 0.001 |
| Vermis X, Cerebellum | 0.18 | 4.31 | 0.002 |
| Left Hippocampus | 0.17 | 4.18 | 0.002 |
| Vermis VII, Cerebellum | 0.17 | 4.15 | 0.002 |
| Vermis VIII, Cerebellum | 0.19 | 4.12 | 0.002 |
| Right Postcentral Gyrus | -0.12 | -3.79 | 0.005 |
| Left Putamen | 0.09 | 3.32 | 0.017 |
| Right Lobule VIII, Cerebellum | 0.13 | 3.28 | 0.018 |
| Superior Sensorimototr Network (0,-31,67) | -0.14 | -3.17 | 0.023 |
| Right Crus I, Cerebellum | 0.08 | 3.12 | 0.025 |
| Right Thalamus | 0.11 | 3 | 0.032 |
| Left Temporal Fusiform Cortex | 0.12 | 2.92 | 0.037 |
| Right Lobule IX, Cerebellum | 0.11 | 2.91 | 0.037 |

| | | | |
|---|---|---|---|
| Right Crus I, Cerebellum | 0.08 | 2.91 | 0.037 |
| Left Amygdala | 0.08 | 2.89 | 0.037 |
| Vermis VIII, Cerebellum | 0.11 | 2.87 | 0.039 |
| Left Juxtapositional Lobule Cortex | -0.12 | -2.84 | 0.040 |
| Left Middle Frontal Gyrus | -0.09 | -2.82 | 0.041 |
| Dorsal Attentional Network (Intraparietal cortex; 39,-42,54) | -0.09 | -2.79 | 0.043 |
| Right Middle Frontal Gyrus | -0.1 | -2.74 | 0.047 |
| Default Mode Network (Posterior Cingulate Cortex; 1,-61,38) | 0.09 | 2.72 | 0.049 |
| Lobule V | | | |
| Right Lobule IV & V, Cerebellum | 1.24 | 25.69 | 0.000 |
| Right Lobule VI, Cerebellum | 0.64 | 22.26 | 0.000 |
| Right Lobule V, Cerebellum | 0.61 | 20.79 | 0.000 |
| Right Lobule I-IV, Cerebellum | 0.63 | 15.51 | 0.000 |
| Vermis VI, Cerebellum | 0.68 | 15.48 | 0.000 |
| Left Lobule IV & V, Cerebellum | 0.67 | 15.16 | 0.000 |
| Vermis IV & V, Cerebellum | 0.58 | 10.43 | 0.000 |
| Vermis VI, Cerebellum | 0.47 | 9.57 | 0.000 |
| Anterior Cerebellar Network (0,-63,-30) | 0.42 | 9.42 | 0.000 |
| Right Temporal Occipital Fusiform Gyrus | 0.33 | 9.33 | 0.000 |
| Left Lobule IV, Cerebellum | 0.52 | 7.97 | 0.000 |
| Right Lobule III, Cerebellum | 0.22 | 7.49 | 0.000 |
| Left Lobule III, Cerebellum | 0.28 | 7.3 | 0.000 |
| Vermis VII, Cerebellum | 0.36 | 6.77 | 0.000 |
| Vermis III, Cerebellum | 0.31 | 6.66 | 0.000 |
| Right Lingual Gyrus | 0.32 | 6.15 | 0.000 |
| Left Parahippocampal Gyrus | 0.19 | 5.36 | 0.000 |
| Left Lingual Gyrus | 0.26 | 5.27 | 0.000 |
| Vermis VIII, Cerebellum | 0.24 | 5.26 | 0.000 |
| Vermis VIIb, Cerebellum | 0.17 | 4.58 | 0.001 |
| Vermis IX, Cerebellum | 0.17 | 4.55 | 0.001 |
| Right Crus I, Cerebellum | 0.15 | 4.34 | 0.002 |
| Right Occipital Fusiform Gyrus | 0.15 | 4.33 | 0.002 |
| Left Temporal Occipital Fusiform Gyrus | 0.17 | 4.25 | 0.002 |
| Right Crus I, Cerebellum | 0.16 | 4.18 | 0.002 |
| Right Parahippocampal Gyrus | 0.2 | 4.08 | 0.003 |
| Right Lobule VIIb, Cerebellum | 0.11 | 3.96 | 0.004 |
| Right Lobule IX, Cerebellum | 0.14 | 3.61 | 0.009 |
| Vermis I & II, Cerebellum | 0.11 | 3.39 | 0.015 |
| Vermis IX, Cerebellum | 0.12 | 3.21 | 0.022 |

| | | | |
|---|---|---|---|
| Left Hippocampus | 0.1 | 3.09 | 0.029 |
| Right Temporal Fusiform Cortex | 0.1 | 3.01 | 0.034 |
| Left Crus I, Cerebellum | 0.12 | 2.95 | 0.036 |
| Right Lobule VIII, Cerebellum | 0.09 | 2.95 | 0.036 |
| Left Putamen | 0.1 | 2.91 | 0.039 |
| Default Mode Network (Posterior Cingulate Cortex; 1,-61,38) | 0.11 | 2.84 | 0.044 |
| Left Frontal Operculum Cortex | 0.07 | 2.84 | 0.044 |
| Lobule VI | | | |
| Right Lobule VI, Cerebellum | 2.58 | 52.01 | 0.000 |
| Right Lobule V, Cerebellum | 0.61 | 20.79 | 0.000 |
| Anterior Cerebellar Network (0,-63,-30) | 0.82 | 16.69 | 0.000 |
| Right Lobule IV & V, Cerebellum | 0.49 | 15.85 | 0.000 |
| Left Lobule IV & V, Cerebellum | 0.4 | 15.2 | 0.000 |
| Left Lobule IV, Cerebellum | 0.66 | 14.5 | 0.000 |
| Right Temporal Occipital Fusiform Gyrus | 0.5 | 11.88 | 0.000 |
| Vermis VI, Cerebellum | 0.5 | 11.33 | 0.000 |
| Vermis VI, Cerebellum | 0.54 | 10.44 | 0.000 |
| Right Lobule I-IV, Cerebellum | 0.29 | 10.29 | 0.000 |
| Right Crus I, Cerebellum | 0.42 | 9.47 | 0.000 |
| Vermis IV & V, Cerebellum | 0.3 | 9.25 | 0.000 |
| Right Crus I, Cerebellum | 0.45 | 9.16 | 0.000 |
| Vermis VII, Cerebellum | 0.48 | 8.45 | 0.000 |
| Right Occipital Fusiform Gyrus | 0.34 | 7.59 | 0.000 |
| Right Lingual Gyrus | 0.37 | 6.5 | 0.000 |
| Posterior Cerebellar Network (0,-79,-32) | 0.27 | 5.96 | 0.000 |
| Left Crus I, Cerebellum | 0.28 | 5.67 | 0.000 |
| Vermis VIIb, Cerebellum | 0.2 | 5.44 | 0.000 |
| Left Lingual Gyrus | 0.24 | 5.25 | 0.000 |
| Vermis VIII, Cerebellum | 0.21 | 5.17 | 0.000 |
| Vermis III, Cerebellum | 0.18 | 4.67 | 0.001 |
| Vermis IX, Cerebellum | 0.17 | 4.52 | 0.001 |
| Left Temporal Occipital Fusiform Gyrus | 0.21 | 3.99 | 0.004 |
| Vermis IX, Cerebellum | 0.15 | 3.64 | 0.009 |
| Right Lobule III, Cerebellum | 0.12 | 3.5 | 0.013 |
| Right Lobule VIII, Cerebellum | 0.15 | 3.46 | 0.013 |
| Left Lobule III, Cerebellum | 0.11 | 3.39 | 0.015 |
| Right Lobule IX, Cerebellum | 0.12 | 3.17 | 0.026 |
| Left Frontal Operculum Cortex | 0.09 | 2.95 | 0.041 |
| Left Parahippocampal Gyrus | 0.13 | 2.95 | 0.041 |

| Lobule VIIb | | | |
|---|---|---|---|
| Right Lobule VIIb, Cerebellum | 1.34 | 20.89 | 0.000 |
| Right Lobule VIII, Cerebellum | 0.69 | 10.8 | 0.000 |
| Right Lobule V, CerebellumIIa | 0.55 | 9.96 | 0.000 |
| Right Crus I, CerebellumI | 0.61 | 7.84 | 0.000 |
| Vermis VIII, Cerebellum | 0.34 | 7.6 | 0.000 |
| Right Crus II, Cerebellum | 0.56 | 7.51 | 0.000 |
| Left Crus II, Cerebellum | 0.39 | 6.58 | 0.000 |
| Vermis VIII, Cerebellum | 0.27 | 6.47 | 0.000 |
| Posterior Cerebellar Network (0,-79,-32) | 0.36 | 6.19 | 0.000 |
| Left Lobule VIIb, Cerebellum | 0.42 | 6.01 | 0.000 |
| Right Crus I, Cerebellum | 0.26 | 5.84 | 0.000 |
| Left Lobule VIII, Cerebellum | 0.31 | 5.62 | 0.000 |
| Right Crus I, Cerebellum | 0.26 | 5.35 | 0.000 |
| Vermis VIII, Cerebellum | 0.23 | 5.28 | 0.000 |
| Right Lobule IX, Cerebellum | 0.26 | 5.14 | 0.000 |
| Left Precentral Gyrus | 0.1 | 4.87 | 0.001 |
| Right Lobule IX, Cerebellum | 0.21 | 4.66 | 0.001 |
| Left Inferior Frontal Gyrus | 0.13 | 4.55 | 0.001 |
| Language Network (Left Inferior Frontal Gyrus; -51,26,2) | 0.12 | 4.43 | 0.002 |
| Left Lateral Occipital Cortex | 0.1 | 4.42 | 0.002 |
| Right Lobule VIIb, Cerebellum | 0.2 | 3.99 | 0.005 |
| Left Inferior Temporal Gyrus | 0.15 | 3.98 | 0.005 |
| Vermis IX, Cerebellum | 0.13 | 3.83 | 0.006 |
| Left Lobule IX, Cerebellum | 0.2 | 3.79 | 0.007 |
| Salience Network (Anterior Cingulate Cortex; 0,22,35) | -0.12 | -3.77 | 0.007 |
| Right Paracingulate Gyrus | -0.13 | -3.64 | 0.009 |
| Left Inferior Frontal Gyrus | 0.1 | 3.3 | 0.020 |
| Salience Network (Left Rostal Prefrontal Cortex; -32,45,27) | 0.1 | 3.24 | 0.022 |
| Left Middle Frontal Gyrus | 0.09 | 3.15 | 0.026 |
| Left Lateral Occipital Cortex | 0.14 | 3.11 | 0.028 |
| Anterior Cingulate Gyrus | -0.12 | -3.04 | 0.032 |
| Left Crus I, Cerebellum | 0.12 | 2.99 | 0.035 |
| Posterior Cingulate Gyrus | -0.11 | -2.98 | 0.035 |
| Right Heschl's Gyrus | -0.08 | -2.96 | 0.036 |
| Right Inferior Temporal Gyrus | 0.13 | 2.94 | 0.036 |
| Right Inferior Frontal Gyrus | 0.1 | 2.93 | 0.036 |
| Occipital Visual Network (0,-93,-4) | 0.13 | 2.88 | 0.039 |
| Right Lateral Visual Network (38,-72,13) | 0.09 | 2.86 | 0.040 |

| | | | |
|---|---|---|---|
| Anterior Cerebellar Network (0,-63,-30) | 0.12 | 2.84 | 0.041 |
| Left Lateral Visual Network (-37,-79,10) | 0.13 | 2.83 | 0.041 |
| Crus I | | | |
| Right Crus I, Cerebellum | 2.3 | 35.44 | 0.000 |
| Posterior Cerebellar Network (0,-79,-32) | 1.15 | 26.4 | 0.000 |
| Right Crus II, Cerebellum | 0.79 | 16.71 | 0.000 |
| Right Crus I, CerebellumI | 0.67 | 16.05 | 0.000 |
| Anterior Cerebellar Network (0,-63,-30) | 0.55 | 11.54 | 0.000 |
| Left Crus II, Cerebellum | 0.58 | 11.27 | 0.000 |
| Left Crus I, Cerebellum | 0.51 | 11.16 | 0.000 |
| Right Lobule VI, Cerebellum | 0.45 | 9.64 | 0.000 |
| Right Lobule V, Cerebellum | 0.42 | 9.47 | 0.000 |
| Right Occipital Fusiform Gyrus | 0.38 | 8.67 | 0.000 |
| Vermis VII, Cerebellum | 0.38 | 8.43 | 0.000 |
| Right Lobule VIIb, Cerebellum | 0.35 | 8.22 | 0.000 |
| Vermis VIII, Cerebellum | 0.26 | 7.76 | 0.000 |
| Right Lobule VIII, Cerebellum | 0.29 | 7.56 | 0.000 |
| Vermis VIII, Cerebellum | 0.25 | 7.18 | 0.000 |
| Vermis VIIb, Cerebellum | 0.21 | 7.1 | 0.000 |
| Occipital Visual Network (0,-93,-4) | 0.31 | 6.77 | 0.000 |
| Left Lobule VIIb, Cerebellum | 0.28 | 6.46 | 0.000 |
| Left Lobule IV, Cerebellum | 0.23 | 6.23 | 0.000 |
| Right Lateral Occipital Cortex | 0.19 | 6.04 | 0.000 |
| Vermis VI, Cerebellum | 0.31 | 5.84 | 0.000 |
| Right Lobule V, CerebellumIb | 0.26 | 5.84 | 0.000 |
| Right Inferior Temporal Gyrus | 0.18 | 5.57 | 0.000 |
| Right Temporal Occipital Fusiform Gyrus | 0.19 | 5.43 | 0.000 |
| Right Occipital Pole | 0.24 | 5.42 | 0.000 |
| Left Inferior Temporal Gyrus | 0.2 | 5.41 | 0.000 |
| Left Lobule VIII, Cerebellum | 0.23 | 5.01 | 0.000 |
| Vermis IX, Cerebellum | 0.17 | 4.61 | 0.001 |
| Vermis VIII, Cerebellum | 0.2 | 4.6 | 0.001 |
| Right Lobule V, Cerebellum | 0.15 | 4.34 | 0.001 |
| Vermis VI, Cerebellum | 0.2 | 4.2 | 0.002 |
| Right Lingual Gyrus | 0.19 | 4.08 | 0.002 |
| Right Lobule V, CerebellumIIa | 0.17 | 4.02 | 0.003 |
| Vermis IX, Cerebellum | 0.13 | 3.98 | 0.003 |
| Right Lobule IV & V, Cerebellum | 0.12 | 3.83 | 0.004 |
| Default Mode Network (Left Lateral Parietal Cortex; -39,-77,33) | 0.13 | 3.53 | 0.008 |

| | | | |
|---|---|---|---|
| Right Lobule IX, Cerebellum | 0.16 | 3.5 | 0.009 |
| Left Occipital Pole | 0.19 | 3.47 | 0.009 |
| Left Lateral Occipital Cortex | 0.18 | 3.47 | 0.009 |
| Left Lobule IV & V, Cerebellum | 0.11 | 3.46 | 0.009 |
| Left Middle Temporal Gyrus | 0.15 | 3.32 | 0.013 |
| Right Lateral Visual Network (38,-72,13) | 0.12 | 3.24 | 0.015 |
| Right Lobule IX, Cerebellum | 0.14 | 3.15 | 0.018 |
| Right Thalamus | -0.1 | -3.07 | 0.021 |
| Left Inferior Frontal Gyrus | 0.11 | 3.05 | 0.022 |
| Left Lateral Occipital Cortex | 0.14 | 3.04 | 0.022 |
| Right Lobule I-IV, Cerebellum | 0.08 | 2.91 | 0.029 |
| Right Juxtapositional Lobule Cortex | -0.12 | -2.88 | 0.030 |
| Left Heschl's Gyrus | -0.11 | -2.88 | 0.030 |
| Left Lingual Gyrus | 0.12 | 2.74 | 0.041 |
| Left Superior Frontal Gyrus | 0.11 | 2.71 | 0.043 |
| Posterior Cingulate Gyrus | -0.09 | -2.68 | 0.045 |
| Right Superior Parietal Lobule | -0.1 | -2.64 | 0.048 |
| Left Middle Frontal Gyrus | 0.12 | 2.62 | 0.050 |
| Crus II | | | |
| Right Crus II, Cerebellum | 2.21 | 26.13 | 0.000 |
| Right Crus I, Cerebellum | 0.67 | 16.05 | 0.000 |
| Posterior Cerebellar Network (0,-79,-32) | 0.95 | 14.96 | 0.000 |
| Right Crus I, Cerebellum | 0.62 | 13.68 | 0.000 |
| Right Lobule VIIb, Cerebellum | 0.81 | 10.86 | 0.000 |
| Left Crus II, Cerebellum | 0.7 | 10.62 | 0.000 |
| Right Lobule V, CerebellumIb | 0.61 | 7.84 | 0.000 |
| Right Lobule VIII, Cerebellum | 0.39 | 7.61 | 0.000 |
| Left Lobule VIIb, Cerebellum | 0.41 | 7.48 | 0.000 |
| Vermis VIII, Cerebellum | 0.31 | 6.84 | 0.000 |
| Left Lobule VIII, Cerebellum | 0.28 | 6.47 | 0.000 |
| Vermis VIII, Cerebellum | 0.24 | 6.08 | 0.000 |
| Occipital Visual Network (0,-93,-4) | 0.27 | 5.19 | 0.000 |
| Left Crus I, Cerebellum | 0.26 | 5.05 | 0.000 |
| Anterior Cerebellar Network (0,-63,-30) | 0.23 | 4.93 | 0.001 |
| Left Inferior Temporal Gyrus | 0.2 | 4.6 | 0.001 |
| Right Lobule IX, Cerebellum | 0.24 | 4.33 | 0.002 |
| Right Lobule V, CerebellumIIa | 0.25 | 4.21 | 0.003 |
| Left Lateral Visual Network (-37,-79,10) | 0.21 | 4.2 | 0.003 |
| Vermis VII, Cerebellum | 0.25 | 4.17 | 0.003 |

| | | | |
|---|---|---|---|
| Left Occipital Pole | 0.2 | 4.15 | 0.003 |
| Right Occipital Pole | 0.19 | 4.09 | 0.003 |
| Left Lateral Occipital Cortex | 0.22 | 4.06 | 0.004 |
| Right Occipital Fusiform Gyrus | 0.17 | 3.89 | 0.005 |
| Left Inferior Frontal Gyrus | 0.12 | 3.89 | 0.005 |
| Vermis VIII, Cerebellum | 0.2 | 3.82 | 0.006 |
| Salience Network (Left Rostal Prefrontal Cortex; -32,45,27) | 0.11 | 3.75 | 0.007 |
| Right Lateral Occipital Cortex | 0.19 | 3.72 | 0.007 |
| Right Angular Gyrus | -0.1 | -3.69 | 0.007 |
| Left Lateral Occipital Cortex | 0.12 | 3.57 | 0.009 |
| Vermis VIIb, Cerebellum | 0.16 | 3.5 | 0.011 |
| Right Lobule IX, Cerebellum | 0.17 | 3.46 | 0.011 |
| Right Heschl's Gyrus | -0.09 | -3.29 | 0.017 |
| Right Juxtapositional Lobule Cortex | -0.11 | -3.25 | 0.018 |
| Left Frontal Pole | 0.11 | 3.19 | 0.020 |
| Vermis IX, Cerebellum | 0.13 | 3.16 | 0.021 |
| Left Middle Temporal Gyrus | 0.12 | 3.11 | 0.023 |
| Right Thalamus | -0.09 | -3.1 | 0.023 |
| Language Network (Left Inferior Frontal Gyrus; -51,26,2) | 0.11 | 3.04 | 0.025 |
| Right Middle Temporal Gyrus | 0.1 | 3.04 | 0.025 |
| Right Lateral Visual Network (38,-72,13) | 0.15 | 2.96 | 0.029 |
| Right Inferior Temporal Gyrus | 0.11 | 2.89 | 0.034 |
| Left Heschl's Gyrus | -0.12 | -2.82 | 0.040 |
| Anterior Cingulate Gyrus | -0.11 | -2.8 | 0.040 |
| Left Middle Temporal Gyrus | 0.11 | 2.79 | 0.040 |
| Right Lobule VIIb, Cerebellum | 0.12 | 2.77 | 0.041 |
| Left Middle Temporal Gyrus | 0.1 | 2.76 | 0.041 |
| Posterior Cingulate Gyrus | -0.1 | -2.75 | 0.041 |
| Vermis VI, Cerebellum | 0.15 | 2.69 | 0.047 |

**Table A.4 Clusters correlated with Sequence Learning by ROI, dependent variable and stimulation condition.**

| ROI | DV | Stimulation | Region | Cluster Size | x | y | z | p-FDR |
|---|---|---|---|---|---|---|---|---|
| Lobule I-IV | Reaction time | Sham | Left Inferior temporal gyrus | 57 | -58 | -22 | -38 | 0.000 |
| | | | Left Inferior temporal gyrus | 28 | -64 | -16 | -28 | 0.015 |
| | | | Left Inferior temporal gyrus | 28 | 52 | -4 | -42 | 0.015 |
| | | | Left Inferior temporal gyrus | 23 | 66 | -28 | -30 | 0.031 |
| | | | Left Insula | 21 | -44 | 6 | 4 | 0.038 |
| | | | Right Supramarginal gyrus | 20 | 52 | -36 | 28 | 0.040 |
| | | Anodal | Left Superior frontal gyrus | 426 | -26 | 48 | -8 | 0.000 |
| | | | Right Superior frontal gyrus | 175 | 16 | 56 | -6 | 0.000 |
| | | | Right Gyrus rectus | 74 | 2 | 40 | -22 | 0.000 |
| | | | Left Temporal pole, middle temporal gyrus | 45 | -28 | 12 | -40 | 0.000 |
| | | | Right Middle frontal gyrus, orbital part | 38 | 38 | 50 | -12 | 0.001 |
| | | | Left Inferior temporal gyrus | 34 | 36 | 6 | -40 | 0.002 |
| | | | Left Superior occipital gyrus | 26 | -18 | -84 | 14 | 0.010 |
| | | | Left Gyrus rectus | 23 | -2 | 44 | -16 | 0.017 |
| | | | Right Gyrus rectus | 20 | 8 | 62 | -16 | 0.029 |
| | | Cathodal | Right Middle frontal gyrus | 33 | 42 | 38 | 38 | 0.024 |
| | Accuracy | Sham | Left Inferior temporal gyrus | 709 | -58 | -22 | -38 | 0.000 |
| | | | Left Inferior temporal gyrus | 577 | 44 | -14 | -46 | 0.000 |
| | | | Left Temporal pole, middle temporal gyrus | 444 | -46 | 14 | -34 | 0.000 |
| | | | Right Gyrus rectus | 290 | 2 | 26 | -18 | 0.000 |

| | | | | | |
|---|---|---|---|---|---|
| Left Inferior temporal gyrus | 270 | 36 | -2 | -48 | 0.000 |
| Left Inferior frontal gyrus, orbital part | 160 | -52 | 40 | -6 | 0.000 |
| Left Inferior temporal gyrus | 139 | 52 | -10 | -46 | 0.000 |
| Right Crus II, cerebellum | 119 | 44 | -56 | -48 | 0.000 |
| Left Superior frontal gyrus | 99 | -14 | 22 | -24 | 0.000 |
| Right Gyrus rectus | 69 | 12 | 34 | -18 | 0.000 |
| Left Inferior temporal gyrus | 68 | -34 | -10 | -50 | 0.000 |
| Right Medial frontal gyrus, orbital part | 62 | 14 | 46 | -4 | 0.000 |
| Left Parahippocampal gyrus | 54 | -2 | 2 | -34 | 0.000 |
| Right Superior frontal gyrus | 32 | 16 | 22 | -22 | 0.003 |
| Left Temporal pole, middle temporal gyrus | 32 | -22 | 2 | -34 | 0.003 |
| Left Inferior temporal gyrus | 31 | 58 | -26 | -26 | 0.003 |
| Right Inferior frontal gyrus, orbital part | 27 | 38 | 36 | -10 | 0.006 |
| Left Inferior temporal gyrus | 26 | -60 | -58 | -16 | 0.007 |
| Left Inferior temporal gyrus | 25 | 66 | -28 | -30 | 0.009 |
| Left Inferior frontal gyrus, orbital part | 24 | -44 | 24 | -6 | 0.009 |
| Right Fusiform gyrus | 24 | 16 | 6 | -40 | 0.009 |
| Right Lobule VIII, cerebellum | 24 | 26 | -72 | -62 | 0.009 |
| Left Inferior temporal gyrus | 20 | -40 | -4 | -40 | 0.020 |
| Left Lobule VIIb, cerebellum | 20 | -40 | -70 | -56 | 0.020 |

| | | | | | | | | |
|---|---|---|---|---|---|---|---|---|
| | | | Right Lobule IX, cerebellum | 19 | 6 | -42 | -68 | 0.024 |
| | | | Right Lobule VIII, cerebellum | 17 | 6 | -62 | -62 | 0.037 |
| | | Cathodal | Right Inferior frontal gyrus, orbital part | 70 | 50 | 44 | -4 | 0.000 |
| | | | Left Thalamus | 43 | -6 | -30 | 6 | 0.002 |
| | | | Left Precuneus | 42 | 2 | -66 | 38 | 0.002 |
| | | | Right Fusiform gyrus | 41 | 14 | -14 | -46 | 0.002 |
| | | | Right Hippocampus | 30 | 16 | -34 | 8 | 0.010 |
| | | | Left Superior frontal gyrus, medial | 27 | -6 | 44 | 32 | 0.015 |
| | | | Right Lobule VIII, cerebellum | 25 | 24 | -40 | -46 | 0.020 |
| | | | Right Lingual gyrus | 24 | 16 | -56 | 0 | 0.021 |
| | | | Left Inferior frontal gyrus, opercular part | 21 | -52 | 10 | 20 | 0.036 |
| | | | Left Lingual gyrus | 20 | -16 | -88 | -2 | 0.040 |
| | | | Left Superior frontal gyrus | 19 | -18 | 54 | 36 | 0.042 |
| | | | Left Inferior frontal gyrus, triangular part | 19 | -48 | 48 | 14 | 0.042 |
| | | | Left Precuneus | 18 | -2 | -54 | 44 | 0.048 |
| | | | Left Temporal pole, superior temporal gyrus | 17 | -36 | 10 | -22 | 0.050 |
| | | | Left Fusiform gyrus | 17 | -24 | -16 | -46 | 0.050 |
| | | | Right Temporal pole, middle temporal gyrus | 17 | 32 | 8 | -36 | 0.050 |
| Crus I | Reaction Time | Sham | Left Inferior temporal gyrus | 73 | 56 | -18 | -40 | 0.000 |
| | | | Left Middle occipital gyrus | 64 | -50 | -78 | 2 | 0.000 |
| | | | Left Inferior frontal gyrus, orbital part | 60 | -32 | 36 | -10 | 0.000 |
| | | | Right Supplementary motor area | 38 | 14 | -4 | 58 | 0.002 |
| | | | Right Inferior frontal gyrus, orbital part | 36 | 32 | 42 | -4 | 0.003 |

| | | | | | | |
|---|---|---|---|---|---|---|
| | Right Crus II, cerebellum | 35 | 46 | -72 | -46 | 0.003 |
| | Left Inferior temporal gyrus | 29 | -62 | -30 | -26 | 0.007 |
| | Left Inferior temporal gyrus | 26 | -60 | -14 | -30 | 0.011 |
| | Right Caudate nucleus | 19 | 18 | 24 | 6 | 0.041 |
| | Left Median cingulate and paracingulate gyri | 18 | -2 | 0 | 44 | 0.046 |
| Anodal | Right Gyrus rectus | 99 | 8 | 34 | -18 | 0.000 |
| | Right Inferior frontal gyrus, orbital part | 66 | 18 | 22 | -24 | 0.000 |
| | Right Medial frontal gyrus, orbital part | 57 | 6 | 58 | -8 | 0.000 |
| | Right Superior frontal gyrus | 55 | 20 | 34 | -16 | 0.000 |
| | Left Temporal pole, middle temporal gyrus | 45 | -40 | 16 | -38 | 0.001 |
| | Left Gyrus rectus | 37 | -8 | 38 | -16 | 0.002 |
| | Left Gyrus rectus | 35 | -6 | 28 | -20 | 0.003 |
| | Left Medial frontal gyrus, orbital part | 31 | -14 | 70 | -4 | 0.005 |
| | Left Anterior cingulate and paracingulate gyri | 27 | -20 | 46 | 2 | 0.009 |
| | Left Superior frontal gyrus | 26 | -18 | 50 | -14 | 0.010 |
| | Right Inferior frontal gyrus, orbital part | 22 | 38 | 42 | -20 | 0.021 |
| | Right Superior frontal gyrus, medial | 21 | 6 | 70 | 2 | 0.024 |
| | Right Medial frontal gyrus, orbital part | 20 | 4 | 68 | -6 | 0.027 |
| | Left Inferior temporal gyrus | 19 | 36 | 10 | -42 | 0.031 |
| | Right Temporal pole, middle temporal gyrus | 17 | 38 | 18 | -36 | 0.046 |
| | Left Gyrus rectus | 16 | 0 | 62 | -16 | 0.048 |

| | | | | | | | |
|---|---|---|---|---|---|---|---|
| | | Right Inferior frontal gyrus, orbital part | 16 | 32 | 30 | -20 | 0.048 |
| | | Left Gyrus rectus | 16 | -4 | 26 | -24 | 0.048 |
| | | Left Middle temporal gyrus | 273 | -60 | -16 | -22 | 0.000 |
| | | Right Fusiform gyrus | 142 | 42 | -16 | -30 | 0.000 |
| | | Left Inferior temporal gyrus | 113 | 56 | -30 | -24 | 0.000 |
| | | Left Inferior temporal gyrus | 92 | -44 | -8 | -34 | 0.000 |
| | | Left Temporal pole, superior temporal gyrus | 64 | -54 | 14 | -12 | 0.000 |
| | Cathodal | Left Middle temporal gyrus | 39 | -68 | -24 | -12 | 0.002 |
| | | Left Inferior parietal gyrus | 30 | -50 | -22 | 40 | 0.010 |
| | | Left Crus II, cerebellum | 29 | -38 | -74 | -44 | 0.011 |
| | | Right Rolandic operculum | 27 | 34 | -38 | 30 | 0.013 |
| | | Left Middle temporal gyrus | 27 | -46 | -28 | -12 | 0.013 |
| | | Right Lobule VIII, cerebellum | 25 | 24 | -76 | -58 | 0.017 |
| | | Left Inferior temporal gyrus | 920 | -34 | -14 | -48 | 0.000 |
| | | Left Inferior temporal gyrus | 408 | 52 | -6 | -46 | 0.000 |
| | | Left Gyrus rectus | 342 | 0 | 30 | -16 | 0.000 |
| | | Right Fusiform gyrus | 287 | 28 | -10 | -42 | 0.000 |
| Accuracy | Sham | Left Inferior frontal gyrus, orbital part | 195 | -26 | 34 | -12 | 0.000 |
| | | Right Temporal pole, middle temporal gyrus | 161 | 30 | 14 | -32 | 0.000 |
| | | Left Middle occipital gyrus | 158 | -44 | -74 | 0 | 0.000 |
| | | Left Temporal pole, middle temporal gyrus | 157 | -44 | 6 | -46 | 0.000 |

| | | | | | |
|---|---|---|---|---|---|
| Left Inferior frontal gyrus, orbital part | 122 | -52 | 34 | -10 | 0.000 |
| Left Lobule VIIb, cerebellum | 108 | -46 | -58 | -56 | 0.000 |
| Left Inferior frontal gyrus, orbital part | 91 | -32 | 36 | -10 | 0.000 |
| Left Gyrus rectus | 83 | -6 | 32 | -24 | 0.000 |
| Left Inferior temporal gyrus | 73 | -52 | -4 | -38 | 0.000 |
| Right Superior frontal gyrus | 65 | 16 | 22 | -22 | 0.000 |
| Right Crus II, cerebellum | 63 | 50 | -64 | -50 | 0.000 |
| Left Inferior temporal gyrus | 43 | 48 | 10 | -42 | 0.000 |
| Left Inferior temporal gyrus | 43 | 48 | -8 | -50 | 0.000 |
| Right Inferior frontal gyrus, orbital part | 40 | 34 | 36 | -8 | 0.001 |
| Right Superior frontal gyrus | 37 | 22 | 36 | -12 | 0.001 |
| Right Lobule VIII, cerebellum | 36 | 22 | -46 | -62 | 0.001 |
| Left Inferior frontal gyrus, orbital part | 35 | -22 | 26 | -24 | 0.001 |
| Left Inferior temporal gyrus | 35 | 60 | -42 | -28 | 0.001 |
| Left Parahippocampal gyrus | 34 | -12 | 2 | -34 | 0.002 |
| Left Inferior temporal gyrus | 34 | 66 | -26 | -30 | 0.002 |
| Right Gyrus rectus | 33 | 2 | 8 | -28 | 0.002 |
| Left Median cingulate and paracingulate gyri | 30 | 0 | -2 | 46 | 0.003 |
| Right Anterior cingulate and paracingulate gyri | 28 | 12 | 36 | -6 | 0.004 |

| | | | | | | |
|---|---|---|---|---|---|---|
| | Left Inferior temporal gyrus | 26 | -64 | -14 | -28 | 0.006 |
| | Right Calcarine fissure | 22 | 28 | -74 | 12 | 0.013 |
| | Left Medial frontal gyrus, orbital part | 22 | 0 | 40 | -12 | 0.013 |
| | Left Inferior temporal gyrus | 22 | 68 | -18 | -28 | 0.013 |
| | Left Superior parietal gyrus | 19 | -34 | -62 | 50 | 0.024 |
| | Right Inferior frontal gyrus, orbital part | 18 | 26 | 34 | -10 | 0.029 |
| | Right Olfactory cortex | 17 | 14 | 16 | -16 | 0.035 |
| | Left Middle temporal gyrus | 17 | -56 | -40 | -2 | 0.035 |
| | Right Crus II, cerebellum | 16 | 50 | -48 | -46 | 0.040 |
| | Right Lobule X, cerebellum | 16 | 20 | -34 | -48 | 0.040 |
| | Right Parahippocampal gyrus | 16 | 20 | 0 | -30 | 0.040 |
| | Left Fusiform gyrus | 15 | -2 | -16 | -54 | 0.047 |
| | Right Middle temporal gyrus | 15 | 66 | -4 | -28 | 0.047 |
| | Left Temporal pole, middle temporal gyrus | 15 | -32 | 16 | -38 | 0.047 |
| Anodal | Right Temporal pole, middle temporal gyrus | 25 | 46 | 8 | -32 | 0.034 |
| | Left Inferior temporal gyrus | 1014 | -64 | -48 | -22 | 0.000 |
| | Left Inferior temporal gyrus | 235 | 68 | -28 | -26 | 0.000 |
| Cathodal | Right Middle temporal gyrus | 180 | 64 | -6 | -26 | 0.000 |
| | Left Temporal pole, superior temporal gyrus | 148 | -52 | 12 | -14 | 0.000 |
| | Right Lobule VIII, cerebellum | 87 | 26 | -56 | -62 | 0.000 |

| | | | | | |
|---|---|---|---|---|---|
| Right Superior parietal gyrus | 53 | 18 | -62 | 68 | 0.000 |
| Left Precuneus | 46 | -10 | -74 | 62 | 0.001 |
| Left Middle temporal gyrus | 44 | -68 | -26 | -12 | 0.001 |
| Right Inferior frontal gyrus, orbital part | 32 | 46 | 42 | -4 | 0.006 |
| Left Crus II, cerebellum | 32 | -38 | -74 | -44 | 0.006 |
| Left Middle temporal gyrus | 31 | -62 | 0 | -18 | 0.007 |
| Right Middle temporal gyrus | 29 | 66 | -2 | -20 | 0.009 |
| Left Rolandic operculum | 28 | -62 | 4 | 2 | 0.009 |
| Right Olfactory cortex | 28 | 12 | 6 | -14 | 0.009 |
| Right Lobule IX, cerebellum | 27 | 8 | -44 | -70 | 0.010 |
| Left Fusiform gyrus | 25 | -34 | -16 | -22 | 0.014 |
| Left Lobule VIIb, cerebellum | 24 | -40 | -50 | -44 | 0.016 |
| Right Supramarginal gyrus | 23 | 36 | -34 | 30 | 0.018 |
| Left Lobule X, cerebellum | 23 | -18 | -24 | -38 | 0.018 |
| Left Lobule VIIb, cerebellum | 19 | -46 | -54 | -56 | 0.037 |
| Left Superior frontal gyrus, medial | 19 | -10 | 56 | 22 | 0.037 |
| Right Lobule VIII, cerebellum | 18 | 24 | -40 | -54 | 0.041 |
| Right Lobule VIII, cerebellum | 18 | 10 | -62 | -56 | 0.041 |
| Left Lobule IX, cerebellum | 18 | -4 | -62 | -60 | 0.041 |
| Right Median cingulate and paracingulate gyri | 17 | 12 | -38 | 44 | 0.045 |

| | | | | | | |
|---|---|---|---|---|---|---|
| | Left Middle occipital gyrus | 17 | -32 | -98 | 8 | 0.045 |
| | Left Middle temporal gyrus | 17 | -68 | -14 | -22 | 0.045 |

**Table A.5 Clusters correlated with working memory by ROI, dependent variable and stimulation condition.**

| ROI | DV | Stimulation | Region | Cluster Size | x | y | z | p-FDR |
|---|---|---|---|---|---|---|---|---|
| Lobule I-IV | Reaction Time | Anodal | Left Calcarine fissure | 57 | -12 | -86 | 14 | 0.000 |
| | | | Left Median cingulate and paracingulate gyri | 26 | -10 | -14 | 38 | 0.017 |
| | | Cathodal | Left Inferior occipital gyrus | 25 | -44 | -70 | -14 | 0.038 |
| | Accuracy | Anodal | Left Temporal pole, middle temporal gyrus | 234 | -30 | 12 | -40 | 0.000 |
| | | | Left Superior frontal gyrus | 228 | -22 | 46 | -12 | 0.000 |
| | | | Left Temporal pole, middle temporal gyrus | 169 | -42 | 22 | -36 | 0.000 |
| | | | Right Temporal pole, middle temporal gyrus | 157 | 44 | 26 | -34 | 0.000 |
| | | | Right Fusiform gyrus | 146 | 24 | 12 | -42 | 0.000 |
| | | | Left Middle frontal gyrus, orbital part | 89 | -42 | 54 | -10 | 0.000 |
| | | | Left Fusiform gyrus | 85 | -28 | -6 | -48 | 0.000 |
| | | | Right Temporal pole, middle temporal gyrus | 65 | 44 | 14 | -40 | 0.000 |
| | | | Left Medial frontal gyrus, orbital part | 29 | -4 | 68 | -10 | 0.003 |
| | | | Right Superior frontal gyrus | 23 | 10 | 48 | -22 | 0.010 |
| | | | Left Inferior frontal gyrus, orbital part | 21 | -36 | 50 | -12 | 0.014 |
| | | | Right Inferior frontal gyrus, orbital part | 18 | 40 | 46 | -18 | 0.026 |
| | | Cathodal | Left Rolandic operculum | 58 | -64 | -6 | 12 | 0.000 |
| | | | Right Temporal pole, middle temporal gyrus | 50 | 22 | 14 | -34 | 0.001 |
| | | | Left Gyrus rectus | 45 | -4 | 22 | -28 | 0.001 |
| | | | Left Inferior temporal gyrus | 32 | -66 | -56 | -6 | 0.008 |

| | | | | | | | | |
|---|---|---|---|---|---|---|---|---|
| | | | Left Temporal pole, middle temporal gyrus | 23 | -34 | 12 | -32 | 0.034 |
| | | | Left Gyrus rectus | 23 | -6 | 50 | -16 | 0.034 |
| | | | Left Middle occipital gyrus | 22 | -18 | -10 4 | 4 | 0.036 |
| | | | Left Lobule VIII, cerebellum | 20 | -32 | -40 | -56 | 0.043 |
| | | | Left Middle frontal gyrus, orbital part | 20 | -40 | 48 | -4 | 0.043 |
| Crus I | Reaction Time | Anodal | Left Temporal pole, middle temporal gyrus | 266 | -40 | 6 | -44 | 0.000 |
| | | | Left Inferior temporal gyrus | 120 | 38 | -2 | -48 | 0.000 |
| | | | Left Inferior temporal gyrus | 117 | 32 | 10 | -44 | 0.000 |
| | | | Left Temporal pole, middle temporal gyrus | 105 | -32 | 16 | -36 | 0.000 |
| | | | Left Middle temporal gyrus | 93 | -56 | 4 | -34 | 0.000 |
| | | | Left Inferior temporal gyrus | 90 | 46 | 8 | -44 | 0.000 |
| | | | Right Middle frontal gyrus, orbital part | 85 | 40 | 56 | -8 | 0.000 |
| | | | Left Superior frontal gyrus | 71 | -16 | 62 | -6 | 0.000 |
| | | | Left Superior frontal gyrus | 56 | -14 | 72 | 4 | 0.000 |
| | | | Left Middle frontal gyrus, orbital part | 47 | -26 | 38 | -16 | 0.000 |
| | | | Left Gyrus rectus | 41 | -12 | 30 | -20 | 0.001 |
| | | | Left Middle frontal gyrus, orbital part | 36 | -34 | 54 | -10 | 0.001 |
| | | | Left Middle frontal gyrus, orbital part | 30 | -24 | 42 | -16 | 0.003 |
| | | | Right Medial frontal gyrus, orbital part | 27 | 10 | 66 | -12 | 0.006 |
| | | | Left Inferior frontal gyrus, triangular part | 25 | -54 | 34 | 6 | 0.007 |

| | | | | | | | |
|---|---|---|---|---|---|---|---|
| | | Left Middle frontal gyrus, orbital part | 25 | -44 | 56 | -10 | 0.007 |
| | | Right Fusiform gyrus | 24 | 22 | 12 | -42 | 0.009 |
| | | Right Gyrus rectus | 22 | 2 | 48 | -22 | 0.012 |
| | | Left Temporal pole, middle temporal gyrus | 21 | -34 | 26 | -36 | 0.014 |
| | | Left Inferior temporal gyrus | 21 | 62 | -10 | -38 | 0.014 |
| | | Left Inferior temporal gyrus | 20 | -66 | -10 | -26 | 0.016 |
| | | Left Inferior frontal gyrus, opercular part | 17 | -60 | 18 | 4 | 0.029 |
| | | Right Medial frontal gyrus, orbital part | 17 | 6 | 68 | -8 | 0.029 |
| | Cathodal | Right Precuneus | 43 | 6 | -58 | 56 | 0.002 |
| | | Right Angular gyrus | 37 | 26 | -46 | 42 | 0.003 |
| | Sham | Left Inferior parietal gyrus | 75 | -56 | -34 | 40 | 0.000 |
| | | Right Supramarginal gyrus | 44 | 62 | -30 | 44 | 0.000 |
| Accuracy | Anodal | Left Temporal pole, middle temporal gyrus | 274 | -40 | 8 | -42 | 0.000 |
| | | Left Inferior temporal gyrus | 149 | 34 | 10 | -46 | 0.000 |
| | | Right Temporal pole, middle temporal gyrus | 115 | 26 | 16 | -38 | 0.000 |
| | | Left Inferior temporal gyrus | 97 | -58 | 0 | -36 | 0.000 |
| | | Left Inferior temporal gyrus | 88 | 42 | 8 | -44 | 0.000 |
| | | Right Middle frontal gyrus, orbital part | 76 | 40 | 56 | -16 | 0.000 |
| | | Left Medial frontal gyrus, orbital part | 70 | -12 | 68 | 0 | 0.000 |
| | | Left Fusiform gyrus | 59 | -20 | 8 | -42 | 0.000 |
| | | Left Superior frontal gyrus | 43 | -20 | 40 | -20 | 0.000 |
| | | Left Inferior frontal gyrus, orbital part | 35 | -44 | 48 | -12 | 0.002 |

| | | | | | | |
|---|---|---|---|---|---|---|
| | Left Gyrus rectus | 35 | -4 | 56 | -18 | 0.002 |
| | Left Temporal pole, superior temporal gyrus | 34 | -28 | 24 | -34 | 0.002 |
| | Left Inferior frontal gyrus, triangular part | 25 | -54 | 34 | 6 | 0.008 |
| | Left Temporal pole, middle temporal gyrus | 25 | -30 | 12 | -44 | 0.008 |
| | Left Inferior temporal gyrus | 24 | -68 | -18 | -28 | 0.009 |
| | Right Superior frontal gyrus | 23 | 10 | 70 | -4 | 0.010 |
| | Right Gyrus rectus | 23 | 6 | 60 | -18 | 0.010 |
| | Left Gyrus rectus | 22 | -12 | 40 | -16 | 0.012 |
| | Left Inferior frontal gyrus, orbital part | 20 | -40 | 48 | -10 | 0.017 |
| | Left Inferior frontal gyrus, orbital part | 19 | -50 | 36 | -20 | 0.020 |
| | Right Middle temporal gyrus | 19 | 62 | 2 | -34 | 0.020 |
| | Left Middle frontal gyrus, orbital part | 18 | -30 | 60 | -6 | 0.023 |
| | Left Inferior frontal gyrus, orbital part | 18 | -46 | 50 | -12 | 0.023 |
| | Left Inferior frontal gyrus, opercular part | 17 | -60 | 18 | 4 | 0.026 |
| | Left Inferior frontal gyrus, orbital part | 17 | -30 | 46 | -16 | 0.026 |
| | Right Middle frontal gyrus | 16 | 30 | 62 | 24 | 0.031 |
| | Left Superior frontal gyrus | 16 | -18 | 62 | -6 | 0.031 |
| | Left Inferior frontal gyrus, orbital part | 14 | -32 | 44 | -18 | 0.043 |
| | Left Middle frontal gyrus, orbital part | 14 | -22 | 36 | -22 | 0.043 |
| | Left Inferior temporal gyrus | 14 | -60 | -18 | -36 | 0.043 |
| Cathodal | Left Gyrus rectus | 40 | 0 | 30 | -14 | 0.011 |

| | | | | | | |
|---|---|---|---|---|---|---|
| | Left Temporal pole, superior temporal gyrus | 30 | -40 | 18 | -24 | 0.032 |